78-10022
CR-156647

# DIGITAL IMAGE CORRELATION TECHNIQUES APPLIED TO LANDSAT MULTISPECTRAL IMAGERY



L. O. Bonrud
W. J. Miller

CONTROL DATA CORPORATION
Minneapolis, Minnesota

(E78-10022) DIGITAL IMAGE CORRELATION TECHNIQUES APPLIED TO LANDSAT MULTISPECTRAL IMAGERY (Control Data Corp.) 118 p HC A06/MF A01 CSCL 05B N78-12499 Unclas G3/43 00022

January, 1976
Contract NAS 5-20570

National Aeronautics and Space Administration
Goddard Space Flight Center
Greenbelt, Maryland



CONTROL DATA
CORPORATION

# DIGITAL IMAGE CORRELATION TECHNIQUES APPLIED TO LANDSAT MULTISPECTRAL IMAGERY

L. O. Bonrud
W. J. Miller

Original photography may be purchased from:
EROS Data Center

Sioux Falls, SD

## FOREWORD

This report was prepared by Control Data Corporation, Minneapolis, Minnesota, for the National Aeronautics and Space Administration (NASA), located at Goddard Space Flight Center (GSFC). The work performed and described in the report, under contract number NAS5-20570, constitutes a part of the continuing effort at GSFC to further the application of remote sensing.

Control Data Corporation performed digital image registration and resampling techniques on three sets of LANDSAT multispectral scanner (MSS) imagery. Major emphasis in regard to registration techniques was placed on an automatic registration system that achieves registration accuracies resulting in mean radial displacement errors less than 0.25 pixel.

Control Data's program effort was directed by L. O. Bonrud. W. J. Miller, the Project Leader, was responsible for all processing procedures and results, and R. R. Hoyt provided consultation in processing techniques. J. D. Johnston assisted Mr. Miller in software development, processing, and analysis. Image reproduction was performed by J. D. Johnston and K. Schroeder. Graphics and publications services were provided by A. A. Yost, D. M. Olson and F. M. Dailey.

The program was funded under the above named contract during the period June 1974 through 30 September 1975. The NASA Program Monitor was Mr. B. Peavey, whose assistance and cooperation is gratefully acknowledged.

This technical report was submitted on behalf of Control Data by L. O. Bonrud and W. J. Miller on January 16, 1975. The report has been reviewed and is approved.

ABSTRACT

Automatic image registration and resampling techniques applied to LANDSAT data achieved accuracies resulting in mean radial displacement errors of less than 0.2 pixel. The process method utilizes recursive computational techniques and line-by-line updating on the basis of feedback error signals. Goodness of local feature matching is evaluated through the implementation of a correlation algorithm.

An automatic restart procedure allows the system to derive control point coordinates over a portion of the image and to restart the process utilizing this new control point information as initial estimates. By this technique excellent registration is efficiently obtained over the entire image.

Excellent registration was obtained in the presence of significant temporal changes. Greatest dependability is typically obtained by correlation of data derived in the same spectral band, though effective performance was obtained for interband registration as well.

Two dimensional sin X/X resampling is indicated to provide superior overall radiance and spatial frequency properties compared with nearest neighbor and four-point bilinear resampling, but at a severe penalty in process rate.

TABLE OF CONTENTS

TABLE OF CONTENTS (CONT.)

LIST OF ILLUSTRATIONS

LIST OF ILLUSTRATIONS (CONT.)

## LIST OF TABLES

LIST OF TABLES (CONT.)

# 1.0 INTRODUCTION

Remote sensing technology provides man with a versatile capability which can be applied to the management of his resources and ultimately contribute to an orderly development for the betterment of mankind. Yet, unless information can be appropriately extracted from the vast amounts of data which are collected daily the potential of remote sensing will not be reached [1].

LANDSAT multispectral scanner imagery is currently being collected and investigated for a wide range of applications. Interpretation of this data generally requires some method of classification and may involve a number of spectral images of the same scene. It follows that precise registration becomes important in order that the information contained in the various images can be properly coordinated.

The accuracy of registration that is needed is dependent upon the applicational requirements. Thus, there may be many useful applications of LANDSAT data in which it is entirely satisfactory to register two data products to within several pixels. However, other researchers involved in crop classification, for example, may wish to evaluate areas so small as 40 acres. For current LANDSAT resolution (nominally 75 meters) this means that it may be necessary to register and classify areas containing 40 pixels or less. It thus becomes important to relate pixel to pixel, and subpixel registration accuracy must be achieved.

Elements of the image scene are classified on the basis of radiometric values contained in the various spectral scenes. Therefore, it is important to minimize the degradation of these values during processing of the data.

Thus, effective classification of scene content is highly dependent upon the quality of registration processing. Oftentimes comparisons are made over an elapsed time interval and are thus complicated with temporal changes. These changes together with variations in spectral detail and terrain, present significant challenges to machine processing of remotely sensed data.

Sensor capability and the potentially great need for large amounts of processed data have established a requirement for cost-effective automatic processing techniques. Hence, precise automatic registration techniques are important to the success of machine processing of LANDSAT data.

The work described in this report investigates the applicability of an automatic registration process for registering LANDSAT multispectral imagery without using any ancillary data, such as spacecraft attitude, location, or ground truth. The method depends upon correlating one image with another.

An early paper by Rosenfeld [2] includes a consideration of various possible coefficients of correlation as measures of the quality of image registration. Application of image correlation to change detection has been reported by Lillestrand [3], and those techniques developed for the registration of radar data are evaluated in this study for their usefulness in automatic registration of LANDSAT data.

## 1.1 Objectives

The goal of this program is to demonstrate and evaluate the performance of an automatic registration technique with LANDSAT data of varying qualities. Specific objectives are:

- Achieve Sub-Pixel Registration Accuracy

This objective is to achieve image-to-image registration accuracies with mean radial displacement errors less than 0.25 pixel. A requirement is that the registration procedure must rely solely on information contained in the test data (reference and collateral).

- Minimize Radiometric Degradation

Processing methods are evaluated for their capability to preserve collateral radiometric values through warping to the reference image.

- Establish Sensitivity to Image Properties

The objective of this requirement is to characterize scene content and associated correlation parameters which will produce optimum performance results.

- Characterization of Technique vs. Image Property

Effectiveness of automatic registration processing using fixed parameter and process dependent techniques are evaluated for various types of test data. Sensitivity to autoband, interband, and intrascene registration is investigated.

- Outline Efficiency of Registration Procedure

Processing rates are investigated as a function of resampling technique.

## 1.2 Summary

Four pairs of LANDSAT multispectral imagery were registered with an automatic digital process (TRAK) to demonstrate and evaluate its performance capabilities with respect to imagery qualities. The scenes were selected to provide examples of cultural development, foothills, mountains, and desert-like terrain in order that registration performance could be evaluated for these varying conditions. Moreover, process techniques were tested in the presence of temporal and spectral changes under conditions of autoband, interband, and intrascene processing (defined in Section 3.2.2).

All four scenes were registered by using the TRAK process augmented with process dependent modes AUTODAMP, AUTOVLIM, and RESTART. In addition, Scenes A and B (defined in TABLE 3-1) were processed with fixed parameters.

RESTART proved to be particularly effective in obtaining precision results quickly because of its automatic computation of precise initial offsets. Registration accuracies represented by mean radial displacement errors less than 0.2 pixel were obtained for all terrain types and for autoband, interband, and intrascene processing.

Nearest neighbor resampling compared with 4-point bilinear and two dimensional sin X/X resampling resulted in the least radiance degradation as measured by two methods: average radiance and pixel-by-pixel differences of conjugate radiance values in the raw and warped collateral images. Nearest neighbor resampling is subject to local displacements of $\pm 0.5$ pixel, however, and depresses radiance values at feature edges.

Two dimensional sin X/X resampling ranked ahead of nearest neighbor and 4-point bilinear resampling on the basis of overall statistical evaluation of radiance parameters. Sin X/X resampling also maintains frequency fidelity, while 4-point bilinear interpolation blurs the image.

Though sin X/X resampling was not optimized it is concluded that it would allow TRAK registration to reach its greatest precision. On the basis of the current work it would achieve this precision at 1/9 the process rate that can be achieved with nearest neighbor resampling.

The speed of the registration process using nearest neighbor resampling is approximately 3000 pixels per second (central processor time) on the Control Data 6600 computer system. It is of interest to note that the process rate can be increased to one million pixels per second (or more) with system architecture built upon Control Data's Flexible Processor, a microprogrammable machine.

As described above incorporation of AUTODAMP, AUTOVLIM, and RESTART in the automatic registration processor minimized processor sensitivity to diverse imagery characteristics. Mean radial displacement errors less than 0.2 pixel were obtained in autoband, intrascene, and interband combinations. Thus, the TRAK registration process which depends upon subregion image correlation, is proving to be very effective on a wide variety of image qualities.

The procedures and results which have been summarized here are discussed in detail in the following sections. Contents of this report are discussed under the following five topics:

1.0 INTRODUCTION
2.0 REGISTRATION TECHNIQUE
3.0 EXPERIMENTAL INVESTIGATION
4.0 REGISTRATION ACCURACIES
5.0 RADIOMETRIC DEGRADATION

Additional summary details of the investigation may be found at the close of Sections 4.0 and 5.0.

## 2.0 REGISTRATION TECHNIQUE

Registration of pairs of data sets was obtained with an automatic processing technique implemented in program TRAK, which is also known as the Strip Processor. The method utilizes recursive computation to update the spatial transformation for each scan line on the basis of correlation performed within correlation paths or strips running in the process direction. In this manner Program TRAK allows continuous progressive processing of image data with modest memory requirements.

The process spatially transforms a collateral image to register with a similar reference image. It is also capable of correcting the collateral image to make the radiometric values of the collateral image match those of the reference image on a statistical basis. This technique is particularly advantageous in change detection applications where it is desired to minimize the effect of systematic processing variables which may have influenced the quality of the original images.

No radiometric corrections were used in preparing the results of this study since it was desired to maintain radiometric fidelity. However, for the sake of completeness a description of the radiometric correction feature is included. If so desired, the algorithm can be modified to accept radiometric calibration data and related error signals in place of those signals which are now generated on the basis of comparison with the reference image. In this way radiometric corrections can be implemented in the Strip Processor.

Three automatic adaptive features, RESTART, AUTODAMP, and AUTOVLIM, augment the basic process. These features are described separately.

AUTODAMP is a process dependent technique for computing servo decay constants. This technique automatically adjusts the servo decay constants for both geometric coordinate directions as a function of the size of feature detail (correlation distance).

AUTOVLIM is a process dependent technique for adjusting the Harness Channel Width (VLIM). AUTOVLIM adjusts the circular area around the predicted offset in which the process can apply its correction.

RESTART generates new registration control points while processing a portion of the image. When a specified number of control points have been determined, the registration process is reinitiated at the beginning of the image strip using the new control points.

A general description of the TRAK process and control parameters is provided in Sections 2.1 and 2.2, respectively, and has been reported by Ulstad [4].

## 2.1 General Description

With the current TRAK program 2 to 12 strips, each N pixels wide, are defined in the reference image (Figure 2-1). The corresponding strips of imagery in the collateral image will be distorted by the existing warp between the images. The objective then is to find matching conjugate locations within the corresponding strips in the reference and collateral images.

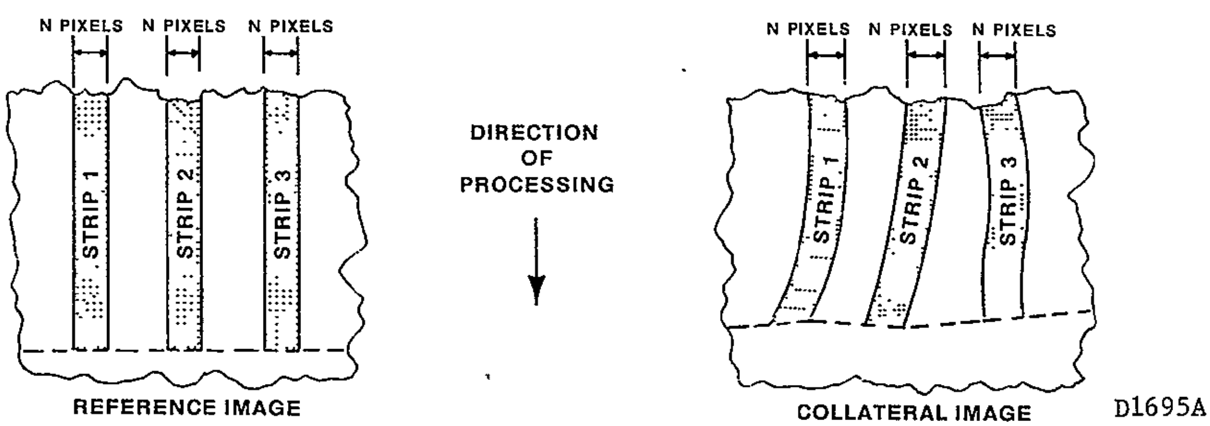


Figure 2-1. Strip Processing Concept



ORIGINAL PAGE IS
OF POOR QUALITY

These matching conjugate locations are identified by performing local correlation computations to match image features. The algorithm is recursive and includes:

- interpolation over five points on the correlation surface,
- a least squares polynomial fit to the matching locations in all of the strips (This also provides for extrapolation to the edge of the image.)
- harnessing and damping factors.

A synthetic scan line is defined in the collateral image by connecting the match points in strips i and i + 1 with straight line segments, as well as by completing straight line extrapolations from the outside strips to the edges of the image (Figure 2-2). Bridging is completed with an appropriate

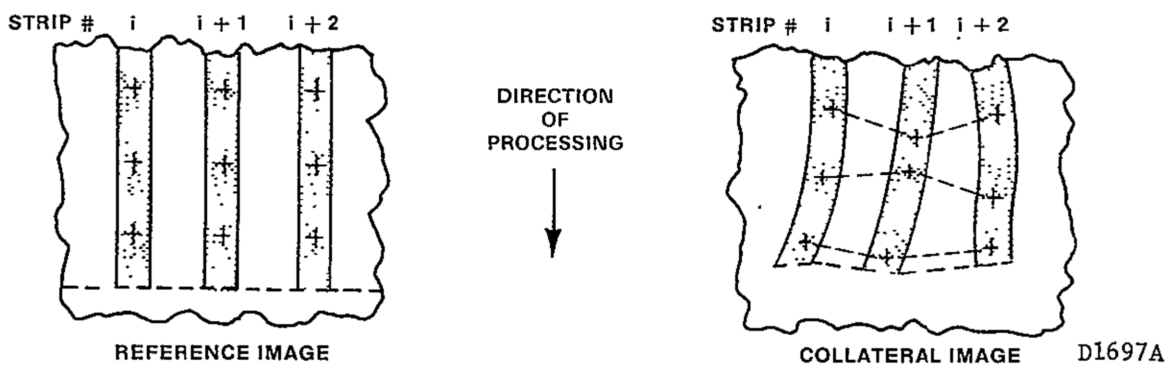


Figure 2-2. Bridging Between Strips

resampling technique, such as nearest neighbor selection, 4 point bilinear interpolation, or $\frac{\sin x}{x}$ interpolation. In this manner a new synthetic scan line is generated from the collateral image to register with the current reference image scan line.

The foregoing process is accomplished with the concept of a numerical scanner (Figure 2-3). The current reference image scan line data (K pixels)

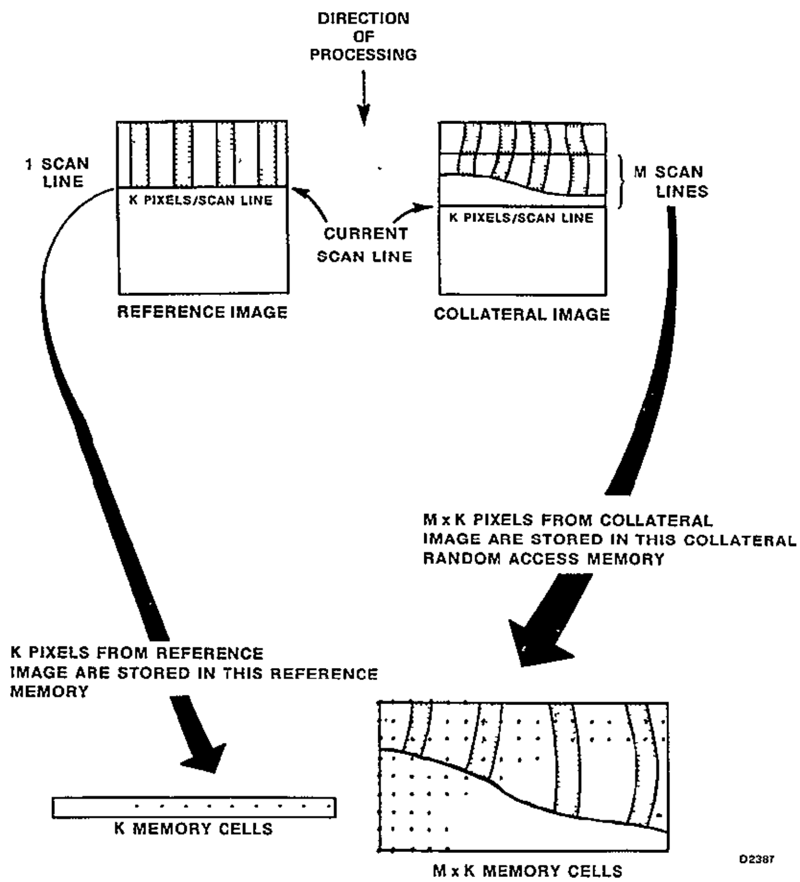


Figure 2-3. Numerical Scanner Concept

is stored until the synthetic collateral image scan line has been computed. The latter is read from a random access memory (M by K pixels) where data for M scan lines is stored. This collateral image window is maintained so that the synthetic scan line data is approximately centered (Figure 2-4). The numerical scanner memory is updated with each scan of the collateral image, while the oldest line is dropped.

In some applications, e.g., change detection, it is desired that the collateral radiometric values be adjusted to match the reference image values. In program TRAK radiometric corrections are made upon the collateral data as the synthetic scan line is read from the buffer memory. Two options, photo-

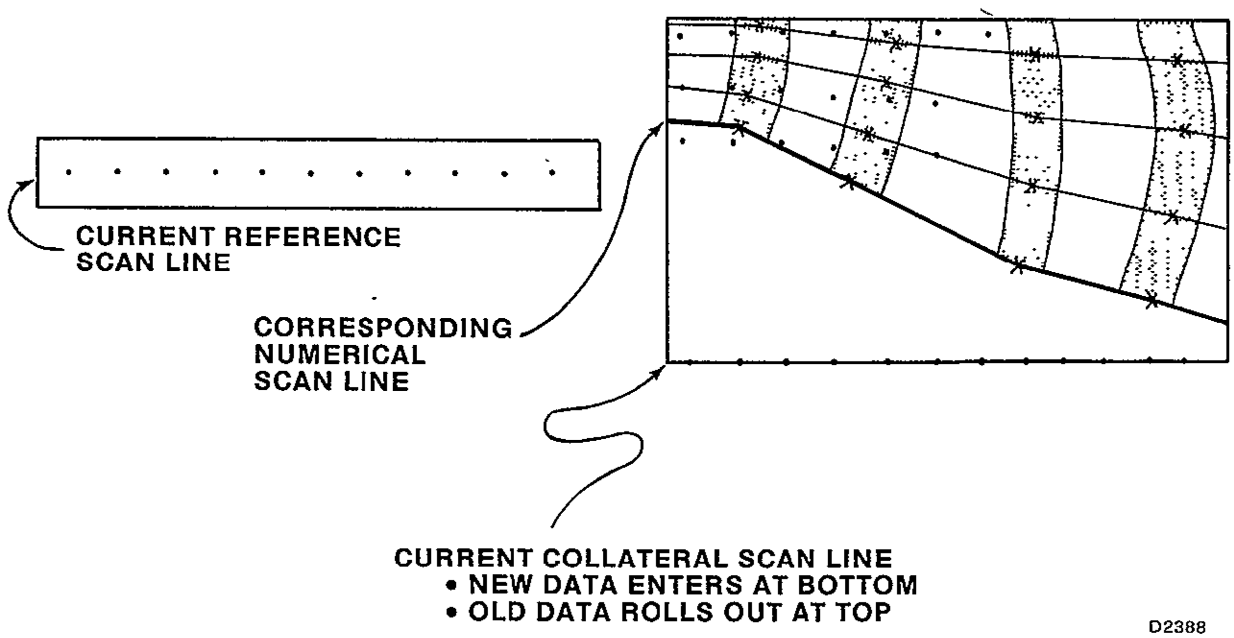


Figure 2-4. Numerical Scan Line

normalization and photoequalization, are available.

With the completion of the foregoing steps the geometric coordinates of the reference and collateral data coincide, and the radiometric values of the two images match statistically.

The above process can be adapted to the particular image characteristics through individual damping of the geometric and radiometric corrective processes. Smoothing of the geometric corrective process is influenced by an exponential decay constant which defines the effective length of the correlation area (patch) for each correlation strip. The effective length of this smoothing and the width of the correlation strip establish the size of the effective correlation patch. As the effective correlation patch is made larger the spatial corrective process becomes more sluggish. Each synthetic scan line is defined through the use of a feedback error signal which corrects the previous estimate of matched locations. Additional smoothing of the warping or registration process is obtained by applying a prescribed fraction of the indicated error. A harness coupling between strips and a two dimensional global warp guide the process through regions where correlation with some strips is low.

Individual accumulators are provided for the computation of spatial correlation and radiometric correction; hence, the damping characteristics for these two processes can be different. Radiometric correction can be decoupled when it is desired to register two images without changing radiometric information. It is important to note that radiometric values in the collateral image will be degraded when radiometric corrections are made on the basis of comparison with the reference image.

As noted above the TRAK process can statistically transform the radiometric values of the collateral image to match those of the reference image by photonormalization or photoequalization. These techniques are particularly useful in matching background detail where systematic errors may have generated different tonal characteristics. Important applications of these techniques, for example, are change detection and photomosaic generation.

The two procedures for radiometric correction differ in the method of computing a radiometric transformation within each correlation strip. However, both methods use a four point linear interpolation to compute the new radiometric value for each pixel position on the given synthetic scan line between correlation strips.

The photonormalization process generates a radiometric transformation by fitting a linear regression line to the joint distribution of radiometric values within the correlation patch (Figure 2-5). The adjusted radiometric values $G_c$ of the collateral image are given by

$$G_c = a_0 + a_1 g_c$$

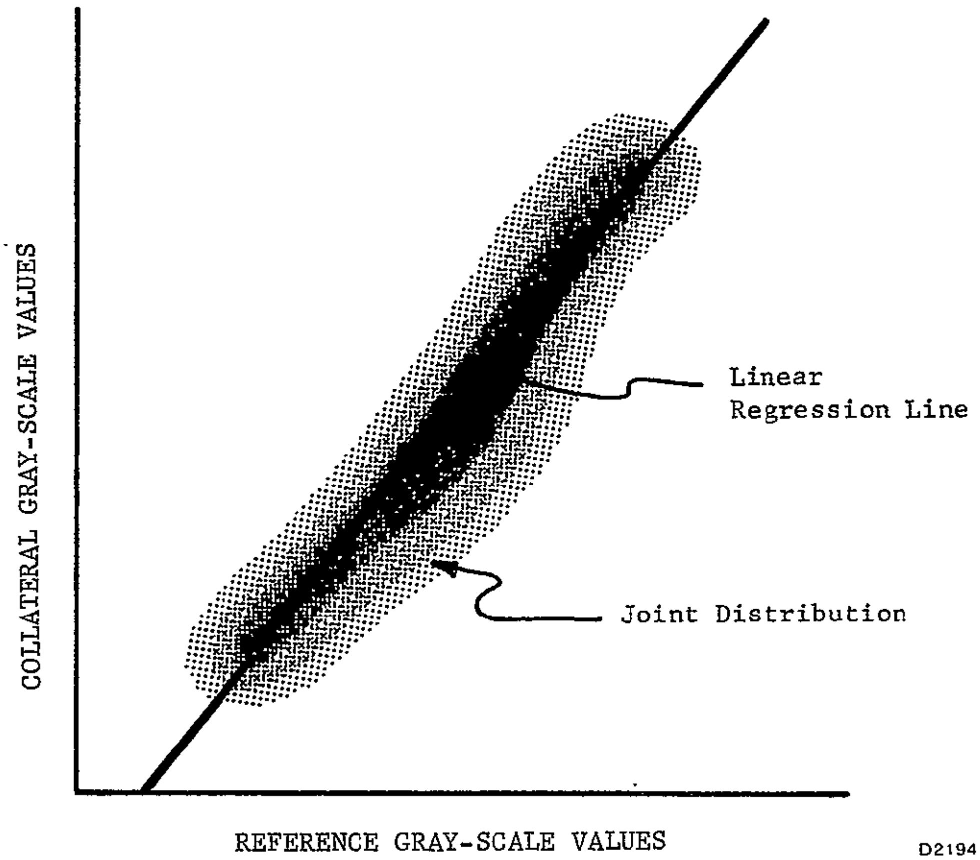


Figure 2-5. Linear Regression Line for Photonormalization

where $g_c$ equals the measured radiometric value. The coefficients $(a_0, a_1)$ are computed from the statistical moments to the second order, assuming approximately gaussian distribution, with the relationship

$$\frac{g_r - \mu_r}{\sigma_r} = \frac{g_c - \mu_c}{\sigma_c}$$

where $g_r$ = radiometric values of the reference image

$g_c$ = radiometric values of the collateral image

$\mu_r$ = average radiometric value of the reference image

$\mu_c$ = average radiometric value of the collateral image

$\sigma_r$ = standard deviation of radiometric values in the reference image

$\sigma_c$ = standard deviation of radiometric values in the collateral image

These moments are available from the correlation process.

In the photoequalization process cumulative distributions of the radiometric values are retained for each correlation strip in the reference and collateral images. Correction is based entirely upon these cumulative distributions; hence, there is no dependence upon the correlation process. The photoequalization process is a mapping of radiometric values from the cumulative collateral distribution to the cumulative reference distribution (Figure 2-6). This process is depicted graphically for two collateral values $g_1$ and $g_2$ which are transformed to values $g_1'$ and $g_2'$. This transformation process

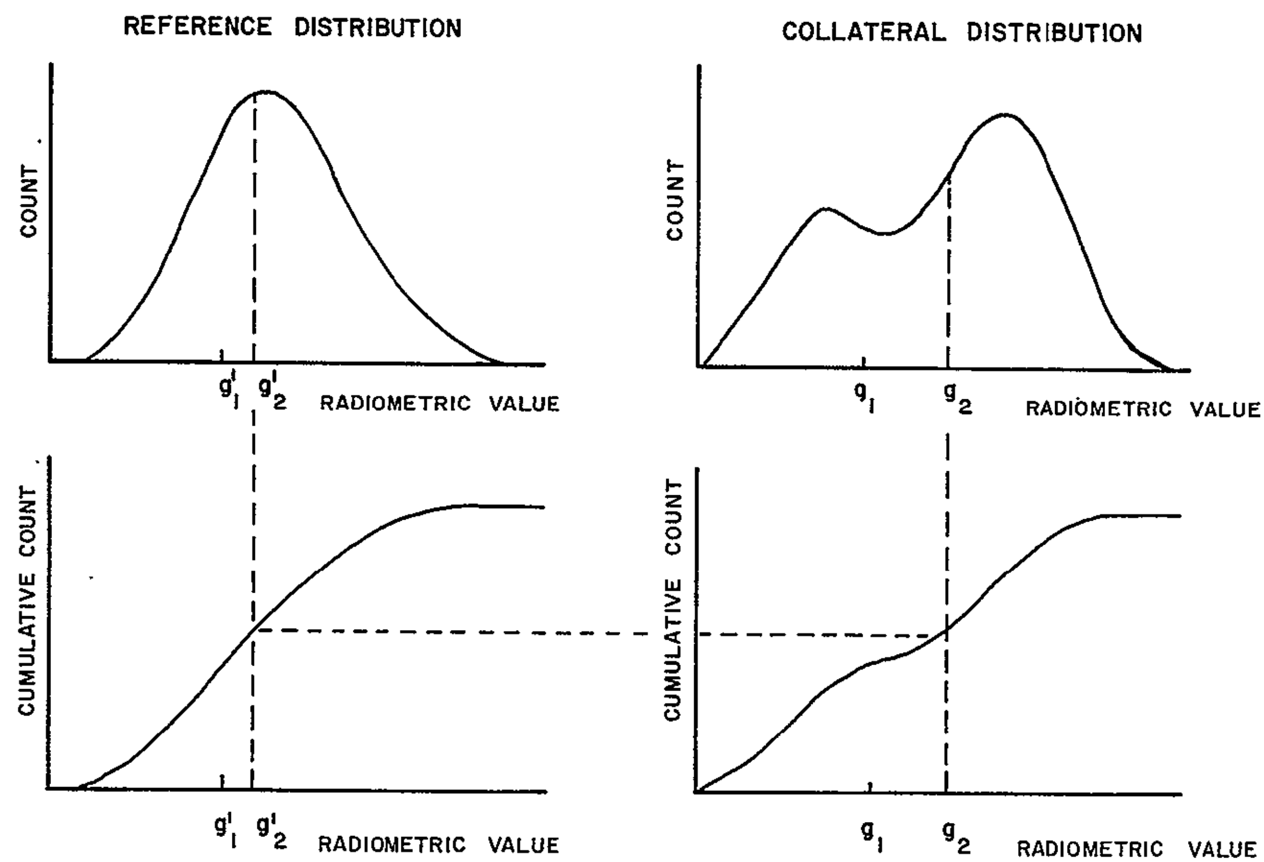


Figure 2-6. Photoequalization

is easily implemented with the use of a look-up table representing the transformation from the collateral cumulative distribution function to the reference cumulative distribution.

## 2.2 Input Control

Four kinds of input control are provided to the TRAK program:

- Identification - Identification is read from the first data card and is used as a heading label on all output.
- Parameters - Parameter data defines process control.
- Registration - Registration data defines conjugate points in the reference and collateral images. This data is used to minimize start-up transients.
- Strip Location - Strip location data defines the start-up location for each correlation strip. The program first distributes the specified number of correlation strips across the specified image width. Then individual strips are relocated to their nearest respective specified strip location.

Default values are automatically assigned when control data is not supplied by the operator. For example, default strip positioning provides uniform distribution of strips across the image. Default registration specifies no warp.

A total of 25 parameters are currently employed in the TRAK process. Proper selection of these parameters makes possible effective registration and photocorrection of imagery of many types and quality. A brief description of each parameter follows.

Scan Line Length (NP). This parameter determines the length of the records which are buffered in from the input files for both the reference and collateral image. It need not match the record length. However, if it is greater than the number of image characters in a record on either input file it is reduced to the size of the shortest record on either input. Processing time is directly proportional to the length of the input record.

Strip Width (MV). The strip width is chosen such that a square window with sides equal to the intended strip width will generally span identifiable features on both the reference and collateral image. Strip width choices less than 100 have no effect on the running time; however, widths greater than 200 increase the process time. This increase depends upon the number of strips.

Number of Strips (NCP). The number of strips is chosen on the basis of anticipated warp complexity and on the required redundance in control regions to insure good correlation in half of the strips. As strip width is increased the number of strips has an increasing effect on process time.

Radiometric Correction Option (NOR). This option allows the operator the choice of making or not making radiometric corrections. Enabling the radiometric correction approximately doubles the total process time on typical images.

Radiometric Smoothing Length (RDMP). This parameter controls the extent of image area over which radiometric smoothing is effected. A typical value is 200 for aerial photography and side-looking radar imagery when the equivalent ground resolution of the digitized image is in the range of 2 to 20 feet. A rule of thumb is to set this parameter equal to 4 to 6 times the strip width. If the radiometric smoothing length is large there may be a noticeable start-up transient in the radiometric corrections depending upon image correlation.

Radiometric Correction Type (NRO). This parameter enables the user to choose either the photonormalization or photoequalization correction.

X-Axis Damping and Y-Axis Damping (XDMP, YDMP). These parameters define the response distance of the spatial warp correction process in the X (perpendicular to scan line) and Y (parallel to scan line) directions.

Airborne line scanners, such as SLR, infrared and multispectral scanners, may have very complicated warps requiring 10 to 50 pixels (or lines) of damping. If large damping values are used then good registration data is required to diminish the start-up transient. (See RESTART technique).

Global Warp Control (HRN). Several forms of interstrip coupling are provided to guide strips through areas of low correlation. These methods are listed together with their code names in the following table:

| HRN | COUPLING |
|---|---|
| -1 | No coupling |
| 0 | Constrained, Y-axis only |
| 1 | Hard coupled, Y-axis only |
| 2 | Constrained, X and Y axis |
| 3 | Hard Coupled, X and Y axis |
| 4 | Constrained, X and Y axis (Match points used) |

In the hard coupled technique all strip positions are weighted by the correlation at that position and fitted with a least square polynomial. The order of the polynomial is defined by the Y-axis order of global fit.

Constrained harness coupling allows each strip to be independent provided a strip finds maximum correlation within the Harness Deviation Tolerance. This tolerance defines a circular error region about a center determined by the Y-axis fit polynomial. Under these controls the correlation strip is guided to within the circular error of global fit, and the correlation process directs the location of the strip to the point of best match within this area. Constrained option 4 involves another dimension in that strip locations are guided by initial match points in addition to the correlation process.

It has been found that two dimensional control tends to be more universally capable of process control than the one dimensional control. Fixed coupling has proven to be less accurate as a general rule.

Y-Axis Order of Global Fit (HRNO). This parameter establishes the order of a one dimensional polynomial along the Y-axis and operates in conjunction with the global warp control. The selected order should be as low as possible, typically 1 and rarely over 2. This polynomial can be fit to known distortions in the Y-axis. When a constrained harness coupling is used the Y-axis fit polynomial defines the center of the Harness Deviation Tolerance zone.

When the global fit is smoothed over a large area it is not subject to local transients as an individual strip is. Global control of this type provides the means to guide a strip through transient areas based upon the performance of the remaining strips.

X-Axis Order of Global Fit (HRND). This parameter defines a recursive smoothing of the coefficients for the Y-axis order of global fit along the X-axis. Thus it operates in conjunction with the Global Warp Control, the Y-axis Order of Global Fit, and the Harness Deviation Tolerance. The smoothing distance is generally selected to be 3 to 6 times the X-axis damping distance.

Harness Deviation Tolerance (VLIM). This is a circular error tolerance (VLIM) of the global fit approximation. It should not exceed the correlation distance of the imagery.

Satellite Correlation Site Separation (STEP). This parameter specifies the distance ahead of the reference scan line that the predicted synthetic scan line is generated. Correlations are determined at this interval (correlation patch separation) and scan predictions are accordingly corrected. Current options limit site separation ranging from 1 to 7 lines.

Pixel Density Determinator (INTP). This parameter selects one of three interpolation processes. These are nearest neighbor, 4 point bilinear, and sin x/x resampling.

First Record (NFST). The first Record parameter specifies the record at which processing is to begin. Prior records are transcribed from the reference and written ahead of the first process record in the output to maintain registration between the output image and the reference image.

If a match to the selected first record cannot be found in the collateral image file, then the first record is increased until the entire match may be found. Thus, this parameter might be increased automatically based upon the input registration data provided. It is never decreased.

Number of Records (NREC). This parameter specifies the number of records to be processed, beginning with the start line. If an End of File is encountered on either file before the number of records is satisfied the process will go to the End of File.

Auxiliary Output (NSKP). This option provides for selecting either of two output formats: (1) synthetic output image and record count or (2) header information, synthetic image, reference image, record count, and miscellaneous array data.

Output Interval (LJ). This parameter specifies the frequency of output on the printer and punch. During the start-up, output is provided for every 5 lines until the line number equal to the output interval is reached. After that point output is at the prescribed interval.

Punch Control (IPUN). This option selects punch output for the following data for each strip: (1) Reference image record, (2) Strip position in the reference record, (3) Matching X position in the collateral source file, (4) Matching Y position in the collateral source file, and (5) Central correlation coefficient.

Reference Maximum (RMAX). This parameter controls a program which in one mode continually searches for the maximum gray-scale value in the reference image for the purpose of detecting saturation and excluding those values from the computation of statistical moments. Accordingly those values have no effect upon the correlation and radiometric correction processes.

In another mode the user can specify a threshold from 0 to 63 (assuming 6 bit data) which will exclude pixel data at greater values from the computation of statistical moments. Thus the user can arbitrarily exclude certain image features, such as clouds, from the correlation and radiometric correction process. Alternatively, the process can be disabled.

Reference Minimum (RMIN). This parameter relates to saturation at minimum values in the same manner as the Reference Maximum parameter relates to saturation at maximum values. The user can specify a threshold from 0 to 63 which excludes values below the threshold from the computation of statistical moments.

Collateral Maximum (CMAX). This parameter serves the same function in the collateral image as the Reference Maximum serves in the reference image.

Collateral Minimum (CMIN). This parameter serves the same function in the collateral image as the Reference Minimum serves in the reference image.

Resampling Points (NPTS). This parameter specifies how many points will be used in the X and Y direction for sin $\Delta X/\Delta X$ sin $\Delta Y/\Delta Y$.

Mode Shape (MODE). This parameter specifies the range in multiples of $\pi$ for the resampling points.

## 3.0 EXPERIMENTAL INVESTIGATION

The intent of this investigation is to demonstrate the existent capabilities of the TRAK registration process in regard to registering LANDSAT imagery [5,6]. Therefore, emphasis was placed upon routine processing of a variety of image samples and analyzing the performance of the registration and interpolation process. Thus, little actual technique development was undertaken.

### 3.1 Description of Image Data

Three sets of LANDSAT multispectral scanner data were supplied for this investigation by the Goddard Space Flight Center (GSFC). The portions of these data sets that were processed are identified as Scenes A, B, C, and D, with the latter two extracted from the third set of data (TABLE 3-1). One fourth of a LANDSAT (ERTS) scene was supplied in each case, and the portion supplied is identified by frame quarter number.

The data is further identified as Reference or Collateral according to its role in the registration process. Collateral data was spatially transformed (warped) to register with the Reference data.

Data was supplied in the form of LANDSAT MSS computer compatible tapes (CCT) complete with Bands 4, 5, 6, and 7. The data was radiometrically calibrated, adjusted for scan line length, and formatted on 9 track, 800 BPI tape at GSFC.

Each of the three quarter frames represents unique sites with considerably different feature characteristics. Scenes C and D also represent distinctly different feature content ranging from fields to mountainous terrain.

### 3.2 Processing Procedures

All processing procedures were totally digital with the exception of

TABLE 3-1. MULTISPECTRAL SCANNER IMAGERY
ERTS-1 SATELLITE

| SCENE | PROCESS FUNCTION | IDENTIFICATION | DATE | FRAME QUARTER |
|---|---|---|---|---|
| A | Reference<br>Collateral | E-1393-17383<br>E-1411-17381 | 28 Aug 1973<br>7 Sept 1973 | 3 |
| B | Reference<br>Collateral | E-1170-05023<br>E-1224-05030 | 9 Jan 1973<br>4 Mar 1973 | 2 |
| C | Reference<br>Collateral | E-1703-17590<br>E-1739-17575 | 26 June 1974<br>1 Aug 1974 | 2 |
| D | Reference<br>Collateral | E-1703-17590<br>E-1739-17575 | 26 June 1974<br>1 Aug 1974 | 4 |

photographic processing of visual data products. These procedures include conversion of data to Control Data formats, registration of scene pairs with Program TRAK, evaluation, and preparation of visual image products.

### 3.2.1 Data Conversion

Program TRAK is written to accept two image files with data encoded to 6 bits. Each scan line of a given image file is represented by one continuous record. Conversion to this format from the LANDSAT bulk format [7] was done with Program CONBLK on a Control Data 6600 computer.

CONBLK converts the 8-bit interleaved format into four files of 6 bit radiance values, where the four files contain the data bands 4, 5, 6, and 7, respectively (Figure 3-1). In this form the desired image pairs are conveniently selected by the operator for subsequent correlation and registration processing.

ORIGINAL PAGE IS
OF POOR QUALITY

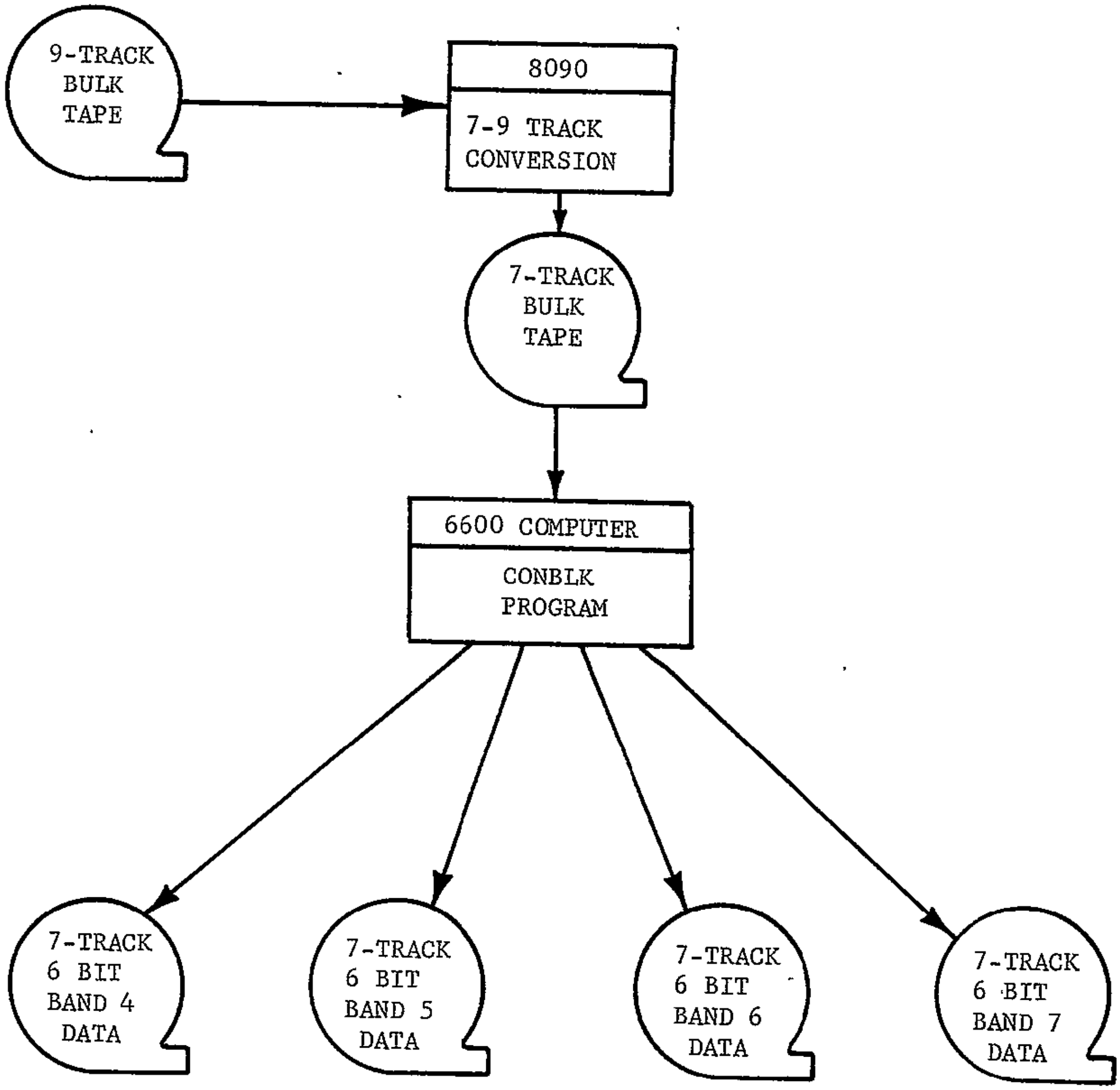


Figure 3-1. Conversion of LANDSAT Data Format

Prior to further processing a visual image of each file is prepared with an Optronics Photowrite Model P1500. This image is used for visual evaluation and for manual measurement of start-up registration points.

### 3.2.2 Registration Processing

All registration processing was done with Program TRAK on a Control Data

6600 computer. As described in Section 2.0 this is a fully automatic registration process which is dependent upon cross correlation of the two images.

A major objective of this program is to demonstrate and analyze the performance of the TRAK process on a variety of scene characteristics, including spectral effects and temporal changes. Three descriptors are defined to describe band and image relationships:

- Intrascene - different spectral bands obtained on the same pass.
- Autoband - same spectral bands for images obtained on different passes.
- Interband - different spectral bands for images obtained on different passes.

Image registration is reported for two modes of operation of the TRAK program. In the first mode, TRAK registration is obtained with fixed parameters which are preselected by the operator. In the second mode three process dependent techniques, AUTODAMP, AUTOVLIM, and RESTART, are incorporated in Program TRAK to allow the registration process to adapt to image features.

AUTODAMP is a method whereby automatic adjustment of the servo decay constants is effected for both geometric coordinate directions. It adjusts the effective correlation area and determines what fraction of the servo error will be applied in addressing the synthetic scan line. Thus, AUTODAMP determines the rate at which registration displacements are corrected, and this is done as a function of measured qualities of the imagery.

A harnessing feature controls the process in correlation strips which lack image structural detail. In such strips the process is constrained to locate a match point within a circular area of tolerance VLIM, the location of which is influenced by the coordinates of match points in adjacent correlation paths. AUTOVLIM automatically adjusts the diameter of this circle of tolerance in accordance with processor evaluation of the image characteristics and performance of the TRAK process. Thus, this parameter may influence the incremental correction that is made in addressing the synthetic scan line.

RESTART is an automatic procedure which allows the system to derive control point coordinates over a portion of the image and to restart the process utilizing this new control point information as initial estimates. Selection of these registration points is based upon the following criteria:

- central correlation tolerance
- servo error tolerance

By this technique excellent registration is efficiently obtained over the entire image, thus avoiding transient misregistration which may otherwise occur over the first 50 to 150 scan lines.

All four scenes were processed with the automatic process control features AUTODAMP, AUTOVLIM, and RESTART. Nearest neighbor interpolation was used in these runs. In addition, Scenes A and B were also registered with fixed parameter processing and with three resampling techniques. These were nearest neighbor, 4-point bilinear and sin x/x resampling.

The choice of an appropriate resampling technique is a trade-off involving the incremental overlap in original digitization, desired geometric and radiometric fidelity, and processing speed (or cost).

## 3.3 Evaluation Techniques

The quality of the registration process is analyzed with three evaluation techniques. The first of these methods, Program DIFF, creates a tonal subtraction image which reveals radiometric differences and misregistration pictorially. The second method is an independent correlation procedure known as Warp Error Check (WECK) which measures the mean radial displacement error. The third method, Program DEGRAD, measures the difference of the radiometric values of the original image and the warped image over selected areas.

### 3.3.1 Program DIFF

Program DIFF generates a tonal subtraction image by subtracting the radiometric values of each sample element in the collateral image from the radiometric values of the conjugate elements in the reference image. In order that these values will fall within the same positive range of values in which the reference and collateral data are found the difference is written:

$$\text{DIFFERENCE}_{ij} = \frac{\text{REFERENCE RADIANCE}_{ij} - \text{COLLATERAL RADIANCE}_{ij}}{2} + 31$$

where i = line count
j = pixel count within each line.

The above equation corresponds to a total radiance range of 64 values (6 bits).

If the two images are identical radiometrically and geometrically a uniform gray value exists across the entire difference image. With misregistration, however, black and white ghosting of feature detail will be apparent. Also, of course, real differences in radiance values will be apparent.

This technique is particularly useful in demonstrating misregistration greater than 1 pixel. For images which are very similar and very closely registered the difference image technique can be made more sensitive by increasing the tonal contrast in the vicinity of the neutral level (31).

Program DIFF reads all inputs from a preamble record on the warped collateral tape. The output consists of basic statistics and histograms for the reference, collateral and difference images.

### 3.3.2 Warp Error Check (WECK)

Program WECK measures the radial displacement between two similar images at a predetermined number of locations. This is done in the following way.

Subregions are defined in the reference image and cross correlation of the radiance values is computed with similar subregions at trial locations in the collateral image (Figure 3-2). At each trial location correlation coefficients are computed at five sites (center, forward, backward, left, and right). A parabolic fit is performed to locate the coordinates of maximum correlation, and the incremental displacement is computed. The magnitude of the maximum correlation coefficient is compared with an assigned threshold value to establish a confidence level.

WECK error analysis conveniently provides an abundance of statistical data comparing two images, and the use of cross correlation provides a very sensitive measure. It must be remembered, however, that the results are influenced by the size of subregions, and the statistical significance of the results is limited by the number of evaluated subregions.

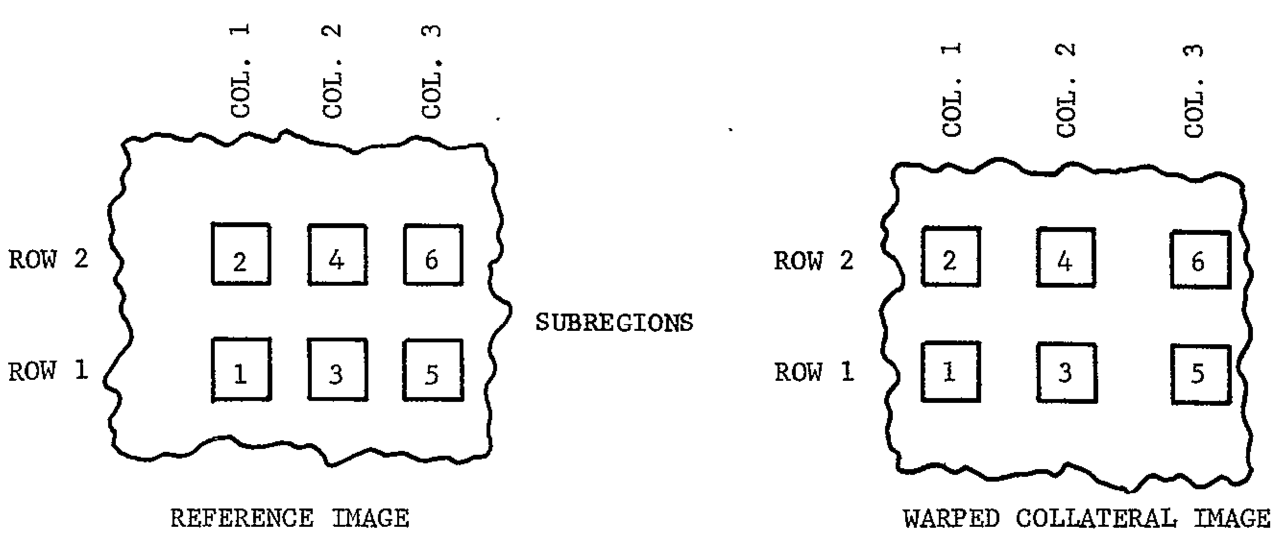


Figure 3-2. WECK Subregions

Program WECK generates a summary edit which includes residual displacements, correlation coefficients, mean displacements, and standard deviations from mean displacements (TABLE 3-2). Additionally, an overall summary provides the mean and root-mean-square displacement error, as well as the standard deviation of displacements from the mean.

Input parameters for Program WECK are described as follows:

Scan Line Length (NY). This parameter dictates the length of records which are buffered in from the input files.

Patch Size (NB). This parameter specifies the number of pixels in each subregion.

Number of Searches (MCST). This parameter is the maximum number of random walks to find the peak correlation around the control site within a particular subregion.

Correlation Threshold (CORREJ). The minimum correlation coefficient for good data (i.e. correlation confidence trail). A value of 0.45 appears to give a sufficient sampling for normal data.

First Column Location (LFC). LFC is a position parameter to locate the first subregion in the X direction.

Last Column Location (LLC). LLC is a position parameter to locate the last subregion in the X direction.

Number of Columns (NC). NC is the total number of columns including the first and last columns.

First Row Location (LFR). LFR is a position parameter to locate the first subregion in the Y direction.

Last Row Location (LLR). LLR is a position parameter to locate the last subregion in the Y direction.

Number of Rows (NW). NW is the total number of rows or sites across the trace including the first and last rows.

TABLE 3-2. WECK SUBREGION EDITS

| PARAMETER | DESCRIPTION |
|---|---|
| REF X | The X coordinate in the reference image at which the entries in the remaining columns were computed. X is measured perpendicular to the scan line. |
| REF Y | The Y coordinate in the reference at which the entries in the remaining columns were computed. REF X and REF Y are defined by the input sample matrix. Y is measured along the scan line. |
| COL X | The Y coordinate in the collateral image of the pixel which corresponds to the pixel at (REF X, REF Y) in the reference image. |
| COL Y | The Y coordinate in the collateral image associated with the point defined for COL X. |
| DX | The algebraic difference between COL X and REF X. |
| DY | The algebraic difference between COL Y and REF Y. |
| DR | The vector sum of DX and DY, otherwise known as the radial distance between the points. $DR = \sqrt{DX \cdot DX + DY \cdot DY}$ |
| CORL | The peak correlation value found between the two images at the above specified coordinates. |
| UX | The mean value of the reference image over the patch specified at the reference coordinates. |
| UY | The mean value of the collateral image over the patch specified at the collateral coordinates. |
| SIG X | The standard deviation over the area defined in UX. |
| SIG Y | The standard deviation over the area defined in UY. |

### 3.3.3 Program DEGRAD

Degradation of radiance values may occur as a result of resampling during the registration process. For example, nearest neighbor interpolation may result in pixel values being displaced as much as one-half pixel spacing.

Therefore, neither radiometric nor geometric accuracy is preserved to sub-pixel accuracy. Four-point bilinear interpolation preserves geometric accuracy, but radiometric values are degraded by the smoothing properties of this interpolation technique. An improvement over these two methods is two dimensional sin x/x resampling which is capable of maintaining both radiometric and geometric fidelity.

Program DEGRAD analyzes radiometric degradation by computing statistics on the difference in radiometric values at conjugate locations in the original (raw) image and warped image. The analysis is performed over selected sub-regions of the original and warped data, and output image products include the warped collateral, original collateral, tonal difference, and a three-level difference image (Figure 3-3). The latter image was produced with thresholds set at $\pm 1$ radiometric unit relative to the neutral level to emphasize any conjugate pixels differing by more than 1 radiometric unit.

An area parameter defines a small square subregion in the warped collateral image that is to be analyzed. Program DEGRAD then locates the conjugate position of this subregion in the original collateral utilizing offset data

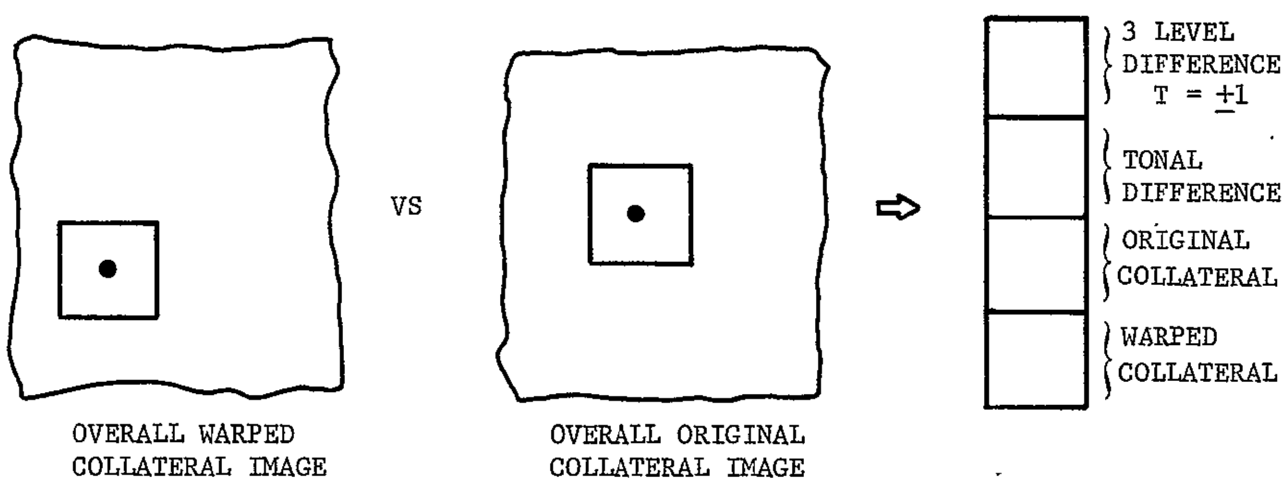


Figure 3-3. Program DEGRAD Image Products

from the registration process. Coordinates in the original collateral image are the sum of the warped collateral coordinates and the known offsets which are available from Program TRAK or by measurement of the respective image products. This analysis is currently applied to small areas with the assumption that there is negligible change in the warp function across the subregion. Hence, the same offset distance is applied to the coordinates of each pixel within this subregion.

A subtraction image is obtained by subtracting the warped collateral radiometric values from the original collateral values on a pixel-by-pixel basis. This subtraction image, when printed, provides for visual evaluation of the spatial distribution of alterations in the radiance values. Program DEGRAD also provides a quantitative evaluation by calculating the occupancy count in sequential bins or sets of these radiance differences. The procedure is described in detail in Section 5.2.

Each of the data products generated by Program DEGRAD is analyzed to provide the following statistics.

- Occupancy count in sequential sets of radiance difference values.
- Mean radiance and standard deviation for each original, warped, and difference image subregion.
- Histograms for each original, warped, and difference image subregion.
- Cross tabulation of subregions (joint distribution).
- Correlation coefficient.
- Least squares equations for regression lines through cluster of cross tabulation.

## 3.4 Implementation

As described previously TRAK registration is investigated for two modes of operation: fixed parameter and process dependent. In Section 4.0 the values of important process parameters are described as a part of the discussion of results. However, principal considerations involving the implementation of

AUTODAMP, AUTOVLIM, and RESTART are summarized in the following

These process dependent operations require the following TRAK input parameters, and values are stated in accordance with the LANDSAT data used in this investigation:

- Scan Line Length is a constant (NP = 810)
- Strip Width depends on feature size ($10 \leq MV \leq 80$)
- Number of Strips is selected to give approximately 100% coverage i.e., strips have little or no separation ($NCP \times MV \approx NP$)
- Global Warp Control is constrained in both x and y directions (NRN = 2)
- First Record (NFST) is specified
- Number of Records (NREC) is specified

The remaining parameters of the total of 25 are set to their default values.

Inital start-up is effected by assigning a straight line offset for all correlation strips to bring the process within its normal search range. For LANDSAT imagery a single translational offset in both coordinate directions is adequate. The actual initial offset values (displacement between reference and collateral images) is computed by RESTART.

Addition of AUTODAMP, AUTOVLIM, and RESTART to TRAK processing reduces the number of operator tasks. The operator's interface to automatic registration processing is depicted schematically in Figure 3-4.

## 3.5 Process Efficiency

Program TRAK is designed to automatically register two similar images and to provide output data describing a number of process parameters. Hence, it is not optimized to deliver registered data at a maximum possible speed. Nevertheless, Program TRAK operating on a Control Data 6600 computer system

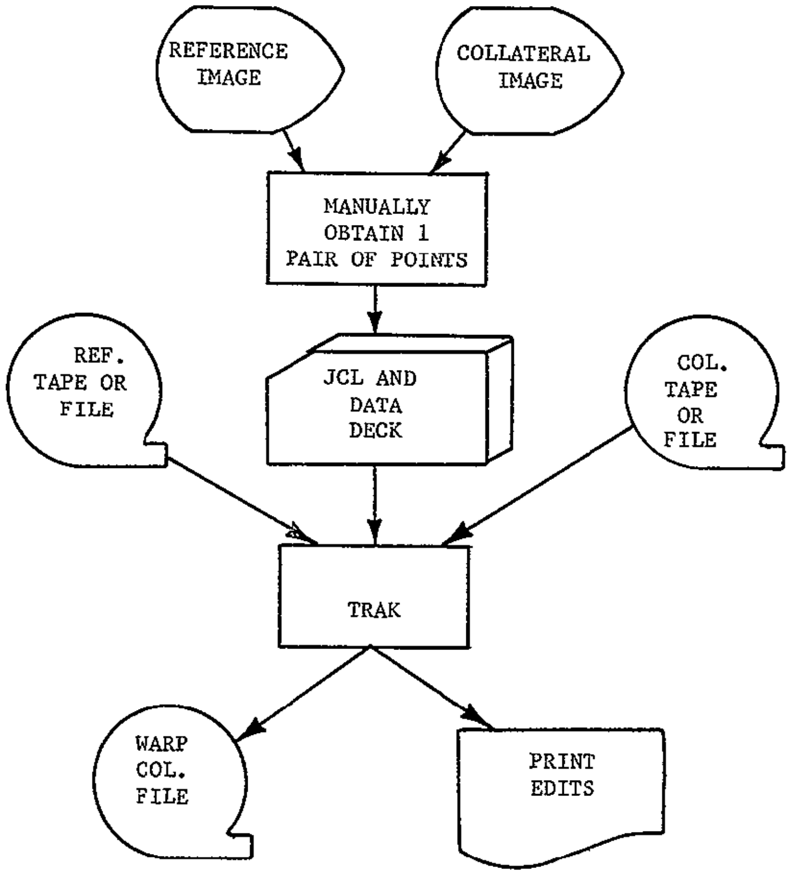


Figure 3-4. Automatic Registration Process Flow Diagram

registers data at 3000 pixels per central processor second. A summary of process times for each of the scenes which were studied is given in TABLE 3-3.

Central processor and I/O times are true process time parameters. System seconds, which includes central processor time and a portion of I/O time, is a measure of the cost of computer usage.

The amount of central memory required for execution is 104000 octal 60-bit words. All entities in TABLE 3-3 are based on image correlation in 10 strips, each 80 pixels wide, and nearest neighbor resampling. Process rates for two dimensional sin X/X, 4-point bilinear, and nearest neighbor resampling

TABLE 3-3. TRAK REGISTRATION PROCESS TIMES ON CONTROL DATA 6600 COMPUTER

• Nearest Neighbor Resampling

| SCENE | CORRELATION TYPE | SCAN LINES | PIXELS PER LINE | I/O SECONDS | CENTRAL PROCESSOR SECONDS | SYSTEM SECONDS |
|---|---|---|---|---|---|---|
| A | AUTOBAND | 722 | 810 | 435 | 183 | 299 |
| B | AUTOBAND | 722 | 400 | 249 | 176 | 243 |
| C | AUTOBAND | 722 | 810 | 623 | 185 | 351 |
| C | INTERBAND | 722 | 810 | 631 | 191 | 360 |
| C | INTRASCENE | 722 | 810 | 657 | 178 | 353 |
| D | AUTOBAND | 722 | 810 | 800 | 183 | 396 |

are summarized in TABLE 3-4.

Current technology allows the registration techniques demonstrated in this report to be accomplished at rates increased by a factor of 10 to 1000. An automatic digital change detection system using microprogrammable processors performs change detection at the rate of 830,000 pixels per second from each of two images [8]. The system performs image correlation, spatial transformation, registration, subtraction, enhancement, and feature oriented processing at 320 million instructions per second (MIPS). Such systems for production image processing are cost-effective [9].

TABLE 3-4. COMPARISON OF PROCESS RATES FOR DATA RESAMPLING TECHNIQUES

| RESAMPLING METHOD | APPROXIMATE RATE PIXELS PER SECOND* |
|---|---|
| TWO DIMENSIONAL SIN X/X RESAMPLING | 340 |
| 4-POINT BILINEAR | 2400 |
| NEAREST NEIGHBOR | 3000 |

*Pixels per central processor second

ORIGINAL PAGE IS
OF POOR QUALITY

## 4.0 REGISTRATION ACCURACIES

The TRAK automatic registration process is evaluated for four LANDSAT multispectral scanner image scenes under conditions of varying terrain, temporal changes, and spectral sensitivity of the sensor. Performance of the process as it relates to registration accuracy is discussed under the following four principal topic headings:

- Autoband Correlation, Scene A
- Autoband Correlation, Scene B
- Comparison of Autoband, Interband, and Intrascene Registration, Scene C
- Autoband Correlation, Scene D

All four scenes were registered by the TRAK process augmented with the process dependent techniques AUTODAMP, AUTOVLIM, and RESTART. Performance of the process is particularly enhanced by the RESTART procedure. However, AUTODAMP weighting factors were not properly tuned, and the result is constant damping in both coordinate directions for each image. The actual damping distance for each image was determined by the clamping value which was assigned to control the minimum distance for a given image. Scenes A and B were also processed with fixed parameters, thus providing for a comparison with process dependent techniques.

Comparison of Autoband, Interband, and Intrascene processing of Scene C provides interesting comparisons of the effect of temporal changes and spectral sensitivity of the sensor. In addition, valuable assessments are made for ultimate registration capability of the TRAK process and sensitivity of WECK error analysis.

Finally, the four scenes represent considerable variation in terrain. Scenes A and C contain much cultural development which results in rectangular tonal patterns of varying size and shape. Scene B is rather amorphous and is difficult to correlate, while Scene D is mountainous.

A major objective of this investigation is to achieve sub-pixel registration accuracy with mean radial displacement errors less than 0.25 pixel, if possible. TRAK registration reached this goal for all four scenes according to WECK error analysis which indicates mean radial displacement errors ranging from 0.14 to 0.25. A detailed description of results follows.

## 4.1 Autoband Correlation, Scene A

Scene A is an area which presents much cultural development and a considerable amount of temporal change between the two passes that are investigated (Figures 4-1 and 4-2). Process results are discussed in this section under two headings:

- Scene A Registration with Process Dependent Techniques
- Scene A Registration with Fixed Parameter Processing

In each case registration was obtained with automatic TRAK processing. The process dependent techniques are AUTODAMP, AUTOVLIM, and RESTART, and these were used with nearest neighbor resampling. Fixed parameter processing includes three resampling techniques: nearest neighbor, 4-point bilinear, and sin X/X.

The results for Scene A represent autoband registration (same band, different passes). Specifically, the collateral image is warped to register with the reference image using data from spectral band 5 for both images. Analysis includes the use of a displacement vector diagram, tonal difference image, and WECK analysis of displacement errors.

Scene A is an area measuring approximately 28 nautical miles square. The data is selected from LANDSAT frames which are identified in TABLE 3-1. The Scene A image area consists of 700 scan lines and each scan line contains 750 pixels. The north edge of the image corresponds to line 300 in the complete quarter frame that was supplied. The area is free of noise lines, has little cloud cover, and is rich in correlative features.


Figure 4-1. LANDSAT 1 Reference Image, Scene A
E-1393-17383 Quarter 3 Band 5

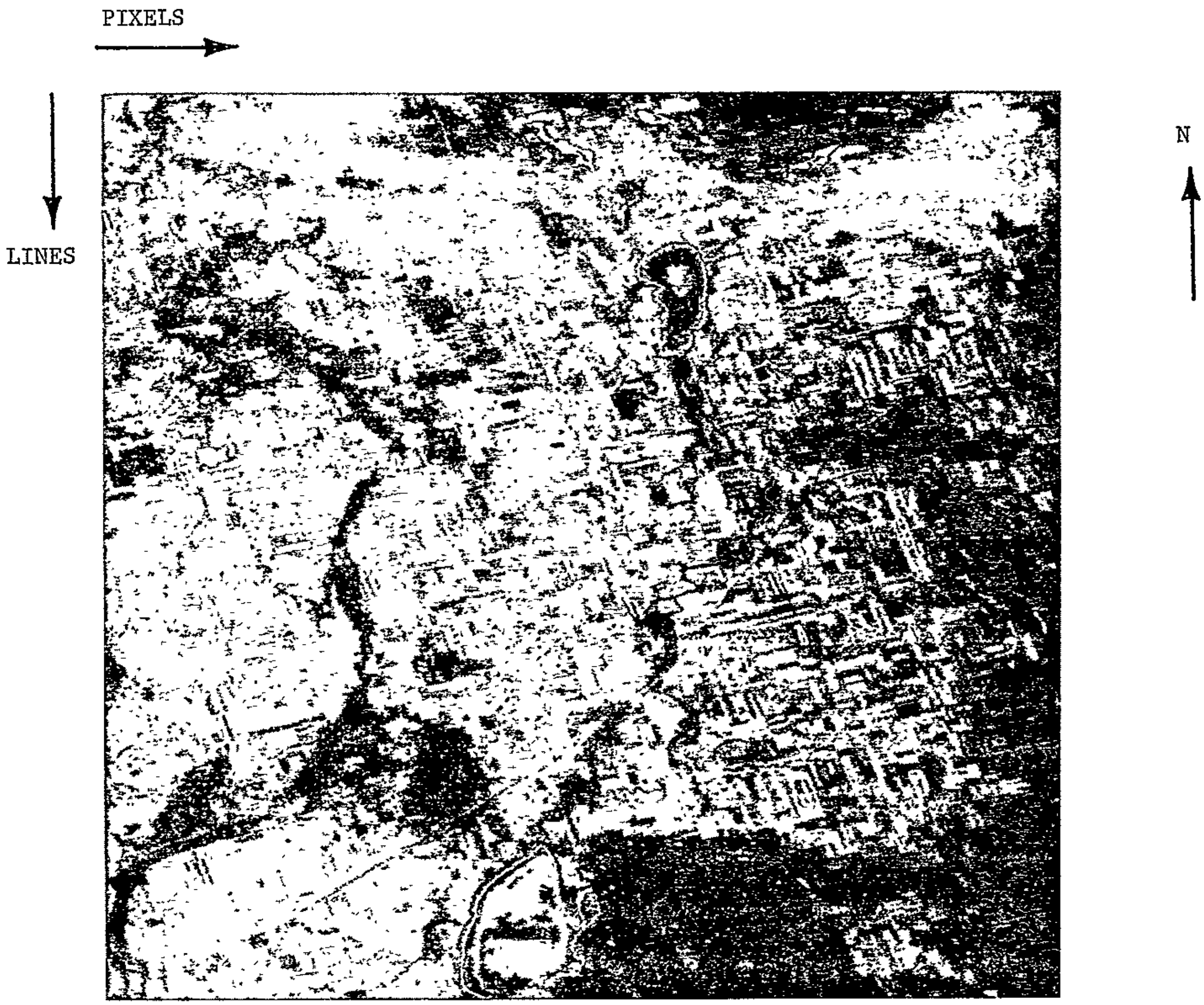


Figure 4-2. LANDSAT 1 Warped Collateral Image, Scene A
E-1411-17381 Quarter 3 Band 5
Nearest Neighbor Radiance Resampling

Each pixel in the printed image is 100 microns (4 mils) square. The scene was digitally enlarged by printing each pixel twice on a given line and repeating each line. Thus, the final image contains 4 elements for each LANDSAT pixel. This procedure is also followed in reproducing the images for Scenes C and D.

A discussion of process results for Scene A follows.

### 4.1.1 Scene A Registration with Process Dependent Techniques

Autoband correlation and registration was obtained using Program TRAK augmented with AUTODAMP, AUTOVLIM, and RESTART. Inclusion of these process dependent techniques was very effective, as will be seen from the following discussion. The results to be described in the following paragraphs are derived from the correlation of band 5 data representing the reference and collateral image pairs of Scene A (TABLE 3-1). The collateral data was spatially transformed (warped) to register with the reference image using nearest neighbor interpolation.

The process results can be visually evaluated by inspecting reproductions of the reference image, warped collateral image, and the vector displacement diagram which demonstrates the amount of warp needed to register these two images (Figures 4-1, 4-2, and 4-3, respectively). Registration is effected by a nearly uniform translation (however, a few vectors display troublesome deviations ranging from 1 to 3 pixels). The vector scale of Figure 4-3 is magnified to reveal fine details of the warp process, and large translational offsets have been subtracted to show these details. In this example for Scene A the actual vector displacement is obtained by adding 50 pixels in the positive orbital (southerly) direction. Typical transverse displacements are in the range of 10 pixels along a scan line and decrease by about 30% from north to south (left to right on the diagram).

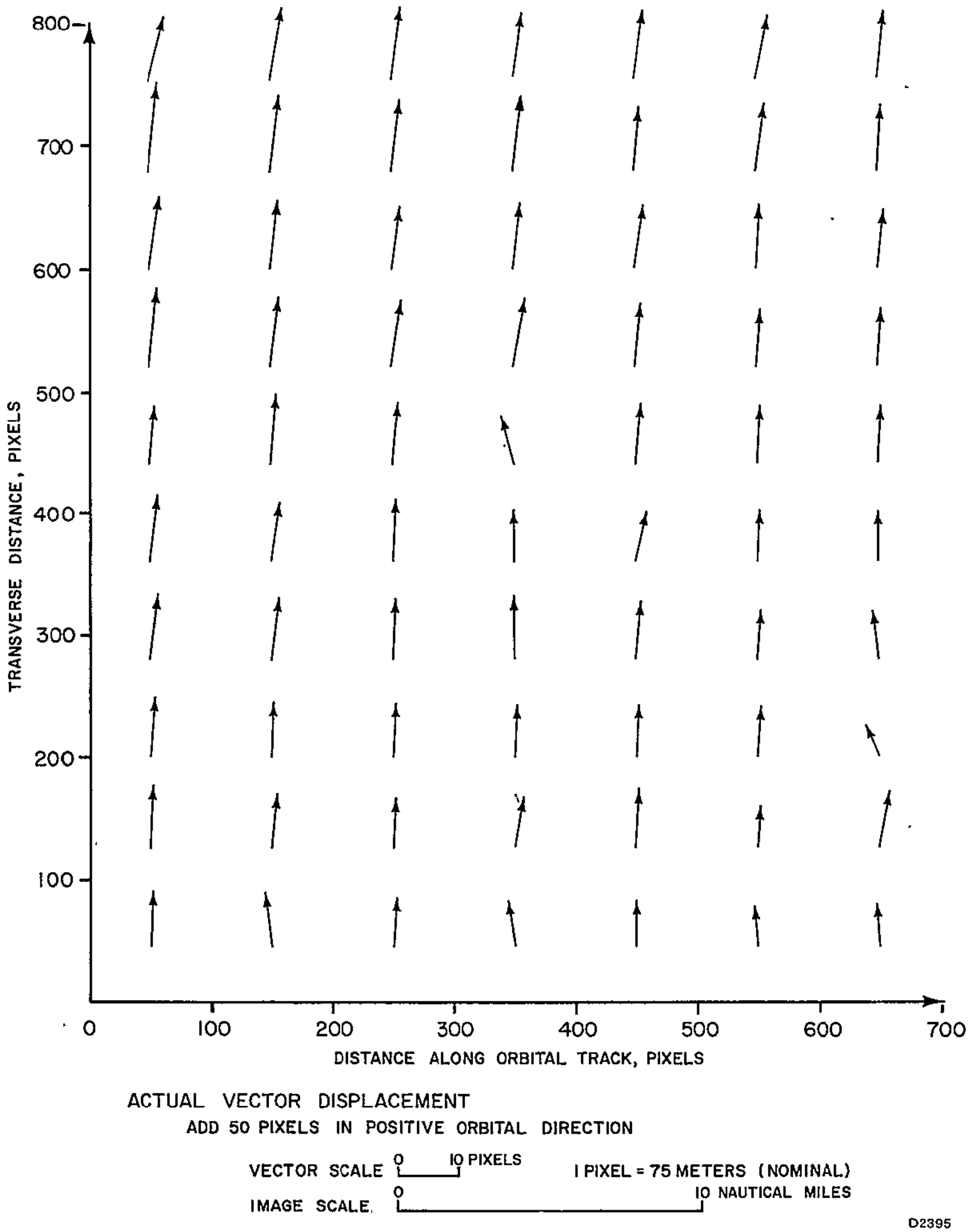


Figure 4-3. Vector Displacement Diagram
Scene A, Autoband Correlation, Band 5.

Registration was accomplished on the basis of image correlation within ten strips, each 80 pixels wide, running from north to south on the imagery. Initial global offsets along the scan line (pixel offsets in the east-west direction) varied from 8.3 to 13.2 pixels, and the scan line offset (north-south direction) varied only from 50.8 to 52.0 (TABLE 4-1). For example, for the first correlation strip this means that scan line 300 on the reference image corresponds to line 350.8 on the original collateral image and pixel 44 of this reference line corresponds to 52.3 on the original collateral line. Offsets at intermediate locations can be estimated with linear interpolation between adjacent values.

After 550 lines of processing the line offsets (X component of displacement) decreased by less than 1 line, and the pixel offsets (Y component of displacement) decreased by 2 to 2.5 pixels in a typical TRAK run (TABLE 4-2). Correlation values are highest at the central correlation site, and average 0.55 over Scene A.

TABLE 4-1. INITIAL GLOBAL OFFSETS FOR SCENE A MEASURED WITH RESTART PROCEDURE, BAND 5

| REFERENCE | | COLLATERAL | |
|---|---|---|---|
| LINE | PIXEL | LINE OFFSET | PIXEL OFFSET |
| 300 | 44 | 50.78 | 8.25 |
| 300 | 123 | 50.92 | 8.80 |
| 300 | 202 | 51.05 | 9.35 |
| 300 | 281 | 51.18 | 9.90 |
| 300 | 360 | 51.32 | 10.45 |
| 300 | 439 | 51.45 | 11.00 |
| 300 | 518 | 51.59 | 11.55 |
| 300 | 597 | 51.72 | 12.10 |
| 300 | 676 | 51.87 | 12.65 |
| 300 | 755 | 51.99 | 13.20 |

TABLE 4-2. TYPICAL TRAK EDIT FOR SCENE A

- AUTOBAND CORRELATION, BAND 5
- AUTODAMP, AUTOVLIM, AND RESTART PROCEDURES
- NEAREST NEIGHBOR RESAMPLING

| REFERENCE | | CORRELATIONS | | | | | SERVO ERRORS | | ESTIMATED WARP | | | |
|---|---|---|---|---|---|---|---|---|---|---|---|---|
| | | | | | | | | | DISPLACEMENT | | VELOCITY | |
| X LINE | Y PIXEL | CENTER | BELOW | LEFT | ABOVE | RIGHT | ΔX | ΔY | X COMPONENT PIXELS | Y COMPONENT PIXELS | X COMPONENT | Y COMPONENT |
| 849 | 44 | .726 | .672 | .631 | .737 | .690 | -.23 | -.78 | 49.710 | 6.262 | -.001 | .003 |
| 849 | 123 | .357 | .296 | .249 | .306 | .260 | -.03 | -.04 | 50.366 | 7.167 | -.000 | .003 |
| 847 | 202 | .645 | .589 | .539 | .556 | .514 | .05 | .11 | 50.283 | 8.034 | -.000 | .004 |
| 849 | 281 | .757 | .731 | .712 | .677 | .636 | .23 | .25 | 50.460 | 8.011 | -.001 | .002 |
| 849 | 360 | .636 | .578 | .573 | .581 | .541 | .10 | -.01 | 50.278 | 8.591 | -.001 | .003 |
| 849 | 440 | .617 | .581 | .589 | .561 | .553 | .20 | .11 | 50.303 | 9.584 | -.001 | .004 |
| 849 | 519 | .583 | .534 | .509 | .507 | .456 | .13 | .11 | 50.725 | 9.193 | -.001 | .002 |
| 849 | 598 | .477 | .413 | .305 | .423 | .330 | -.04 | -.04 | 50.699 | 10.383 | -.001 | .004 |
| 849 | 677 | .672 | .649 | .522 | .630 | .571 | -.10 | .15 | 51.392 | 11.243 | -.000 | .004 |
| 849 | 756 | .753 | .645 | .508 | .690 | .679 | -.27 | -.13 | 51.491 | 10.647 | -.000 | .002 |
| | | | | | | | | | | | | |
| | | | | | | | | | | | | |

Thus, the correlation surface is sufficiently well defined to maintain adequate process control. (Correlation values in columns BELOW, LEFT, ABOVE, and RIGHT are obtained at sites displaced from the estimated location of maximum correlation. Displacements above and below are in positive and negative directions along the scan line, respectively. Displacements to the right and left are in the positive and negative orbital direction, respectively.)

The servo errors, ΔX and ΔY, are corrections which must be added to the previous estimate of warp displacement. With nearest neighbor resampling the servo errors fluctuate between -0.5 and +0.5 pixel (line) over several hundred lines of processing. Small values indicate good process stability.

As stated previously this process run was made with the embodiment of AUTODAMP processing in order that spatial damping distances would be automatically adjusted to optimum values in accordance with scene characteristics. Actually, it is believed that the weighting functions for this process were not properly set, and damping distances along both coordinate directions was maintained at 7 lines. This value corresponds to a minimum limit specified in the software program.

Harnessing of the correlation strips was dynamic under control of AUTOVLIM. Harness channel widths averaged 3.79 and 4.15 in the orbital and transverse directions, respectively. Values ranged from 2.2 to 4.5 pixel.

The velocity components are the estimated spatial rates of change of the estimated warp displacement along each coordinate direction. Zero values indicate pure translation.

Satisfactory correlation and registration was obtained even though significant temporal changes are apparent in a tonal difference image created by subtracting the radiance values of the warped collateral image from the reference image on a pixel-by-pixel basis (Figure 4-4). Some ghosting is apparent in areas of little feature detail, indicating that the registration process was having difficulty in those areas. Correlation is good in the heart of the agricultural area, and the result is little ghosting there.

Registration accuracy was measured with WECK error analysis at 176 subregions, each 100 pixels square. These subregions were distributed over a 600 by 600 pixel area (lines 350 to 950, pixels 100 to 700). The mean radial displacement error between the reference and warped collateral images of Scene A with nearest neighbor resampling is 0.17.

### 4.1.2 Scene A Registration with Fixed Parameter Processing

Registration accuracy depends upon three primary factors:

ORIGINAL PAGE IS
OF POOR QUALITY



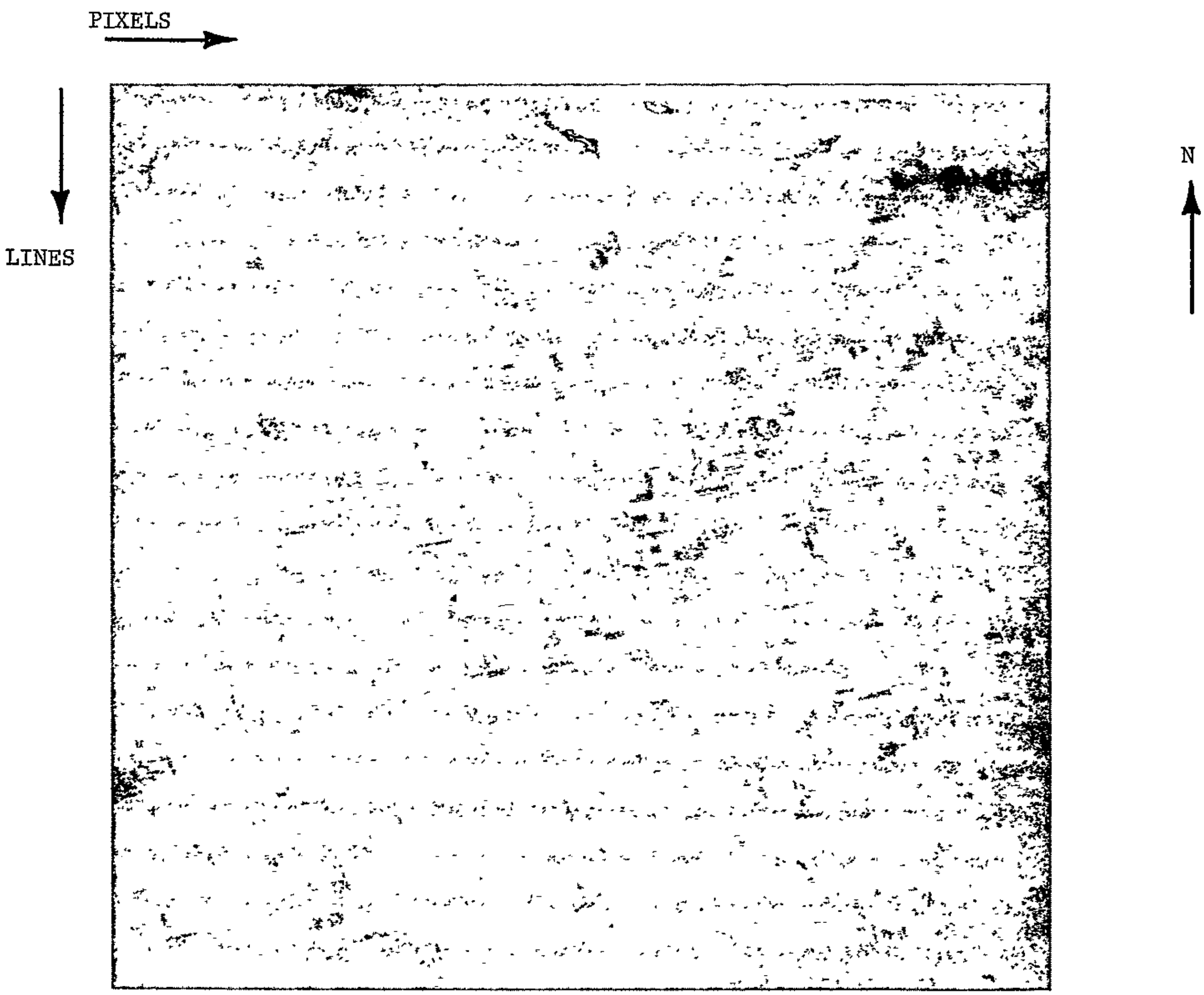


Figure 4-4. Tonal Difference Image, Scene A
Nearest Neighbor Radiance Resampling
Reference: E1393-17383 Strip 3 Band 5
Collateral: E1411-17381 Strip 3 Band 5

- accuracy with which match points are determined
- distance between match points
- interpolation technique

The accuracy of determining match point coordinates is dependent in TRAK processing primarily upon the fundamental capability of cross correlation, the effective size of the correlation subregion, servo damping, and harnessing between correlation strips. Since TRAK computes new match points for every line, the remaining accuracy factors are the spacing of correlation strips and interpolation between these strips.

The effect of these factors was investigated in autoband processing of Scene A (band 5). Interpolation between correlation strips was linear for all runs. Since sub-pixel registration accuracy is achieved it would be desirable to test curvilinear interpolation, or increase the number of correlation strips, especially where the spatial transformations are more complex. This would in general allow for better comparison of various resampling techniques, but it will be discussed that linear interpolation should be adequate for Scene A.

Process parameters were varied in a total of 21 runs, and the results were evaluated by WECK error analysis (TABLE 4-3). Other process conditions are summarized in TABLE 4-4. The parameters are defined in Section 2.

Registration accuracy was measured with WECK error analysis over a 250 by 500 pixel area which includes part of the culturally developed features (lines 425 to 675 and pixels 125 to 675). A total of 150 subregions, each 50 by 50 pixels, were used for this analysis, and typically about 105 subregions were accepted in compiling the statistics. By this analysis the smallest mean radial displacement error between the reference and warped collateral images for each resampling technique over Scene A is as follows (runs 19, 20, and 21):

| RESAMPLING TECHNIQUE | MEAN RADIAL DISPLACEMENT ERROR |
|---|---|
| • nearest neighbor | 0.31 pixel |
| • 4-point bilinear | 0.26 pixel |
| • sin X/X | 0.25 pixel |

This order of performance was repeated in runs 16, 17, and 18 where radiometric correction was operable and is believed to be correct because the warp is very simple over this region (Figure 4-3). Therefore, linear interpolation should be very nearly optimal and allow valid comparison of the resampling techniques.

TABLE 4-3. FIXED PARAMETER PROCESSING, SCENE A (BAND 5)
WECK ERROR ANALYSIS

| RUN NUMBER | INTERPOLATION (INTP) | NUMBER OF STRIPS (NCP) | HARNESS CHANNEL WIDTH (VLIM) PIXELS | DAMPING: ORBITAL (XDMP) LINES | DAMPING: TRANSVERSE (YDMP) PIXELS | RADIAL ERROR PIXELS: MEAN | RADIAL ERROR PIXELS: RMS |
|---|---|---|---|---|---|---|---|
| 1 | | | | 100 | 100 | 0.85 | 0.90 |
| 2 | | | | 125 | 100 | .61 | .65 |
| 3 | | | | 125 | 125 | .49 | .55 |
| 4 | 4-POINT | 8 | 4 | 150 | 150 | .32 | .42 |
| 5 | BILINEAR | | | 100 | 100 | .53 | .64 |
| 6 | | | | 200 | 200 | .44 | .53 |
| 7 | | | 6 | 125 | | N/A | N/A |
| 8 | SIN X/X | | | | | .36 | .48 |
| 9 | NEAREST | | 4 | | | .38 | .45 |
| 10 | NEIGHBOR | | | | | .40 | .47 |
| 11 | | | 2 | | | .27 | .34 |
| 12 | 4-POINT | | | | | .27 | .34 |
| 13 | BILINEAR | | | | | .26 | .32 |
| 14 | | | | 150 | 150 | .27 | .35 |
| 15 | | 12 | | | | .27 | .35 |
| 16 | NEAREST NEIGHBOR | | | | | .32 | .36 |
| 17 | 4-POINT BILINEAR | | 1 | | | .27 | .34 |
| 18 | SIN X/X | | | | | .24 | .32 |
| 19 | NEAREST NEIGHBOR | | | | | .31 | .35 |
| 20 | 4-POINT BILINEAR | | | | | .26 | .32 |
| 21 | SIN X/X | | | | | .25 | .32 |

TABLE 4-4. OTHER CONDITIONS FOR FIXED PARAMETER PROCESSING, SCENE A

| DESCRIPTION | VALUE OR CONDITION |
|---|---|
| SCAN LINE LENGTH (NP), RUNS 1-10<br>RUNS 11-21 | 810 PIXELS<br>750 PIXELS |
| STRIP WIDTH (MV) | 50 PIXELS |
| SATELLITE CORRELATION SITE SEPARATION (STEP) | 1 PIXEL |
| RADIOMETRIC CORRECTION (NOR)<br>RUNS 14, 16, 17, & 18 | YES |
| RADIOMETRIC SMOOTHING LENGTH (RDMP)<br>RUNS 14, 16, 17, & 18 | 200 LINES |
| RADIOMETRIC CORRECTION TYPE (NRO)<br>RUNS 14, 16, 17, & 18 | PHOTONORMALIZATION |
| GLOBAL WARP CONTROL (HRN) | CONSTRAINED ON X & Y AXIS (ADDED CONTROL POINTS, RUNS 8 & 10) |
| Y-AXIS (ALONG SCAN LINE) ORDER OF GLOBAL FIT (HRNO) | FIRST ORDER ONE DIMENSIONAL POLYNOMIAL |
| X-AXIS (ORBITAL DIRECTION) ORDER OF GLOBAL FIT (HRND)<br>RUNS 1-4,8-21<br>RUN 5<br>RUN 6<br>RUN 7 | <br><br>50 LINES<br>300 LINES<br>600 LINES<br>400 LINES |
| REFERENCE AND COLLATERAL MAXIMA (RMAX, CMAX) RUNS 3-21<br>RUNS 1-2 | 55<br>NO THRESHOLD |
| REFERENCE AND COLLATERAL MINIMA (RMIN, CMIN) RUNS 3-21<br>RUNS 1-2 | 10<br>NO THRESHOLD |
| RESAMPLING POINTS (NPTS)<br>SIN X/X ONLY | 5 each axis |
| MODE SHAPE (MODE) SIN X/X | $-2\pi$ to $+2\pi$ |

Moderately stiff damping was used in these runs with damping distances from 100 to 200 pixels (lines). Yet, excellent results were obtained. This would not be the case if the warp were considerably more complex. Optimal damping is indicated to be 150 lines for Scene A by the first 6 runs, and this value gave excellent results in the subsequent runs.

Increasing the number of strips from 8 to 12 (runs 9 and 10) had little effect on performance. Again, this is reasonable because of the simple warp function. Since the area generally abounds in correlative features, harnessing is less important, and small values of the harness channel width are effective.

## 4.2 Autoband Correlation, Scene B

Scene B (Figure 4-5) has little distinctive correlative features, except for the river, and for this reason was the most difficult of the four scenes to correlate. Still a mean radial displacement error as small as 0.25 pixel was achieved.

The area shown in Figure 4-5 consists of 350 scan lines with 400 pixels per line. The first line (north edge) is the first line of the second quarter selected from the complete frame.

Process results are discussed in this section under two headings:

- Scene B Registration with Process Dependent Techniques
- Scene B Registration with Fixed Parameter Processing

Process dependent techniques are AUTODAMP, AUTOVLIM, and RESTART, and results obtained with them are demonstrated with nearest neighbor resampling. Fixed parameter processing results include nearest neighbor, 4-point bilinear, and sin X/X resampling methods.

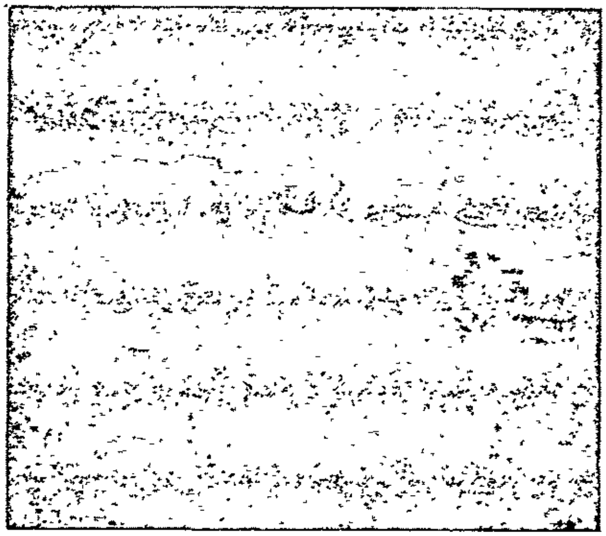

REFERENCE IMAGE

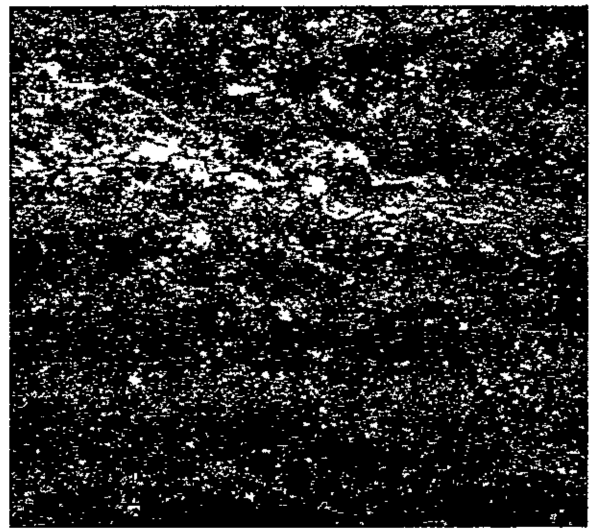

WARPED COLLATERAL IMAGE


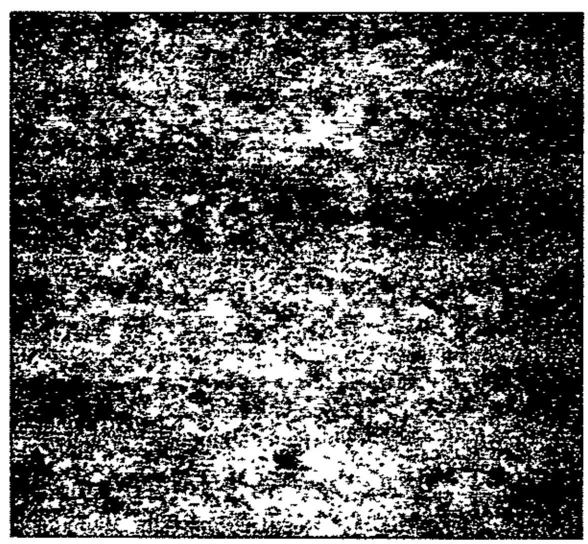

TONAL DIFFERENCE IMAGE

Figure 4-5. Nearest Neighbor Radiance Resampling, Scene B
Reference: E-1170-05012 Band 4 Quarter 2
Collateral: E-1224-05030 Band 4 Quarter 2

### 4.2.1 Scene B Registration with Process Dependent Techniques

The reference and collateral images of Scene B were registered with Program TRAK augmented with AUTODAMP, AUTOVLIM, and RESTART. Cross correlation was performed with band 4 (0.5 to 0.6 micron) data and nearest neighbor resampling was used. The warped collateral and tonal difference images are compared with the reference image in Figure 4-5. The vector displacement diagram (Figure 4-6) demonstrates significantly more process instability than exists for Scenes A, C, and D. It would appear that the true warp should be represented by a smooth and gradual transition.

There is a substantial offset between the two images (TABLE 4-5), and the typical displacement varies by only a few pixels overall. The transverse

TABLE 4-5. INITIAL GLOBAL OFFSETS FOR SCENE B MEASURED WITH RESTART PROCEDURE, BAND 4

| REFERENCE | | COLLATERAL | |
|---|---|---|---|
| LINE | PIXEL | LINE OFFSET | PIXEL OFFSET |
| 1 | 44 | 38.70 | 404.93 |
| 1 | 80 | 38.39 | 404.31 |
| 1 | 116 | 38.07 | 403.70 |
| 1 | 152 | 37.75 | 403.08 |
| 1 | 188 | 37.44 | 402.47 |
| 1 | 224 | 37.12 | 401.85 |
| 1 | 260 | 36.80 | 401.24 |
| 1 | 296 | 36.49 | 400.63 |
| 1 | 332 | 36.17 | 400.01 |
| 1 | 368 | 35.85 | 399.40 |

offset of the reference and collateral images limits common coverage to a width of about 400 pixels. Offsets at line 550 can be compared by reading the displacement components from a typical TRAK edit, TABLE 4-6. The servo errors indicate that the process was quite stable at this point in the first

8 correlation strips (compare with vectors at line 550 in Figure 4-6). Note also the correlations which are greatest at the central correlation site, except the last two in particular. The correlation coefficient was low over the entire image, averaging 0.36.

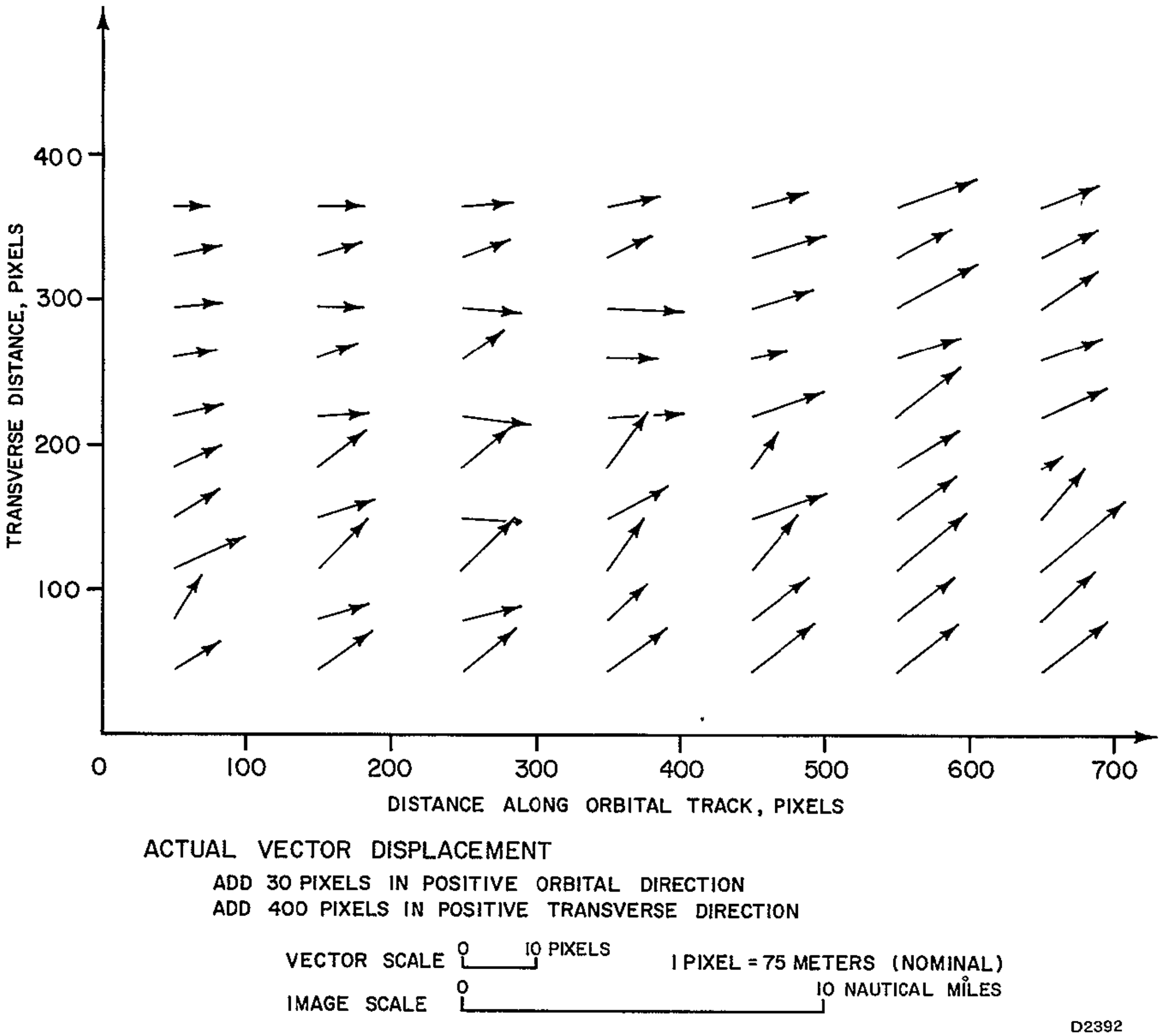


Figure 4-6. Vector Displacement Diagram
Scene B, Autoband Correlation, Band 4

Damping of the registration process in the orbital and transverse (X and Y) directions adjusted at the lower damping level of 7 lines throughout nearly all of the run. Damping in the orbital direction increased to 8 and 10 lines momentarily. Orbital and transverse components of the harness channel width averaged 4.44 and 4.32 pixels, respectively. Values ranged from 3.46 to 4.50, latter being the preset limit. These values of harness channel width were the highest of all runs, and this is reasonable because of poorer correlations.

TABLE 4-6. TYPICAL TRAK EDIT FOR SCENE B

- AUTOBAND CORRELATION, BAND 4
- AUTODAMP, AUTOVLIM, AND RESTART PROCEDURES
- NEAREST NEIGHBOR RESAMPLING

| REFERENCE | | CORRELATIONS | | | | | SERVO ERRORS | | ESTIMATED WARP | | | |
|---|---|---|---|---|---|---|---|---|---|---|---|---|
| | | | | | | | | | DISPLACEMENT | | VELOCITY | |
| X LINE | Y PIXEL | CENTER | BELOW | LEFT | ABOVE | RIGHT | ΔX | ΔY | X COMPONENT PIXELS | Y COMPONENT PIXELS | X COMPONENT | Y COMPONENT |
| 550 | 44 | .403 | .313 | .251 | .387 | .301 | .10 | -.35 | 38.617 | 406.366 | -.001 | -.000 |
| 550 | 79 | .312 | .246 | .247 | .299 | .256 | .04 | -.34 | 37.831 | 406.189 | -.003 | .002 |
| 550 | 114 | .404 | .331 | .282 | .334 | .327 | .11 | -.01 | 39.648 | 407.745 | .001 | .006 |
| 550 | 150 | .458 | .393 | .255 | .380 | .383 | .23 | .05 | 38.397 | 405.823 | .001 | .003 |
| 550 | 185 | .440 | .378 | .230 | .404 | .424 | .43 | -.13 | 38.494 | 405.079 | .000 | .004 |
| 550 | 220 | .280 | .249 | .219 | .287 | .259 | .24 | -.77 | 38.823 | 406.783 | -.005 | .008 |
| 550 | 255 | .342 | .334 | .267 | .321 | .339 | .46 | .23 | 38.407 | 403.185 | .001 | .001 |
| 550 | 291 | .316 | .319 | .234 | .291 | .319 | .54 | .61 | 41.104 | 406.122 | .002 | .010 |
| 550 | 326 | .220 | .198 | .139 | .190 | .257 | 1.35 | .08 | 37.654 | 404.011 | .002 | .000 |
| 550 | 361 | .157 | .150 | .109 | .116 | .212 | 2.50 | .36 | 41.231 | 404.266 | .007 | .007 |
| | | | | | | | | | | | | |
| | | | | | | | | | | | | |

The mean radial displacement error was determined by WECK error analysis to be 0.18 pixel (TABLE 4-7). This evaluation was made with 185 correlation subregions distributed over 71% of Scene B (lines 50 to 350, pixels 17 to 350). Each of the correlation subregions measured 100 by 100 pixels.

TABLE 4-7. REGISTRATION ERROR, SCENE B, BAND 4

- Process Dependent Technique
- WECK Error Analysis

| DESCRIPTION* | | PIXELS |
|---|---|---|
| RMS DISPLACEMENT ERROR | X COMPONENT<br>Y COMPONENT<br>RADIAL | 0.0789<br>0.2044<br>0.2191 |
| MEAN DISPLACEMENT ERROR | X COMPONENT<br>Y COMPONENT<br>RADIAL | 0.0385<br>0.0288<br>0.1815 |
| STANDARD DEVIATION OF DISPLACEMENT | X COMPONENT<br>Y COMPONENT<br>RADIAL | 0.0688<br>0.2023<br>0.1227 |

*X is measured in orbital direction
Y is measured along scan line from west to east

This low displacement error is perhaps somewhat surprising considering the poorer correlation and instability indicated by the vector displacement diagrams. The mean displacement compares with 0.18 pixel obtained for Scene A.

### 4.2.2 Scene B Registration with Fixed Parameter Processing

Considerable difficulty was met initially in registering the reference and collateral image of Scene B, but finally mean radial displacement errors were reduced to 0.25 pixel.

As noted previously Scene B lacks distinctive feature detail. Start-up control points were measured on the band 7 images because they were more easily identified by eye. The initial premise that correlation would be highest with band 7 data was proven wrong, and substantial improvement was obtained by using band 4 data. (TABLE 4-8). Also at run 14 new control points were measured manually on band 7 imagery and contributed to a better start. The start-up difficulties experienced with Scene B emphasize the advantage of the RESTART procedure in which the process determines new start-up control points.

TABLE 4-8. FIXED PARAMETER PROCESSING, SCENE B
WECK ERROR ANALYSIS

| RUN NUMBER | SPECTRAL BAND | INTERPOLATION INTP | HARNESS CHANNEL WIDTH VLIM PIXELS | DAMPING | | RADIAL ERROR PIXELS | |
|---|---|---|---|---|---|---|---|
| | | | | ORBITAL XDMP LINES | TRANSVERSE YDMP PIXELS | MEAN | RMS |
| 1 | | | 1 | 150 | 150 | 2.99 | 3.49 |
| 2 | | | 1 | 5 | 5 | 3.54 | 4.08 |
| 3 | | | 1 | 300 | 300 | 3.24 | 3.84 |
| 4 | | NEAREST | 1 | 25 | 25 | 3.25 | 3.90 |
| 5 | | NEIGHBOR | 1 | 25 | 25 | 1.87 | 2.34 |
| 6 | 7 | | 0.5 | 25 | 25 | 1.64 | 2.05 |
| 7 | | | .5 | 50 | 50 | 2.72 | 3.00 |
| 8 | | | .5 | 15 | 15 | 2.71 | 3.46 |
| 9 | | | .5 | 25 | 25 | 2.93 | 3.81 |
| 10 | | | .5 | 25 | 25 | 2.77 | 3.08 |
| 11 | | | .5 | 25 | 25 | 1.23 | 1.50 |
| 12 | | 4-POINT BILINEAR | .5 | 25 | 25 | .99 | 1.21 |
| 13 | | SIN X/X | .5 | 25 | 25 | 1.10 | 1.33 |
| 14 | | | .5 | 25 | 25 | 0.62 | 0.66 |
| 15 | | 4-POINT BILINEAR | .5 | 25 | 25 | 0.29 | 0.32 |
| 16 | 4 | | .5 | 25 | 25 | 0.25 | 0.29 |
| 17 | | SIN X/X | .5 | 25 | 25 | 0.26 | 0.30 |
| 18 | | NEAREST NEIGHBOR | .5 | 25 | 25 | 0.27 | 0.32 |
| 19 | | SIN X/X | .5 | 25 | 25 | 0.25 | 0.29 |

It was determined that moderately short damping distances in the range of 25 lines provided the necessary responsiveness. This can be compared with process dependent processing for Scenes B and C where damping distances were 7 and 19 lines, respectively. Small harness channel widths of 0.5 and 1 pixel were used, and this can be compared with values averaging between 3.5 and 4.5 in all of the other process dependent runs. Other process conditions which contribute to quality of registration are summarized in TABLE 4-9.

TABLE 4-9. OTHER CONDITIONS FOR FIXED PARAMETER PROCESSING, SCENE B

| DESCRIPTION | VALUE OR CONDITION |
|---|---|
| SCAN LINE LENGTH (NP) | 810 PIXELS |
| STRIP WIDTH (MV) | 30 PIXELS |
| NUMBER OF STRIPS (NCP) | 12 |
| SATELLITE CORRELATION SITE SEPARATION (STEP) | 1 PIXEL |
| GLOBAL WARP CONTROL (HRN) | CONSTRAINED ON X AND Y AXIS |
| Y-AXIS (ALONG SCAN LINE) ORDER OF GLOBAL FIT (HRNO) | FIRST ORDER ONE DIMENSIONAL POLYNOMIAL |
| X-AXIS (ORBITAL DIRECTION) ORDER OF GLOBAL FIT (HRND) | 25 LINES |
| REFERENCE AND COLLATERAL MAXIMA (RMAX, CMAX) | 40 |
| REFERENCE AND COLLATERAL MINIMA (RMIN, CMIN) | 5 |
| RESAMPLING POINTS (NPTS) SIN X/X ONLY | 7 |
| MODE SHAPE (MODE), SIN X/X | |
| RUNS 1-18 | $-2\pi$ TO $+2\pi$ |
| RUN 19 | $-3\pi$ TO $+3\pi$ |

Registration accuracy is evaluated with WECK error analysis over a 400 by 400 pixel area (lines 50 to 450, pixels 50 to 450), which includes the entire area shown in Figure 4-5. The size of each correlation subregion is 100 by 100 pixels. Registration accuracy with band 4 data was better than with band 7 data by a factor of 4 on the basis of mean radial error (TABLE 4-10). SIN X/X and 4-Point bilinear methods were nearly equivalent and somewhat better than nearest neighbor. It should be noted that the SIX X/X process was not optimized.

TABLE 4-10. COMPARISON OF REGISTRATION ACCURACIES, SCENE B

- THREE RESAMPLING TECHNIQUES
- BAND 4 VERSUS BAND 7

(FIXED PARAMETER PROCESSING)

| RESAMPLING PROCEDURE | MEAN RADIAL ERROR, PIXELS | |
|---|---|---|
| | BAND 4 | BAND 7 |
| NEAREST NEIGHBOR | 0.27 | 1.23 |
| 4-POINT BILINEAR | 0.25 | 0.99 |
| SIN X/X, 7 POINTS | | |
| SPREAD $-2\pi$ TO $+2\pi$ | 0.26 | 1.10 |
| SPREAD $-3\pi$ TO $+3\pi$ | 0.25 | |

## 4.3. COMPARISON OF AUTOBAND, INTERBAND, AND INTRASCENE REGISTRATION, SCENE C

The results discussed in this section are particularly interesting and important because autoband, interband, and intrascene registration are compared for the same geographical area. Comparison of autoband and interband registration provide an evaluation of the effect of changing the spectral band in the presence of temporal changes. Intrascene registration provides an excellent test of process accuracy because data obtained at a given time from the various bands of the multispectral scanner are known to be accurately registered.

Scene C, an area possessing well defined, correlative feature content, is well suited for these process comparisons. This scene consists of 700 scan lines and 850 pixels per line (Figure 4-7). The north edge corresponds to line 700 in quarter 2 of the complete frame.

Autoband, interband, and intrascene registration of scene C imagery data are demonstrated by the TRAK registration process augmented with AUTODAMP, AUTOVLIM, and RESTART procedures. Resampling is done with nearest neighbor interpolation. Results are discussed under the following topic headings:

- Autoband Registration, Scene C
- Interband Registration, Scene C
- Intrascene Registration, Scene C

In addition to these three principal topics, evaluations of TRAK registration and WECK analysis based upon autocorrelation are provided. These are found under Intrascene Registration, Scene C.

### 4.3.1 Autoband Registration, Scene C

The reference and collateral images were registered on the basis of correlation of band 5 data in the process dependent mode. The reference image, warped collateral image, and vector displacement diagram are shown in Figures 4-7, 4-8, and 4-9, respectively. Registration was completed with nearest neighbor resampling.

The required warp varies considerably across this image scene; however, smoothness of the result indicates good process stability. The geometric correction of Figure 4-9 compares very well with that of Figure 4-12 which was obtained with correlation of reference band 5 and collateral band 4 data. Again the offset between the reference and collateral image is substantial (TABLE 4-11).

A typical TRAK edit obtained at line 1049 (349 lines south of the north edge) shows the process to be under good control with generally high correlations in the center of each correlation strip (TABLE 4-12). The servo errors are moderate, and the warp velocity vectors, while not large, indicate a rather strongly changing warp.

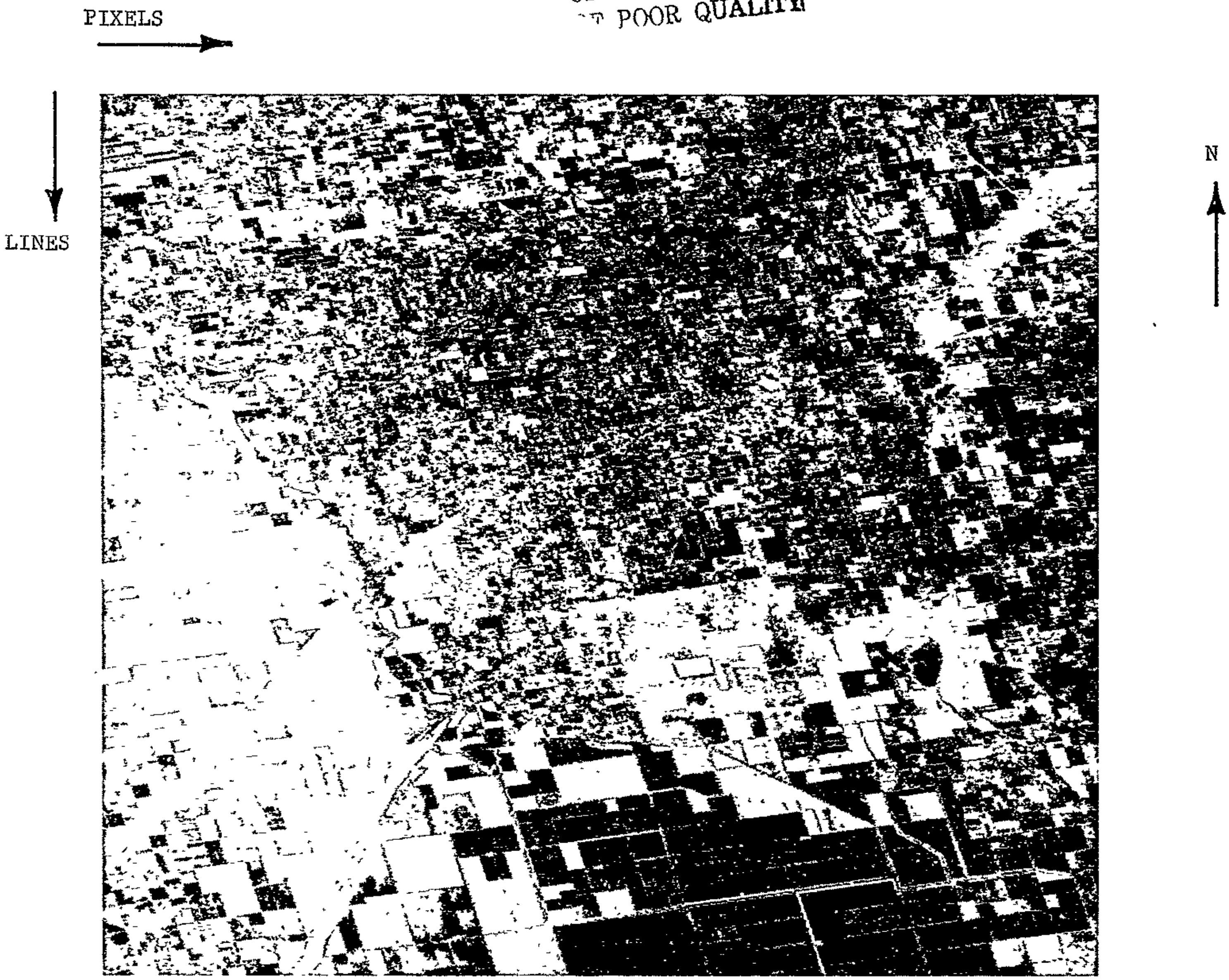


Figure 4-7. LANDSAT 1 Reference Image, Scene C
E-1703-17590 Quarter 2 Band 5


Figure 4-8. LANDSAT 1 Warped Collateral Image
E-1739-17575 Quarter 2 Band 5 Scene C
Nearest Neighbor Radiance Resampling
Autoband Registration (R5 vs C5)

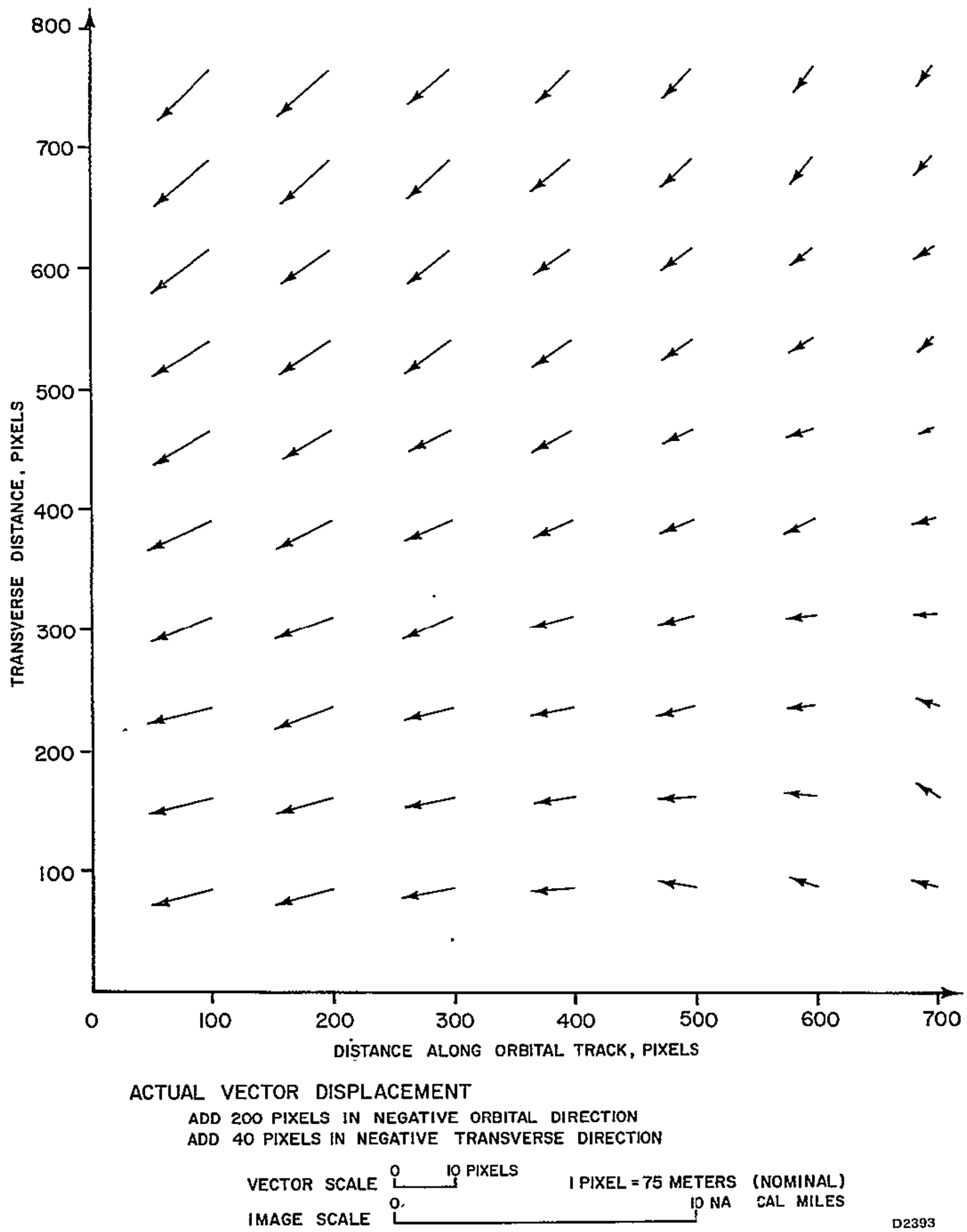


Figure 4-9. Vector Displacement Diagram
Scene C, Autoband Correlation, Band 5

TABLE 4-11. INITIAL GLOBAL OFFSETS FOR SCENE C (AUTOBAND) MEASURED WITH RESTART PROCEDURE, BAND 5

| REFERENCE | | COLLATERAL | |
|---|---|---|---|
| LINE | PIXEL | LINE OFFSET | PIXEL OFFSET |
| 700 | 83 | -209.00 | -41.93 |
| 700 | 159 | -208.78 | -42.55 |
| 700 | 235 | -208.55 | -43.17 |
| 700 | 311 | -208.33 | -43.79 |
| 700 | 387 | -208.11 | -44.42 |
| 700 | 463 | -207.88 | -45.04 |
| 700 | 539 | -207.66 | -45.66 |
| 700 | 615 | -207.44 | -46.28 |
| 700 | 691 | -207.22 | -46.90 |
| 700 | 767 | -206.99 | -47.52 |

Good registration was obtained even though significant temporal changes are readily observed in the tonal difference image (Figure 4-10). Little

TABLE 4-12. TYPICAL TRAK EDIT FOR SCENE C

- AUTOBAND CORRELATION, BAND 5
- AUTODAMP, AUTOVLIM, AND RESTART PROCEDURES
- NEAREST NEIGHBOR RESAMPLING

| REFERENCE | | CORRELATIONS | | | | | SERVO ERRORS | | ESTIMATED WARP | | | |
|---|---|---|---|---|---|---|---|---|---|---|---|---|
| | | | | | | | | | DISPLACEMENT | | VELOCITY | |
| X LINE | Y PIXEL | CENTER | BELOW | LEFT | ABOVE | RIGHT | ΔX | ΔY | X COMPONENT PIXELS | Y COMPONENT PIXELS | X COMPONENT | Y COMPONENT |
| 1049 | 84 | .850 | .839 | .787 | .811 | .715 | .18 | .29 | -206.899 | -40.328 | .009 | .004 |
| 1049 | 160 | .861 | .848 | .825 | .823 | .790 | .16 | .25 | -206.729 | -40.958 | .008 | .004 |
| 1049 | 236 | .645 | .596 | .612 | .630 | .549 | .24 | -.26 | -207.164 | -41.330 | .005 | .006 |
| 1049 | 312 | .617 | .556 | .593 | .562 | .406 | .40 | -.02 | -206.795 | -42.154 | .007 | .004 |
| 1049 | 388 | .585 | .557 | .541 | .537 | .498 | .16 | .13 | -206.353 | -42.751 | .009 | .005 |
| 1049 | 463 | .315 | .265 | .169 | .281 | .291 | -.36 | -.10 | -206.350 | -44.397 | .007 | .004 |
| 1049 | 539 | .750 | .692 | .669 | .706 | .671 | -.01 | -.07 | -206.350 | -44.397 | .007 | .004 |
| 1049 | 615 | .522 | .491 | .401 | .444 | .414 | -.03 | .21 | -206.152 | -44.206 | .006 | .006 |
| 1049 | 691 | .771 | .731 | .765 | .710 | .692 | .43 | .11 | -206.382 | -45.436 | .004 | .005 |
| 1049 | 767 | .748 | .680 | .656 | .693 | .696 | -.14 | -.05 | -205.267 | -45.667 | .008 | .003 |
| | | | | | | | | | | | | |
| | | | | | | | | | | | | |

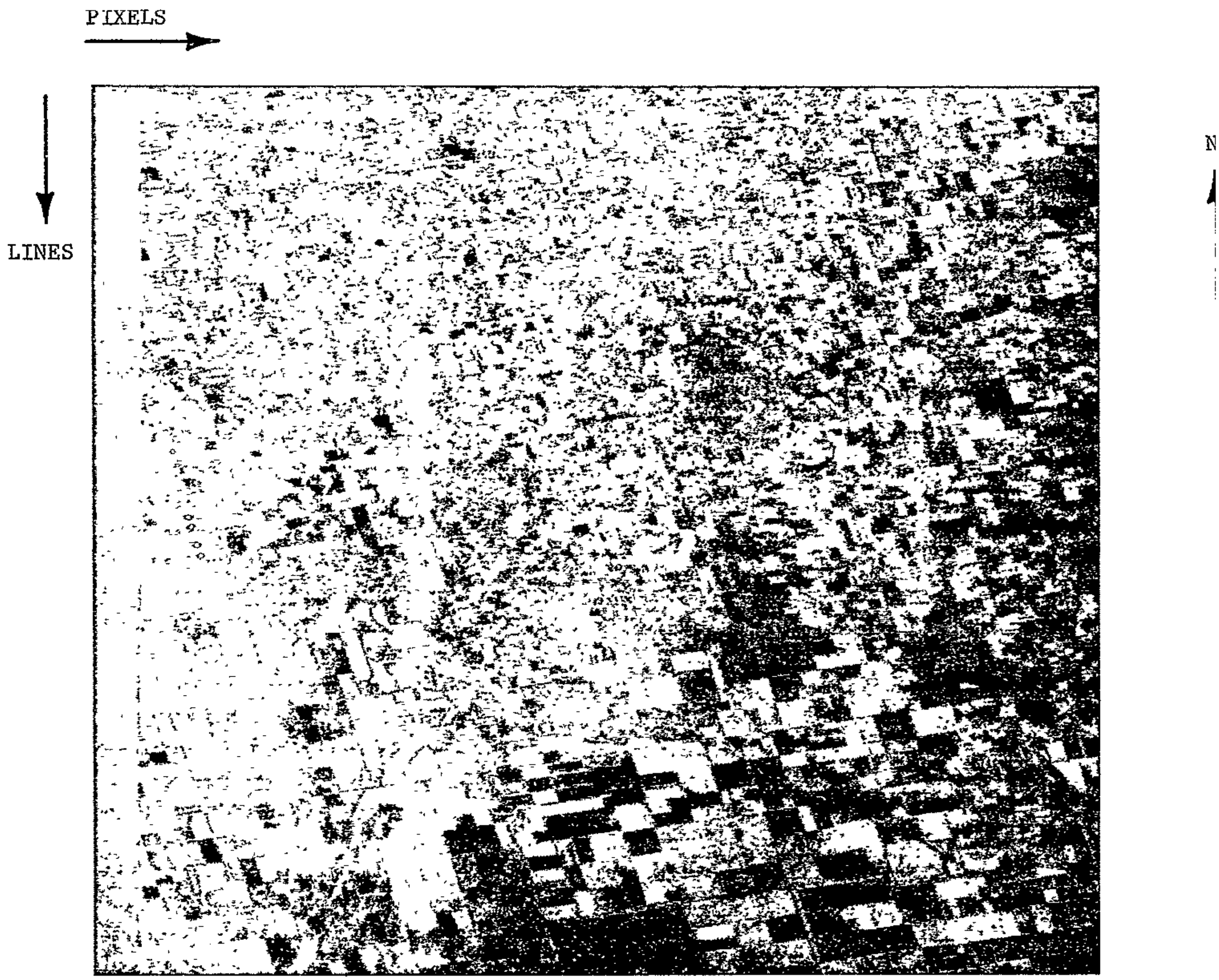


Figure 4-10. Tonal Difference Image, Scene C
Autoband Registration (R5 vs C5)
Nearest Neighbor Radiance Resampling
Reference: E 1703-17590 Band 5 Quarter 2
Collateral: E 1739-17575 Band 5 Quarter 2

ghosting is detectable, indicating good registration. The uniform gray areas at the top and left edge are the result of substituting the reference image where no common coverage existed in the collateral image. This insertion is also evident in the warped collateral image (Figure 4-8).

WECK error analysis indicates a mean radial displacement error of 0.18 pixel (TABLE 4-13). The evaluation was made with 222 subregions, each 100 by 100 pixels, distributed over a 700 x 800 pixel area (lines 700 to 1400, pixels 40 to 850). Thus, nearly all of the registered area was sampled.

In the following section 4.3.2 the same image area is registered with interband correlation, and these results should be compared.

TABLE 4-13. AUTOBAND REGISTRATION ERROR, SCENE C

- Process Dependent Technique
- Nearest Neighbor Resampling
- WECK Error Analysis

| DESCRIPTION* | | PIXELS |
|---|---|---|
| RMS DISPLACEMENT ERROR | X COMPONENT | 0.14 |
| | Y COMPONENT | 0.16 |
| | RADIAL | 0.21 |
| MEAN DISPLACEMENT ERROR | X COMPONENT | 0.09 |
| | Y COMPONENT | 0.07 |
| | RADIAL | 0.18 |
| STANDARD DEVIATION OF DISPLACEMENT | X COMPONENT | 0.12 |
| | Y COMPONENT | 0.14 |
| | RADIAL | 0.11 |

* X is measured along orbital direction
Y is measured along scan line from west to east

4.3.2 Interband Registration, Scene C

Interband registration is demonstrated by warping the collateral image to register with the reference image from Scene C in the process dependent mode. The reference and collateral data are from band 5 (0.6 to 0.7 micrometer) and band 4(0.5 to 0.6 micrometer), respectively. Nearest neighbor resampling is used.

The primary purpose of this example is to investigate the sensitivity of the registration process to a change in the detector wavelength band. In the previous section data obtained on these same flights was registered with autoband correlation (band 5). Those results can thus serve as a reference for the interband registration discussed here.

The reference image (band 5) is shown in Figure 4-7, and the collateral image (band 4) and the vector displacement diagram are shown in Figures 4-11 and 4-12, respectively. The registered area is described in the introduction of Section 4.3.

Initial global offsets were computed for both autoband and interband registration by the RESTART procedure. Hence, the reproducibility of computing offsets as a function of spectral band substitution can be compared (TABLE 4-14). Average differences in the computed offsets were 0.74 line and 0.32 pixel for line offset and pixel offset, respectively.

Correlation values are very similar for autoband and interband registration of this scene (TABLES 4-12 and 4-15). The average correlation coefficient over the registered area is 0.57 and 0.59 for autoband (band 5) and interband (band 4 vs. band 5) correlation, respectively. Comparisons to bands 6 and 7 are not available for this imagery. However, correlation values can be expected to drop for cross correlation of band 4 and 5 with bands 6 or 7 because of significant changes in tonal distribution. For example, comparing features

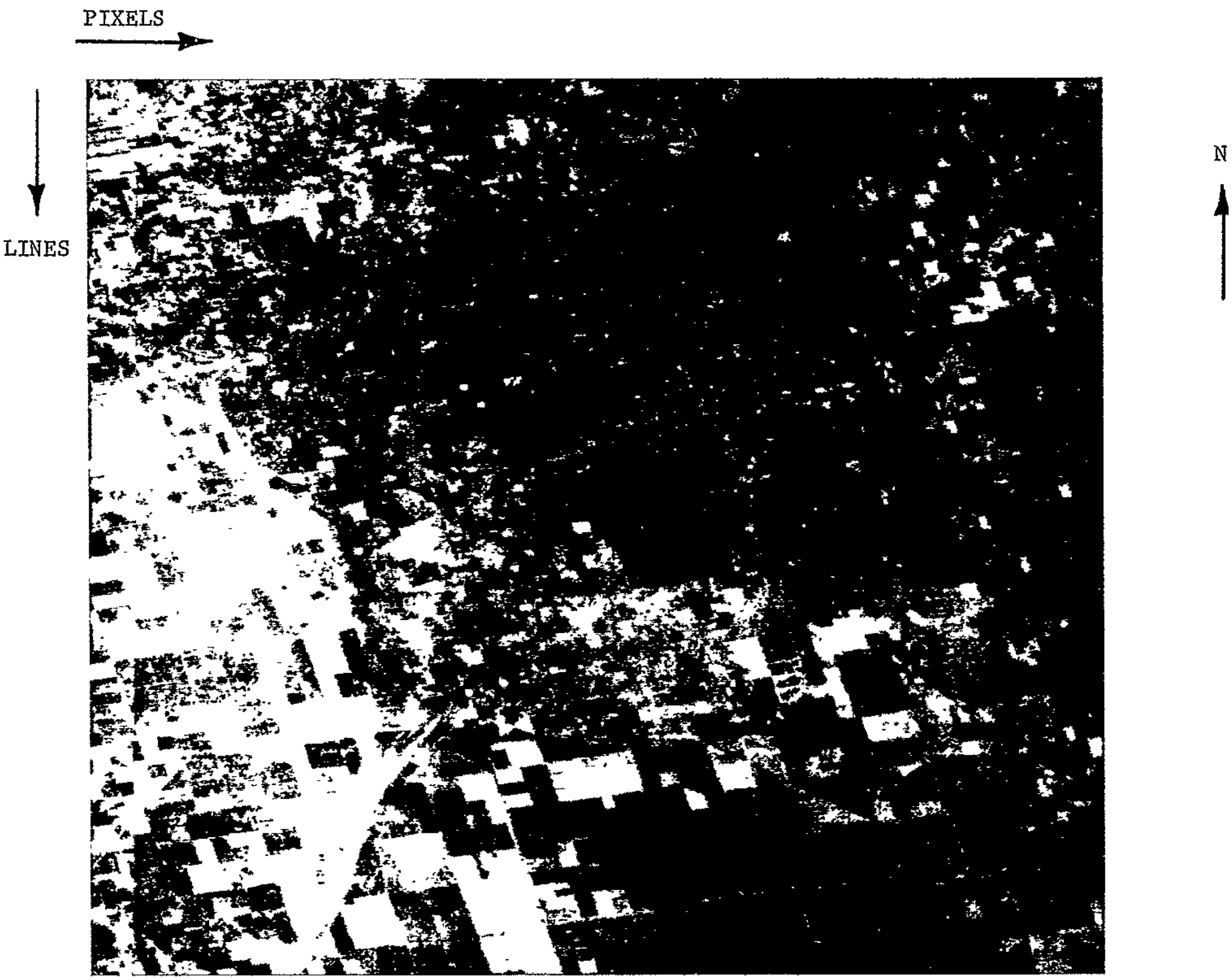


Figure 4-11. LANDSAT 1 Warped Collateral Image, Scene C
E 1739-17575 Quarter 2 Band 4
Nearest Neighbor Radiance Resampling
Interband Registration (R5 vs C4)

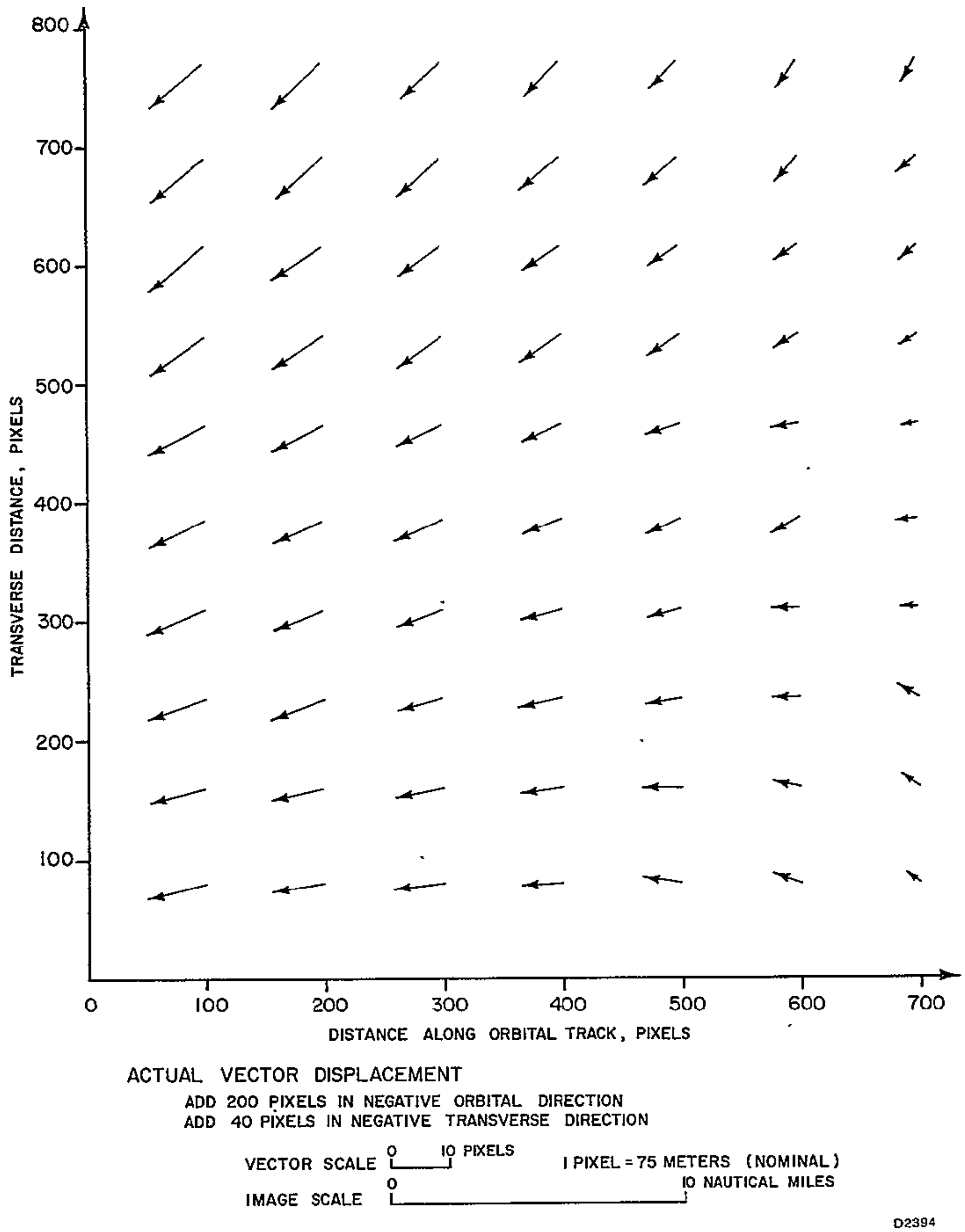


Figure 4-12. Vector Displacement Diagram
Scene C, Interband Correlation
Reference Band 5 versus Collateral Band 4

TABLE 4-14. COMPARISON OF INITIAL GLOBAL OFFSETS COMPUTED IN AUTOBAND AND INTERBAND REGISTRATION WITH RESTART, SCENE C

AUTOBAND REGISTRATION: COLLATERAL BAND 5 WARPED TO REFERENCE BAND 5
INTERBAND REGISTRATION: COLLATERAL BAND 4 WARPED TO REFERENCE BAND 5

| LINE | PIXEL | LINE OFFSET | | | PIXEL OFFSET | | |
|---|---|---|---|---|---|---|---|
| | | AUTOBAND | INTERBAND | DIFFERENCE | AUTOBAND | INTERBAND | DIFFERENCE |
| COL.1 | COL.2 | COL.3 | COL.4 | COL.3-COL.4 | COL.6 | COL.7 | COL.6-COL.7 |
| 700 | 83 | -209.00 | -209.94 | 0.94 | -41.93 | -42.03 | 0.10 |
| 700 | 159 | -208.78 | -209.67 | 0.89 | -42.55 | -42.70 | 0.15 |
| 700 | 235 | -208.55 | -209.40 | 0.85 | -43.17 | -43.37 | 0.20 |
| 700 | 311 | -208.33 | -209.14 | 0.81 | -43.79 | -44.04 | 0.25 |
| 700 | 387 | -208.11 | -208.87 | 0.76 | -44.42 | -44.71 | 0.29 |
| 700 | 463 | -207.88 | -208.60 | 0.72 | -45.04 | -45.38 | 0.34 |
| 700 | 539 | -207.66 | -208.33 | 0.67 | -45.66 | -46.05 | 0.39 |
| 700 | 615 | -207.44 | -208.06 | 0.62 | -46.28 | -46.72 | 0.44 |
| 700 | 691 | -207.22 | -207.79 | 0.57 | -46.90 | -47.39 | 0.49 |
| 700 | 767 | -206.99 | -207.52 | 0.53 | -47.52 | -48.06 | 0.54 |
| AVERAGE | | | | 0.74 | | | 0.32 |

between these spectral regions is often like comparing positive and negative photographs.

As in autoband processing of this scene, interband registration proceeded very smoothly, and the resultant warp (Figure 4-12) agrees very closely with that of autoband processing (Figure 4-9). Discrepancies of 1 or 2 pixels are apparent in the lower right corner (southwest part of scene).

The mean radial displacement error is 0.14 pixel for interband registration of reference band 5 and collateral band 4 (TABLE 4-16). Surprisingly, this is somewhat smaller than the value of 0.18 pixel obtained in autoband registration with band 5 data (TABLE 4-13).

TABLE 4-15. TYPICAL TRAK EDIT FOR INTERBAND REGISTRATION, SCENE C

- COLLATERAL BAND 4 WARPED TO REFERENCE BAND 5
- AUTODAMP, AUTOVLIM, AND RESTART PROCEDURES
- NEAREST NEIGHBOR RESAMPLING

| REFERENCE | | CORRELATIONS | | | | | SERVO ERRORS | | ESTIMATED WARP | | | |
|---|---|---|---|---|---|---|---|---|---|---|---|---|
| | | | | | | | | | DISPLACEMENT | | VELOCITY | |
| X LINE | Y PIXEL | CENTER | BELOW | LEFT | ABOVE | RIGHT | ΔX | ΔY | X COMPONENT PIXELS | Y COMPONENT PIXELS | X COMPONENT | Y COMPONENT |
| 1049 | 84 | .858 | .843 | .794 | .811 | .717 | .19 | .26 | -206.866 | -40.301 | .012 | .004 |
| 1049 | 160 | .864 | .853 | .815 | .823 | .804 | .05 | .28 | -206.951 | -40.768 | .009 | .005 |
| 1049 | 236 | .609 | .564 | .556 | .592 | .526 | .11 | -.23 | -207.321 | -41.316 | .007 | .006 |
| 1049 | 312 | .562 | .504 | .542 | .505 | .383 | .40 | -.01 | -206.961 | -41.912 | .008 | .006 |
| 1049 | 388 | .574 | .543 | .506 | .535 | .523 | -.07 | .06 | -206.397 | -42.646 | .011 | .006 |
| 1049 | 463 | .298 | .260 | .177 | .263 | .279 | -.36 | -.01 | -206.430 | -43.093 | .008 | .005 |
| 1049 | 539 | .686 | .643 | .609 | .644 | .624 | -.05 | -.01 | -206.370 | -44.302 | .009 | .005 |
| 1049 | 615 | .500 | .462 | .363 | .429 | .404 | -.09 | .15 | -206.071 | -43.989 | .008 | .007 |
| 1049 | 691 | .768 | .694 | .763 | .744 | .670 | .45 | -.25 | -206.375 | -45.458 | .006 | .005 |
| 1049 | 767 | .736 | .670 | .671 | -.695 | .646 | .08 | -.11 | -205.527 | -45.627 | .009 | .004 |
| | | | | | | | | | | | | |
| | | | | | | | | | | | | |

TABLE 4-16. INTERBAND REGISTRATION ERROR, SCENE C

- Collateral Band 4 Warped to Reference Band 5
- Process Dependent Technique
- Nearest Neighbor Resampling
- WECK Error Analysis

| DESCRIPTION | | PIXELS |
|---|---|---|
| RMS DISPLACEMENT ERROR | X COMPONENT | 0.09 |
| | Y COMPONENT | 0.13 |
| | RADIAL | 0.16 |
| MEAN DISPLACEMENT ERROR | X COMPONENT | 0.02 |
| | Y COMPONENT | 0.04 |
| | RADIAL | 0.14 |
| STANDARD DEVIATION OF DISPLACEMENT | X COMPONENT | 0.09 |
| | Y COMPONENT | 0.13 |
| | RADIAL | 0.08 |

* X is measured along orbital direction
Y is measured along scan line from west to east

The evaluation of registration accuracy over Scene C was obtained by WECK analysis over a 700 by 800 pixel area (lines 700 to 1400, pixels 50 to 850). Correlations were computed for 225 subregions, each 100 by 100 pixels.

4.3.3 Intrascene Registration, Scene C

The multispectral scanner is known to provide precisely registered data in the four spectral bands. Intrascene registration (same time, different bands) accordingly provides a means of evaluating performance of the registration process.

In this section accuracies obtained in intrascene registration by the TRAK process are measured by WECK error analysis. The geometric displacement of raw data from band 4 and band 5 is also measured with WECK analysis and serves as a comparison for results obtained with TRAK processing. Ultimate accuracies of both TRAK processing and WECK analysis are discussed for an autocorrelation test.

TRAK Registration. Band 4 and Band 5 data from the reference image of Scene C (E-1703-17590) are used to demonstrate intrascene registration. The band 4 image is warped to register with the band 5 image using TRAK registration with AUTODAMP, AUTOVLIM, and RESTART procedures (Figure 4-13).

Resampling is performed with nearest neighbor interpolation. The registered area is described in the introduction of Section 4.3 and is identical to the area evaluated for autoband and interband correlation. The noise lines appearing in band 4 were present in the raw data. They did not interfere with the continuity of processing, however. Such noise lines can be replaced with interpolations from good data to improve the appearance of the imagery if so desired.

Registration match points were obtained in 10 correlation strips, each 80 pixels wide. Initial offsets measured by RESTART are generally less than 0.25 pixel along either coordinate (TABLE 4-17). WECK error analysis of the raw data indicated mean displacements of 0.012 lines and -0.08 pixel along a


Figure 4-13. LANDSAT 1 Warped Reference Image, Scene C
E-1703-17590 Quarter 2 Band 4
Nearest Neighbor Radiance Resampling
Intrascene Registration (R5 vs R4)

TABLE 4-17. INITIAL GLOBAL OFFSETS FOR SCENE C (INTRASCENE)* MEASURED WITH RESTART PROCEDURE

| BAND 5 | | BAND 4 | |
|---|---|---|---|
| LINE | PIXEL | LINE OFFSET | PIXEL OFFSET |
| 700 | 45 | 0.035 | 0.159 |
| 700 | 125 | -.001 | .166 |
| 700 | 205 | -.015 | .174 |
| 700 | 285 | -.006 | .183 |
| 700 | 365 | .026 | .194 |
| 700 | 445 | .080 | .207 |
| 700 | 525 | .157 | .221 |
| 700 | 605 | .256 | .236 |
| 700 | 685 | .378 | .253 |
| 700 | 765 | .523 | .272 |

* E-1703 - 17590

scan line (TABLE 4-19). It would be of interest to compare these results with manufacturing quality assurance measurements of the sensors.

The autodamp process was clamped to restrict damping distances from falling below 33 pixels along either coordinate. The result was constant damping distances of 33 pixels in both the orbital and transverse directions (XDMP and YDMP).

Global harnessing with AUTOVLIM was variable. Components of the Harness Channel Width averaged 2.2 and 4.1 pixels in the orbital and transverse directions, respectively. The orbital component varied from 0.5 to 4.5 pixel with largest values occurring in the northern area and smallest values in the central region. The transverse component remained near 4.5, except for a decrease to 2.5 near the south edge of the scene.

The TRAK process follows a well defined correlation surface with correlations generally being significantly greater at the center trial site (TABLE 4-18). The average correlation coefficient for the 10 strips over Scene C is 0.896.

The process is evidently very stable with high correlation values, low servo errors in the range of 0.01 to 0.1, and low warp velocity corrections ranging generally less than 0.001 and never greater than 0.006.

At the beginning of the registration process (Scene C) the warp displacement components are indicated to be less than 0.2 pixel. When nearest neighbor resampling is used the process accumulates errors, and the displacement components grow to 0.5 pixel. As the process concinues the displacement components fluctuate between -0.5 and +0.5 pixel. The transverse component is generally positive in this example, however.

TABLE 4-18. TYPICAL TRAK EDIT FOR INTRASCENE REGISTRATION, SCENE C

- E-1703-17590 (REFERENCE), BAND 4 WARPED TO BAND 5
- AUTODAMP, AUTOVLIM, AND RESTART PROCEDURES
- NEAREST NEIGHBOR RESAMPLING

| REFERENCE | | CORRELATIONS | | | | | SERVO ERRORS | | ESTIMATED WARP | | | |
|---|---|---|---|---|---|---|---|---|---|---|---|---|
| | | | | | | | | | DISPLACEMENT | | VELOCITY | |
| X LINE | Y PIXEL | CENTER | BELOW | LEFT | ABOVE | RIGHT | ΔX | ΔY | X COMPONENT PIXELS | Y COMPONENT PIXELS | X COMPONENT | Y COMPONENT |
| 1049 | 46 | 0.823 | 0.752 | 0.713 | 0.750 | 0.691 | -.05 | -.01 | -0.261 | 0.495 | -.001 | .001 |
| 1049 | 126 | .941 | .903 | .822 | .895 | .799 | -.04 | -.05 | - ..463 | .475 | -.001 | .000 |
| 1049 | 206 | .948 | .894 | .878 | .906 | .868 | -.03 | .06 | .202 | .466 | .001 | .000 |
| 1049 | 285 | .942 | .871 | .772 | .855 | .727 | -.06 | -.05 | - .478 | .472 | -.001 | .000 |
| 1049 | 365 | .910 | .735 | .652 | .748 | .647 | -.01 | .02 | - .487 | .487 | -.001 | .000 |
| 1049 | 445 | .938 | .820 | .791 | .850 | .784 | -.01 | .07 | - .495 | .468 | -.001 | .000 |
| 1049 | 525 | .943 | .841 | .845 | .871 | .851 | .02 | .09 | - .514 | .514 | -.001 | .001 |
| 1049 | 604 | .951 | .822 | .759 | .855 | .750 | -.01 | .07 | .121 | .480 | .000 | .000 |
| 1049 | 684 | .958 | .887 | .850 | .880 | .868 | .05 | -.03 | - .458 | .497 | -.001 | .001 |
| 1049 | 764 | .954 | .864 | .854 | .868 | .834 | -.04 | .01 | - .501 | .453 | -.001 | .000 |
| | | | | | | | | | | | | |
| | | | | | | | | | | | | |

The foregoing intrascene registration results obtained by TRAK processing were further tested by WECK error analysis. In the analysis 225 subregions, each 100 by 100 pixels, were distributed over a 700 by 810 pixel area (essentially all of Scene C). Very high correlation coefficients, averaging 0.950, were obtained in the comparison of the registered data (bands 4 and 5), and the analysis should therefore be reliable.

The mean radial displacement between warped band 4 and band 5 data is 0.08 pixel by this analysis (TABLE 4-19). The same measurement was made on raw data from bands 4 and 5, and the same mean displacement was obtained (TABLE 4-19). TRAK processing did cause increases in the mean orbital (X) displacement, the RMS displacements, and standard deviation of displacement, however.

TABLE 4-19. INTRASCENE REGISTRATION ERROR, SCENE C (REFERENCE DATA)

- Process Dependent Technique
- Nearest Neighbor Resampling
- WECK Error Analysis

| DESCRIPTION* | | PIXELS | | |
|---|---|---|---|---|
| | | NASA RAW DATA | | AFTER TRAK REGISTRATION |
| | | BAND 4 vs BAND 4 | BAND 5 vs BAND 4 | BAND 5 vs BAND 4 |
| RMS DISPLACEMENT ERROR | X COMPONENT | 0.0018 | 0.017 | 0.038 |
| | Y COMPONENT | .0017 | .084 | .095 |
| | RADIAL | .0025 | .086 | .103 |
| MEAN DISPLACEMENT ERROR | X COMPONENT | -.0001 | .012 | .020 |
| | Y COMPONENT | .0001 | -.080 | .070 |
| | RADIAL | .0020 | .082 | .080 |
| STANDARD DEVIATION OF DISPLACEMENT | X COMPONENT | .0018 | .012 | .033 |
| | Y COMPONENT | .0017 | .025 | .064 |
| | RADIAL | .0015 | .025 | .064 |

*X is measured along orbital direction
Y is measured along scan line from west to east

TRAK Registration with Fixed Parameters. Intrascene registration for an area adjacent to the north edge of Scene C was obtained with TRAK processing in another run. The first 700 lines of band 4 data are registered to band 5 data using fixed parameters and nearest neighbor interpolation. The mean radial displacement error measured by WECK analysis is 0.055 pixel, which is significantly smaller than the value obtained over Scene C.

Autocorrelation Test of TRAK Process. TRAK processing performance was investigated in an autocorrelation test on collateral band 4 data (E-1739-17575). The process was tested over the first 1000 lines and therefore included the first 300 lines of Scene C. Fixed parameters and nearest neighbor resampling were used.

Servo errors obtained in autocorrelation are still smaller than those obtained in intrascene registration of band 4 and band 5 data. Warp displacement components gradually grow from very small values with fluctuations increasing to $\pm 0.4$ pixel during the processing of the first 1000 lines. The correlation coefficient is 1.00 in every case.

Autocorrelation Test of WECK Error Analysis. The sensitivity and potential accuracy of WECK error analysis was investigated in an autocorrelation test on reference band 4 data (E-1703-17590). The measurement was made over the first 700 lines and therefore includes part of the area which was used in the autocorrelation test of the TRAK process.

WECK analysis has a residual mean radial error of 0.002 pixel in this autocorrelation test (Band 4 vs. Band 4, TABLE 4-19). Correlation coefficients are 1.00.

Conclusions from Intrascene Processing. WECK analysis, which has been used to evaluate registration accuracies, has inherent sensitivity and accuracy exceeding any other process results obtained. Hence, it is concluded that Program WECK provides an acceptable evaluation of registration accuracy.

TRAK registration appears to have registration capabilities to produce mean radial displacement errors measuring in tenths of pixels. However, nearest neighbor resampling limits local performance to $\pm 0.5$ pixel.

## 4.4 Autoband Correlation, Scene D

Scene D is chosen to represent a mountainous terrain. The results of autoband registration on this scene can be compared with results for the culturally developed areas of Scenes A and C or the more amorphous Scene B.

The reference image, warped collateral image, and vector displacement diagram are shown in Figures 4-14, 4-15, and 4-16, respectively. Registration of band 5 data was obtained with the TRAK process augmented with AUTODAMP, AUTOVLIM, and RESTART procedures. The data was resampled with nearest neighbor interpolation.

Scene D lies about 50 nautical miles east of Scene C. Both scenes are common to the same LANDSAT image frame and are obtained from quarters 4 and 2, respectively. The area of scene D consists of 700 scan lines and 810 pixels per line. The north edge of the scene is line 1000 in the complete quarter frame which was supplied.

Offset between the reference and collateral data is about 200 lines and varies in the range of 50 to 60 pixels along a scan line. Initial global offsets computed with RESTART are presented in TABLE 4-20.

The TRAK process generally maintained good control in registering Scene D, and the resultant warp displacement diagram is quite smooth (Figure 4-16). Note that this warp is significantly different than the warp in Scene C (Figure 4-9).

As described previously TRAK registration was performed in the process dependent mode. Global damping in the orbital and transverse directions was

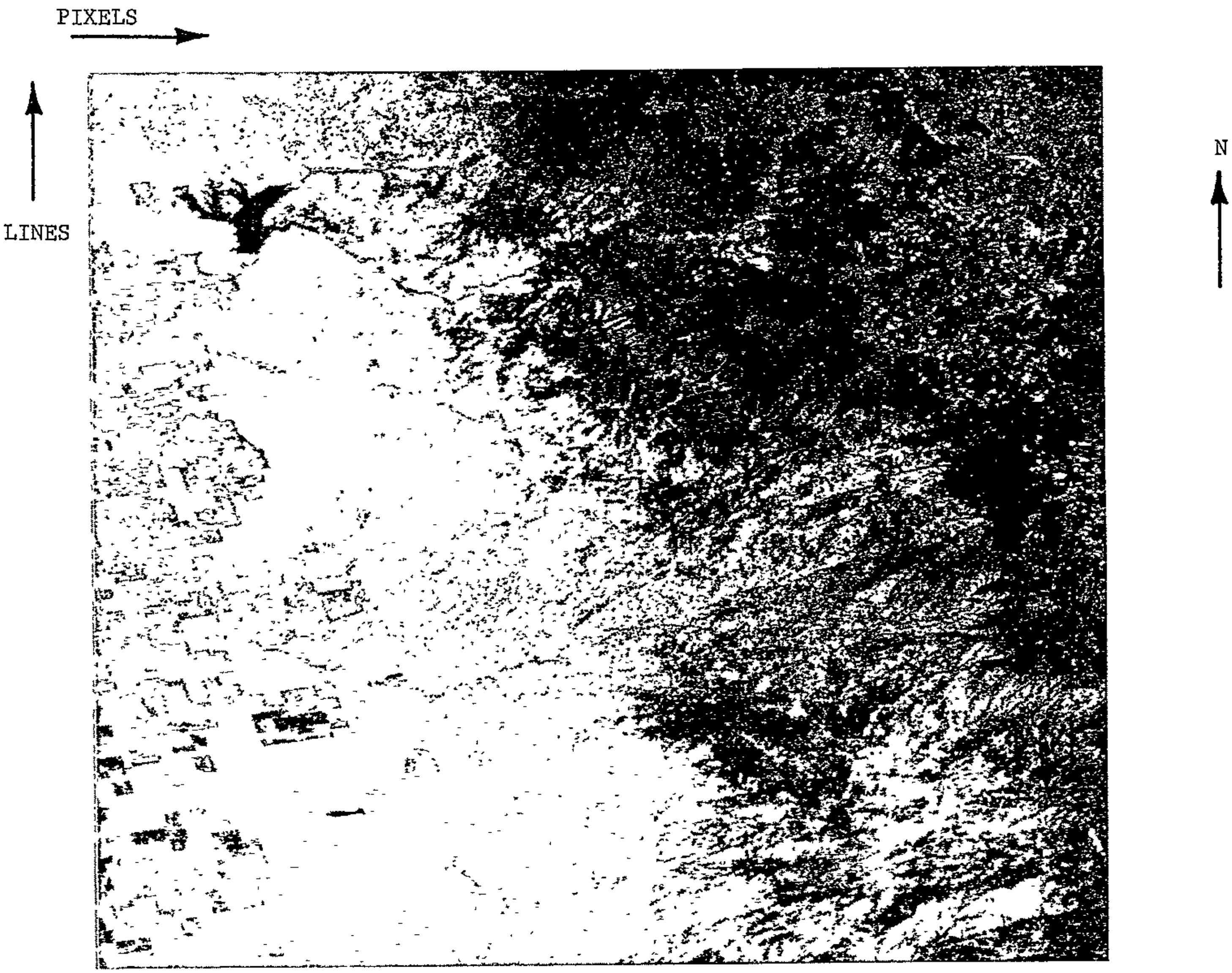


Figure 4-14. LANDSAT 1 Reference Image, Scene D
E 1703-17590 Band 5 Quarter 4

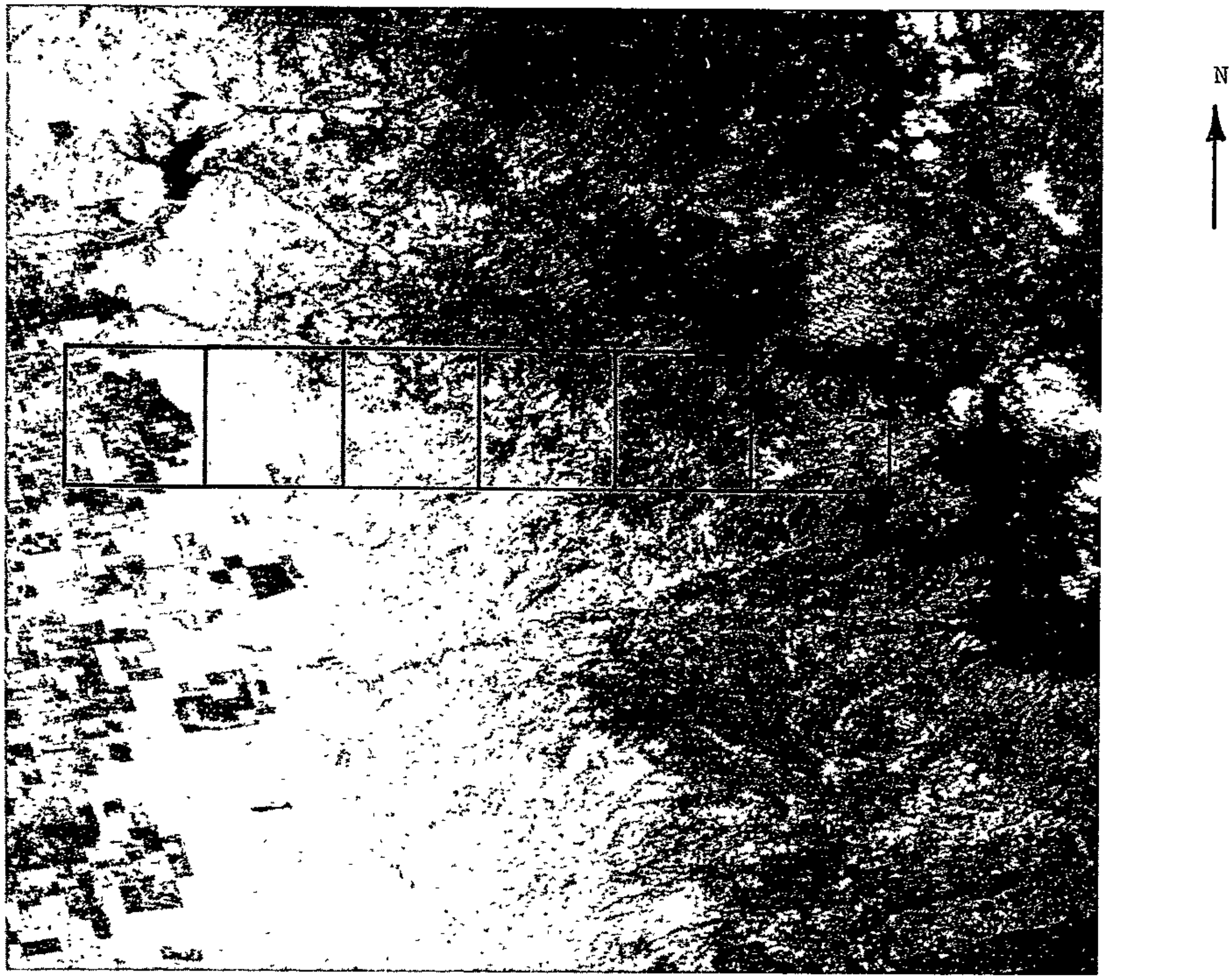


Figure 4-15. LANDSAT 1 Warped Collateral Image, Scene D
Nearest Neighbor Radiance Resampling
E 1739-17575 Band 5 Quarter 4

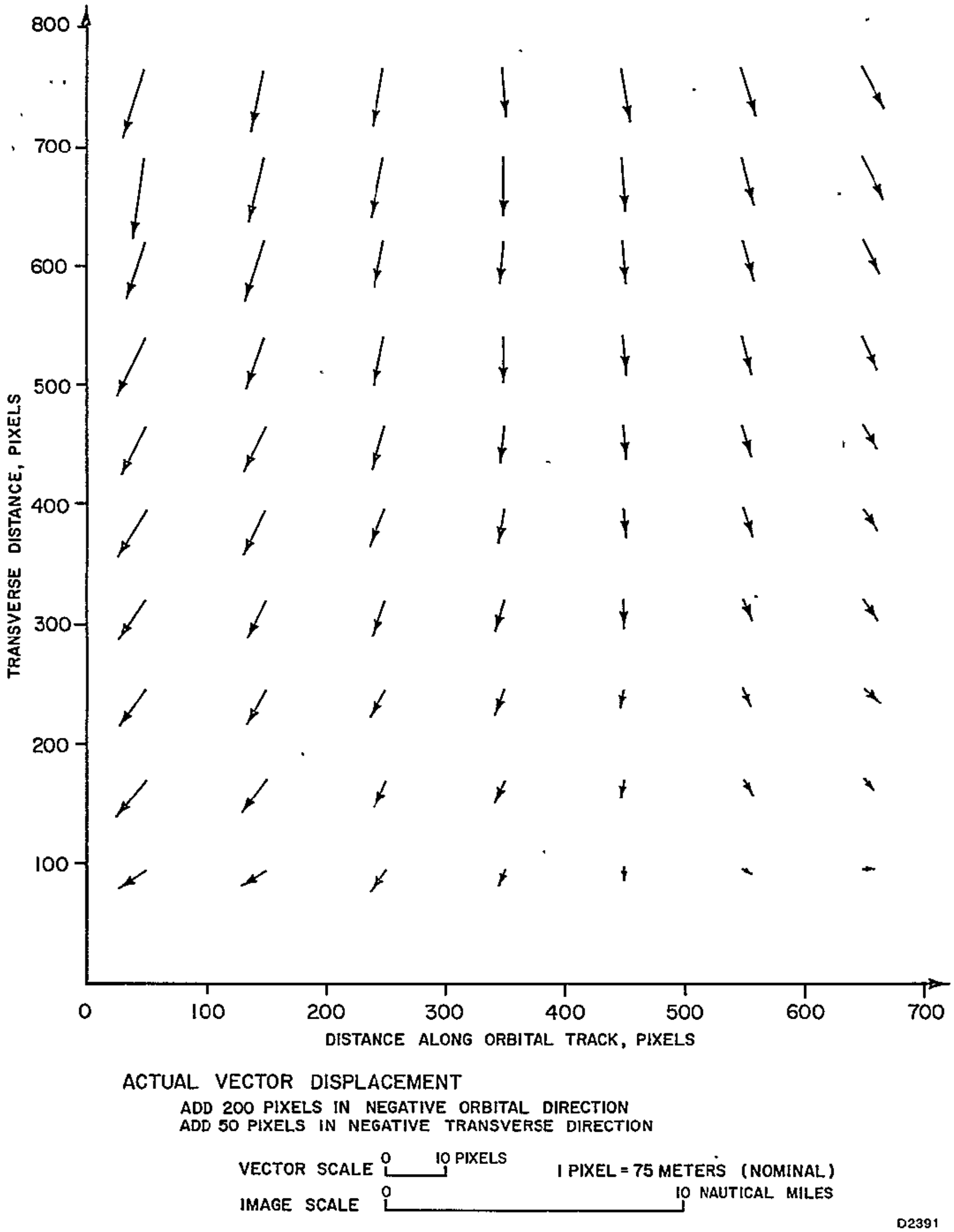


Figure 4-16. Vector Displacement Diagram
Scene D, Autoband Correlation (Band 5)

TABLE 4-20. INITIAL GLOBAL OFFSETS FOR SCENE D MEASURED WITH RESTART PROCEDURE, BAND 5

| REFERENCE | | COLLATERAL | |
|---|---|---|---|
| LINE | PIXEL | LINE OFFSET | PIXEL OFFSET |
| 1000 | 101 | -203.31 | -55.22 |
| 1000 | 175 | -202.96 | -55.91 |
| 1000 | 249 | -202.62 | -56.60 |
| 1000 | 323 | -202.27 | -57.29 |
| 1000 | 377 | -201.93 | -57.99 |
| 1000 | 471 | -201.58 | -58.68 |
| 1000 | 545 | -201.24 | -59.37 |
| 1000 | 619 | -200.89 | -60.06 |
| 1000 | 693 | -200.55 | -60.76 |
| 1000 | 767 | -200.21 | -61.45 |

clamped to restrict these values from falling below 7 lines (pixels). Process conditions maintained the damping distances for both coordinates at this lower limit. The Harness Channel Width was variable, however, and averaged 4.15 in the orbital direction and 3.75 in the transverse direction. The transverse channel width decreased to 2.6 in the central region of Scene D.

The correlation coefficient measured in TRAK averaged a moderate 0.66. At line 1349 the tenth correlation strip is in difficulty with a poorly defined correlation surface (TABLE 4-21). This is in the vicinity of clouds appearing in the east central region of the collateral image, and so this is not surprising.

The tonal difference image reveals temporal changes in the west and cloud changes in the northeast (Figure 4-17). Some scattered ghosting in the mountains reveals small errors in registration in those areas. The uniform gray area along the west and north edges results from the substitution of reference image data in the warped collateral image to fill out the scene.

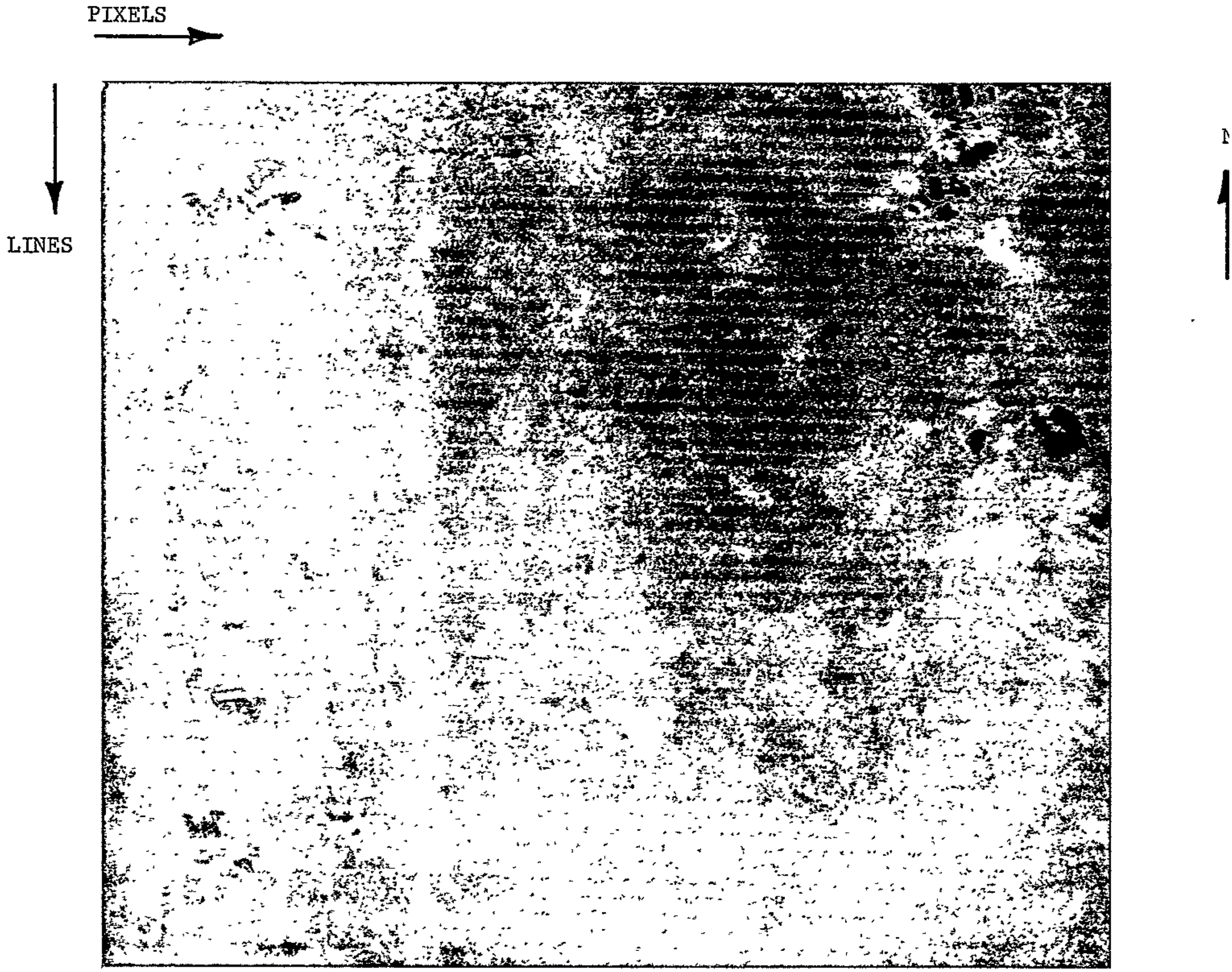


Figure 4-17. Tonal Difference Image, Scene D
Autoband Registration (R5 vs C5)
Nearest Neighbor Radiance Resampling
Reference: E 1703-17590 Band 5 Quarter 4
Collateral: E 1739-17575 Band 5 Quarter 4

TABLE 4-21. TYPICAL TRAK EDIT FOR AUTOBAND REGISTRATION, SCENE D COLLATERAL BAND 5 WARPED TO REFERENCE BAND 5

- AUTOBAND CORRELATION, BAND 5
- AUTODAMP, AUTOVLIM, AND RESTART PROCEDURES
- NEAREST NEIGHBOR RESAMPLING

| REFERENCE | | CORRELATIONS | | | | | SERVO ERRORS | | ESTIMATED WARP | | | |
|---|---|---|---|---|---|---|---|---|---|---|---|---|
| | | | | | | | | | DISPLACEMENT | | VELOCITY | |
| X LINE | Y PIXEL | CENTER | BELOW | LEFT | ABOVE | RIGHT | ΔX | ΔY | X COMPONENT PIXELS | Y COMPONENT PIXELS | X COMPONENT | Y COMPONENT |
| 1349 | 96 | .917 | .867 | .862 | .909 | .917 | 0.51 | -.37 | -201.218 | -52.568 | -.008 | .007 |
| 1349 | 170 | .881 | .818 | .815 | .840 | .860 | .26 | -.11 | -201.500 | -53.622 | -.010 | .007 |
| 1349 | 245 | .899 | .817 | .782 | .813 | .806 | .06 | .01 | -201.295 | -54.021 | -.011 | .006 |
| 1349 | 319 | .816 | .710 | .536 | .684 | .643 | .12 | .05 | -201.434 | -54.970 | -.011 | .006 |
| 1349 | 394 | .847 | .759 | .652 | .793 | .780 | .24 | -.12 | -200.963 | -55.301 | -.011 | .007 |
| 1349 | 468 | .833 | .738 | .633 | .710 | .796 | .34 | .07 | -200.721 | -56.202 | -.013 | .007 |
| 1349 | 543 | .700 | .551 | .597 | .654 | .508 | -.15 | -.26 | -200.218 | -57.521 | -.013 | .006 |
| 1349 | 617 | .786 | .650 | .627 | .749 | .668 | .08 | -.28 | -200.481 | -57.154 | -.014 | .008 |
| 1349 | 692 | .871 | .828 | .718 | .738 | .687 | -.05 | .20 | -199.908 | -59.610 | -.015 | .005 |
| 1349 | 766 | .293 | .269 | .271 | .297 | .301 | 1.02 | -.70 | -199.707 | -58.148 | -.016 | .009 |
| | | | | | | | | | | | | |
| | | | | | | | | | | | | |

Mountainous terrain such as this could cause considerably greater registration problems if it were photographed at much lower altitudes. At lower altitudes relief induced displacement becomes very complex. Fortunately, this problem is greatly reduced in LANDSAT imagery because of the great flying height.

The accuracy of TRAK registration was evaluated by WECK error analysis with 190 correlation subregions, each measuring 100 by 100 pixels, distributed over the entire scene. The mean radial displacement error between the reference image and the warped collateral image measures 0.20 pixel (TABLE 4-22).

TABLE 4-22. AUTOBAND REGISTRATION ERROR, SCENE D

- Process Dependent Technique
- Nearest Neighbor Resampling
- WECK Error Analysis

| DESCRIPTION* | | PIXELS |
|---|---|---|
| RMS DISPLACEMENT ERROR | X COMPONENT | 0.13 |
| | Y COMPONENT | 0.17 |
| | RADIAL | 0.22 |
| MEAN DISPLACEMENT ERROR | X COMPONENT | 0.12 |
| | Y COMPONENT | -0.04 |
| | RADIAL | 0.20 |
| STANDARD DEVIATION OF DISPLACEMENT | X COMPONENT | 0.07 |
| | Y COMPONENT | 0.17 |
| | RADIAL | 0.09 |

*X is measured in orbital direction
Y is measured along scan line from west to east

## 4.5 Summary of Registration Accuracies

Automatic TRAK registration processing demonstrated a capability to effect precise registration of LANDSAT data without using any ancillary information, such as spacecraft attitude, location, or ground truth. Mean radial displacement errors less than 0.2 pixel were obtained in each of the four scenes (TABLE 4-23). These results were obtained under the following range of conditions:

- AUTOBAND (same band, different times)
- INTERBAND (different bands, different times)
- INTRASCENE (different bands, same time)
- Cultural development, foothills, mountains, and desert-like terrains

TABLE 4-23. SUMMARY OF TRAK CORRELATION AND REGISTRATION ACCURACIES

| SCENE | DESCRIPTION | AVERAGE CORRELATION COEFFICIENT | | MEAN RADIAL ERROR (1) PIXELS | |
|---|---|---|---|---|---|
| | | FIXED PARAMETERS | AUTO FEATURES (2) | FIXED PARAMETERS | AUTO FEATURES (2) |
| A | AUTOBAND | 0.54 | 0.55 | 0.31 | 0.17 |
| B | AUTOBAND | 0.44 | 0.36 | 0.27 | 0.18 |
| C | AUTOBAND | | 0.57 | | 0.18 |
| | INTERBAND | | 0.59 | | 0.14 |
| | INTRASCENE | | 0.90 | | 0.08 |
| D | AUTOBAND | | 0.66 | | 0.20 |

1) NEAREST NEIGHBOR INTERPOLATION
2) AUTOVLIM, AUTODAMP, AND RESTART

Some general trends are concluded:

- Registration accuracy increases with increasing correlation coefficient.
- Registration accuracy is better with data from bands 4 and 5 than from bands 6 and 7.
- Sin X/X resampling is followed by 4-point bilinear and nearest neighbor resampling, in that order, on the basis of registration accuracy. (This is a tentative conclusion based upon only a few trials with non-optimum sin X/X interpolation).
- Nearest neighbor resampling limits TRAK registration to $\pm 0.5$ pixel locally, though the statistical mean can be as low as 0.08 pixel for Intrascene processing.
- RESTART improves TRAK processing performance significantly.
- Intrascene correlation is very high.
- Correlation is greater for cultural development than for mountains, and perhaps least for deserts.

ORIGINAL PAGE IS
OF POOR QUALITY

## 5.0 RADIOMETRIC DEGRADATION

In this section LANDSAT multispectral scanner imagery which has been spatially transformed to register with another image of the same area is analyzed for possible radiometric degradation. Data for this study is selected from examples of automatic TRAK registration which are described in Section 4.0. Included in this selection are comparisons of three resampling techniques: 1) nearest neighbor, 2) 4-point bilinear, and 3) two dimensionsl sin X/X. While sin X/X resampling procedures were not optimized, results were sufficiently instructive to be included.

Degradation of radiometric values is investigated statistically over small subregions enclosing the same feature detail in the raw collateral and warped collateral images. Statistical measures were obtained with Programs WECK and DEGRAD (Section 3.0). Radiometric degradation is evaluated on the basis of average radiance values, standard deviation of radiance, correlation coefficient, mean radial displacement error, regression line for the joint distribution diagram, and distribution of radiance in the difference image. The results are illustrated, as well, with printed images.

The following discussion is organized under five topics which discuss results for Scenes A, B, C, and D separately. The concluding topic is a brief summary.

### 5.1 Scene A

Analysis of radiometric degradation in Scene A is based upon TRAK registration with fixed parameter processing. Specifically, data is chosen from runs 19, 20, and 21 which demonstrate nearest neighbor, 4-point bilinear, and sin X/X resampling, respectively (TABLE 4-3). In this instance sin X/X resampling embodies 5 points weighted over the interval $-2\pi$ to $+2\pi$ along each coordinate axis.

Radiometric statistics are compiled over six subscenes, each 50 pixels square (TABLE 5-1). As described in Section 3.0 radiance values of the warped collateral data are compared with raw collateral data over the same feature contained in a given subscene. Thus, any alteration of radiance values that occurs because of inaccurate registration and resampling can be analyzed statistically.

Radiance values of the raw collateral and warped collateral data sets are compared on the basis of mean radial displacement error, average radiance over the subscene, standard deviation of radiance, correlation coefficient, and a joint distribution regression line (TABLE 5-2). Average values are computed for each of these descriptors over the six subscenes to facilitate an integrated comparison of the three resampling techniques.

Mean radial displacement error and cross correlation of the reference image with the warped collateral image were obtained by WECK analysis. The reference and collateral images are described in TABLE 3-1, and an analysis of registra-

TABLE 5-1. COORDINATES OF SUBSCENES USED IN TONAL DEGRADATION ANALYSIS, SCENE A

| SUB-SCENE NUMBER | CENTER COORDINATES | | | |
|---|---|---|---|---|
| | RAW COLLATERAL | | WARPED COLLATERAL | |
| | LINE | PIXEL | LINE | PIXEL |
| 1 | 551 | 461 | 500 | 450 |
| 2 | 651 | 511 | 600 | 500 |
| 3 | 676 | 637 | 625 | 625 |
| 4 | 786 | 259 | 735 | 250 |
| 5 | 826 | 409 | 775 | 400 |
| 6 | 851 | 520 | 800 | 510 |

# TABLE 5-2. ANALYSIS OF RADIANCE DEGRADATION, SCENE A

• TRAK REGISTRATION WITH FIXED PARAMETERS

| RESAMPLING | SUBSCENE | MEAN RADIAL DISPLACE-MENT PIXELS | AVERAGE RADIANCE | | STANDARD DEVIATION OF RADIANCE | | | CORRELATION COEFFICIENT | | JOINT DISTRIBUTION REGRESSION LINE | | |
|---|---|---|---|---|---|---|---|---|---|---|---|---|
| | | | RAW COLLATERAL | WARPED COLLATERAL | RAW COLLATERAL | WARPED COLLATERAL | DIFFERENCE | REFERENCE VS WARPED COLLATERAL | RAW COLLATERAL VS WARPED COLLATERAL | SLOPE | INTERCEPT | STANDARD DEVIATION PERPENDICULAR* |
| NEAREST NEIGHBOR | 1 | .24 | 24.30 | 24.27 | 5.71 | 5.72 | 2.60 | .841 | .766 | .998 | .08 | 2.76 |
| | 2 | .37 | 23.47 | 23.51 | 3.06 | 3.07 | 1.35 | .624 | .724 | .996 | .06 | 1.60 |
| | 3 | .24 | 23.62 | 23.76 | 2.77 | 2.63 | 1.48 | .765 | .559 | 1.095 | -2.40 | 1.96 |
| | 4 | N/A | 23.76 | 23.74 | 3.10 | 3.07 | 1.31 | N/A | .730 | 1.012 | - .26 | 1.62 |
| | 5 | N/A | 24.44 | 24.47 | 3.31 | 3.33 | 1.24 | N/A | .804 | .994 | .12 | 1.46 |
| | 6 | N/A | 24.90 | 24.88 | 2.95 | 2.94 | 1.53 | N/A | .645 | 1.005 | - .12 | 1.76 |
| | AVE | .28 | 24.08 | 24.11 | 3.48 | 3.46 | 1.59 | .743 | .705 | 1.017 | - .42 | 1.86 |
| 4 POINT BILINEAR | 1 | .17 | 24.30 | 23.81 | 5.71 | 5.44 | 2.00 | .855 | .828 | 1.060 | - .94 | 2.45 |
| | 2 | .37 | 23.47 | 23.10 | 3.06 | 2.87 | 1.11 | .666 | .763 | 1.089 | -1.68 | 1.57 |
| | 3 | .07 | 23.62 | 23.21 | 2.77 | 2.43 | 1.18 | .819 | .605 | 1.235 | -5.04 | 2.00 |
| | 4 | N/A | 23.76 | 23.28 | 3.10 | 2.94 | 1.13 | N/A | .730 | 1.074 | -1.24 | 1.69 |
| | 5 | N/A | 24.44 | 24.01 | 3.31 | 3.24 | .95 | N/A | .846 | 1.027 | - .23 | 1.32 |
| | 6 | N/A | 24.90 | 24.41 | 2.95 | 2.77 | 1.38 | N/A | .620 | 1.108 | -2.14 | 1.45 |
| | AVE | .20 | 24.08 | 23.64 | 3.48 | 3.28 | 1.29 | .780 | .732 | 1.099 | -1.88 | 1.75 |
| SIN X/X 5 POINTS -2π TO +2π | 1 | .14 | 24.30 | 23.79 | 5.71 | 5.71 | 2.21 | .844 | .802 | .999 | .54 | 2.54 |
| | 2 | .11 | 23.47 | 23.08 | 3.06 | 3.11 | 1.27 | .674 | .718 | .980 | .84 | 1.61 |
| | 3 | .03 | 23.62 | 23.20 | 2.77 | 2.68 | 1.33 | .796 | .562 | 1.060 | - .96 | 1.91 |
| | 4 | N/A | 23.76 | 23.23 | 3.10 | 3.10 | 1.27 | N/A | .677 | 1.001 | .52 | 1.76 |
| | 5 | N/A | 24.44 | 23.99 | 3.31 | 3.35 | 1.04 | N/A | .818 | .986 | .80 | 1.40 |
| | 6 | N/A | 24.90 | 24.37 | 2.95 | 2.97 | 1.52 | N/A | .562 | .988 | .82 | 1.93 |
| | AVE | .09 | 24.08 | 23.61 | 3.48 | 3.49 | 1.44 | .771 | .690 | 1.002 | .43 | 1.86 |

*PERPENDICULAR TO JOINT DISTRIBUTION LINE tion accuracy over the three subscenes which were analyzed is better than the results indicated in TABLE 4-3 (runs 19, 20, and 21). Over these three subscenes sin X/X resampling was much superior in registration accuracy with its low mean radial displacement of 0.09 pixel.

Normally, cross correlation between raw collateral and warped collateral data will be higher than that between reference and warped collateral if the measurement is made over a sufficiently small subregion so that relative distortion is insignificant. This conclusion assumes the additional assumptions that the center of each subregion is accurately registered, and that the reference and collateral images may be represented by different spectral bands or contain temporal changes. Results obtained in Scenes B, C, and D support this conclusion. However, only 1 of the two subscenes in Scene A support it. The discrepancy may be explained by the fact that cross correlation of reference and warped collateral data were not obtained over precisely the same area as was used for correlation of raw collateral and warped collateral data. The former was obtained from WECK analysis and the latter from DEGRAD analysis. Locations of the subscenes differed by 5 to 30 pixels in WECK and DEGRAD analyses. In this instance, since the subscenes are only 50 pixels square, local variations in correlation and small sample statistics can easily produce local inconsistencies. For the examples analyzed over Scene A 4-point bilinear resampling provided the highest correlation.

Radiance statistics, including cross correlation of raw collateral and warped collateral data, were obtained with Program DEGRAD. The analysis reveals that 4-point bilinear and sin X/X resampling depress the average value of radiance in the warped collateral by nearly 0.5 units on a radiance scale of 64 units.

Similarity of two radiance distributions is measured by the joint distribution diagram which is created by plotting warped collateral radiance versus raw collateral radiance (Figure 5-1). If both distributions are identical the joint distribution is a straight line through the origin at 45 degrees.

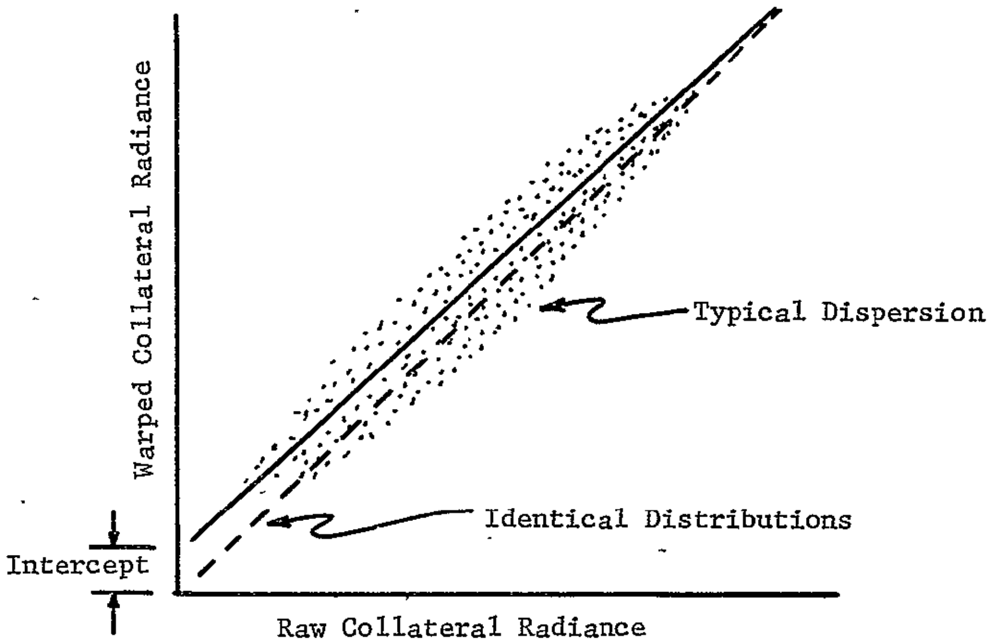


Figure 5-1. Joint Distribution Diagram

Otherwise the distribution is dispersed and a regression line intercepts one of the axes at a point displaced from the origin.

A linear regression line was computed on the basis of a least squares fit to the displacements perpendicular to the regression line. For Scene A the regression line has the following equation:

$$G_0 = m\, G_W + G_{01}$$

where $G_o$ = radiance of raw collateral

$G_W$ = radiance of warped collateral

$G_{01}$ = intercept on raw collateral radiance axis

m = slope of regression line

Identical distributions are described by slope m = 1, intercept $G_{01}$ = 0, and standard deviation perpendicular to the regression line = 0.

For the process results obtained over Scene A two dimensional sin X/X resampling in the warped collateral image provides the closest match to the raw data based upon slope and intercept. Four-point bilinear resampling is slightly superior with respect to standard deviation perpendicular to the regression line.

The three resampling techniques are ranked as follows on the basis of the radiance measures obtained over Scene A:

| RESAMPLING TECHNIQUE | RANK VALUE |
|---|---|
| Two Dimensional Sin X/X (5 points spread $-2\pi$ to $+2\pi$) | 2.1 |
| Nearest Neighbor | 2.0 |
| 4-Point Bilinear | 1.9 |

This ranking was obtained by assigning rank values r from 1 to 3, with 3 representing best performance. Equal weights were assigned to the following factors:

- Average radiance in raw and warped collateral data
- Standard deviation of radiance in raw and warped data
- Standard deviation of radiance in the difference of raw and warped data
- Correlation coefficient for raw and warped collateral data
- Regression slope
- Regression intercept
- Standard deviation perpendicular to the regression line

A weighted rank value R is obtained from

$$R = \frac{\Sigma nr}{\Sigma n}$$



C-2

where n = number of times a given rank is assigned to a given factor

r = rank value assigned for each factor

When two techniques are equivalent in one of the factors the sum of the corresponding rank values are divided equally between the two techniques.

Results of this ranking analysis indicate a small superiority for two dimensional sin X/X resampling even though the technique is not considered to be optimized. However, the results are not particularly conclusive considering the narrow spread of rank values and arbitrary assignment of equal weight to each evaluation factor.

In regard to image qualities it is noted that nearest neighbor resampling, and to a lesser extent 4-point bilinear resampling, depresses the average radiance at feature edges. Four-point bilinear resampling is inferior because of marked blurring of the image. Sin X/X resampling provides the advantage of interpolation without blurring.

5.2 Scene B

As for Scene A radiometric degradation over Scene B is based upon TRAK registration with fixed parameters. Data was chosen from runs 16, 17, 18, and 19 which demonstrate nearest neighbor, 4-point bilinear, and two dimensional sin X/X resampling (TABLE 4-8). Sin X/X was performed with two different weightings: 7 points spread from $-2\pi$ to $+2\pi$ and 7 points spread from $-3\pi$ to $+3\pi$.

Radiometric statistics are compiled over six subscenes, each 100 pixels square (TABLE 5-3). Comparisons of the raw collateral and warped collateral data were obtained over these subscenes with Program DEGRAD (TABLE 5-4). Mean radial displacement error and correlation of the reference and warped collateral images were obtained from WECK analysis over approximately the same subscenes. The reference and collateral data for Scene B are identified in TABLE 3-1.

Average values of the mean radial displacement measured over the six

TABLE 5-3. COORDINATES OF SUBSCENES USED IN TONAL DEGRADATION ANALYSIS, SCENE B

| SUB-SCENE NUMBER | CENTER COORDINATE | | | |
|---|---|---|---|---|
| | RAW COLLATERAL | | WARPED COLLATERAL | |
| | LINE | PIXEL | LINE | PIXEL |
| 1 | 137 | 504 | 100 | 100 |
| 2 | 137 | 602 | 100 | 200 |
| 3 | 137 | 700 | 100 | 300 |
| 4 | 237 | 504 | 200 | 100 |
| 5 | 237 | 603 | 200 | 200 |
| 6 | 237 | 702 | 200 | 300 |

subscenes are almost identical with results discussed in Section 4.2.2 (TABLE 4-8). The small differences are not statistically significant.

As would be expected cross correlation of raw collateral and warped collateral data is greater than that of the reference and warped collateral data (ref., discussion in Section 5.1). Four-point bilinear resampling yielded somewhat higher correlations than the other methods.

Nearest neighbor resampling provided the closest match of raw and warped collateral images on the basis of average radiance and standard deviation of radiance (exact matches). As was found in Scene A the average values of radiance in the warped collateral image is depressed about 0.5 unit on a radiance scale of 64 units.

The parameters defining the regression line fit to the joint distribution have the same definition as for Scene A (Section 5.1). Nearest neighbor resampling provides the best match on the basis of the regression line; however, two dimensional sin X/X is very nearly as good.

Ranking the four resampling techniques by the method described in Section 5.1 the following order is obtained:

# TABLE 5-4. ANALYSIS OF RADIANCE DEGRADATION, SCENE B

• TRAK REGISTRATION WITH FIXED PARAMETERS

| RESAMPLING | SUBSCENE | MEAN RADIAL DISPLACEMENT PIXELS | AVERAGE RADIANCE | | | STANDARD DEVIATION OF RADIANCE | | | CORRELATION COEFFICIENT | | JOINT DISTRIBUTION REGRESSION LINE | | |
|---|---|---|---|---|---|---|---|---|---|---|---|---|---|
| | | | RAW COLLATERAL | WARPED COLLATERAL | DIFFERENCE | RAW COLLATERAL | WARPED COLLATERAL | DIFFERENCE | REFERENCE VS. WARPED COLLATERAL | RAW COLLATERAL VS. WARPED COLLATERAL | SLOPE | INTERCEPT | STANDARD DEVIATION PERPENDICULAR* |
| NEAREST NEIGHBOR | 1 | .29 | 27.32 | 27.33 | 30.77 | 3.99 | 3.98 | 1.53 | .775 | .713 | 1.000 | -.01 | 2.13 |
| | 2 | .06 | 26.97 | 26.98 | 30.76 | 3.81 | 3.82 | 1.54 | .696 | .681 | .995 | .12 | 2.14 |
| | 3 | .51 | 26.28 | 26.23 | 30.73 | 3.50 | 3.47 | 1.66 | .540 | .558 | 1.013 | -.30 | 2.35 |
| | 4 | .11 | 25.47 | 25.49 | 30.83 | 2.67 | 2.69 | 1.07 | .570 | .698 | .989 | .25 | 1.46 |
| | 5 | .28 | 26.09 | 26.10 | 30.78 | 2.76 | 2.77 | 1.24 | .499 | .612 | .990 | .26 | 1.70 |
| | 6 | .40 | 25.43 | 25.42 | 30.75 | 2.77 | 2.78 | 1.33 | .516 | .560 | .994 | .16 | 1.83 |
| | AVERAGE | .28 | 26.26 | 26.26 | 30.77 | 3.25 | 3.25 | 1.40 | .599 | .637 | .997 | .08 | 1.94 |
| 4 POINT | 1 | .27 | 27.32 | 26.85 | 30.52 | 3.99 | 3.79 | 1.41 | .793 | .745 | 1.085 | -1.81 | 2.12 |
| | 2 | .02 | 26.97 | 26.47 | 30.50 | 3.81 | 3.56 | 1.39 | .722 | .727 | 1.098 | -2.10 | 2.11 |
| | 3 | .51 | 26.28 | 25.75 | 30.49 | 3.50 | 3.22 | 1.52 | .567 | .608 | 1.149 | -3.31 | 2.41 |
| | 4 | .15 | 25.47 | 25.00 | 30.53 | 2.67 | 2.39 | .89 | .606 | .783 | 1.148 | -3.22 | 1.35 |
| | 5 | .23 | 26.09 | 25.63 | 30.53 | 2.76 | 2.50 | 1.11 | .545 | .671 | 1.158 | -3.60 | 1.74 |
| | 6 | .32 | 25.43 | 24.90 | 30.51 | 2.77 | 2.50 | 1.23 | .549 | .588 | 1.190 | -4.25 | 2.00 |
| | AVERAGE | .25 | 26.26 | 25.77 | 30.51 | 3.25 | 2.99 | 1.26 | .630 | .687 | 1.138 | -3.05 | 1.96 |
| SINX/X 7 POINTS -2π TO + 2π | 1 | .26 | 27.32 | 26.82 | 30.50 | 3.99 | 3.96 | 1.38 | .775 | .765 | 1.009 | .26 | 1.94 |
| | 2 | .04 | 26.97 | 26.45 | 30.49 | 3.81 | 3.81 | 1.47 | .705 | .710 | 1.001 | .51 | 2.05 |
| | 3 | .52 | 26.28 | 25.72 | 30.48 | 3.50 | 3.46 | 1.63 | .557 | .570 | 1.022 | - .00 | 2.33 |
| | 4 | .15 | 25.47 | 24.97 | 30.50 | 2.67 | 2.68 | .92 | .598 | .784 | .995 | .63 | 1.24 |
| | 5 | .27 | 26.09 | 25.61 | 30.51 | 2.76 | 2.76 | 1.13 | .529 | .682 | .996 | .59 | 1.55 |
| | 6 | .30 | 25.43 | 24.91 | 30.49 | 2.77 | 2.75 | 1.32 | .535 | .558 | 1.011 | .24 | 1.86 |
| | AVERAGE | .26 | 26.26 | 25.75 | 30.50 | 3.25 | 3.24 | 1.31 | .617 | .678 | 1.006 | .37 | 1.83 |
| SINX/X 7 POINTS -3π TO + 3π | 1 | .28 | 27.32 | 26.82 | 30.50 | 3.99 | 3.99 | 1.53 | .780 | .715 | 1.000 | .50 | 2.13 |
| | 2 | .07 | 26.97 | 26.45 | 30.49 | 3.81 | 3.80 | 1.49 | .701 | .701 | 1.005 | .40 | 2.09 |
| | 3 | .54 | 26.28 | 25.75 | 30.49 | 3.50 | 3.80 | 1.59 | .549 | .593 | 1.013 | .18 | 2.25 |
| | 4 | .16 | 25.47 | 24.98 | 30.51 | 2.67 | 2.67 | 1.02 | .594 | .729 | .997 | .57 | 1.39 |
| | 5 | .23 | 26.09 | 25.61 | 30.51 | 2.76 | 2.77 | 1.22 | .538 | .630 | .992 | .69 | 1.67 |
| | 6 | .24 | 25.43 | 24.93 | 30.50 | 2.77 | 2.77 | 1.37 | .548 | .526 | 1.002 | .46 | 1.91 |
| | AVERAGE | .25 | 26.26 | 25.76 | 30.50 | 3.25 | 3.30 | 1.37 | .618 | .649 | 1.002 | .47 | 1.91 |

*PERPENDICULAR TO JOINT DISTRIBUTION REGRESSION LINE

| | RADIOMETRIC DEGRADATION |
|---|---|
| RESAMPLING TECHNIQUE | RANK VALUE |
| Two Dimensional Sin X/X (7 points spread $-2\pi$ to $+2\pi$ | 3.0 |
| Two Dimensional Sin X/X (7 points spread $-3\pi$ to $+3\pi$) | 2.6 |
| Nearest Neighbor | 2.5 |
| 4-Point Bilinear | 2.2 |

Ranking is computed for the same seven factors described previously, but since there are four techniques the rank values range from 1 to 4 (instead of 1 to 3). Even though correlation was more difficult with Scene B than with Scene A the rank orders are identical for both cases.

As described in Section 3.3.3 Program DEGRAD provides the means for visual evaluation by creating the following images: raw collateral, warped collateral, tonal difference, and threshold difference. The results obtained with nearest neighbor resampling in three subscenes are presented in Figure 5-2. Areas of exact match between raw and warped collateral data are a uniform gray in the tonal difference image. All white areas in the threshold image include pixels which differ only by 1 radiance value or less (on a scale of 64). Black areas represent pixels differing by more than 1 radiance value.

The differences in radiance values obtained by subtracting the warped collateral image from the raw collateral image have been classified into 11 bins $B_i$ which contain the count of differences $D_i$. The bins and corresponding ranges of differences are defined by:

$B_i$, $D_i = 0$, $i = 0$

$B_i$, $i - 1 < D_i \leq i$, $1 \leq i \leq 9$

$B_i$, $D_i < 9$, $i = 10$

Thus $B_0$ corresponds to exact match. The remaining bins are grouped at integer increments of radiance units, with $B_{10}$ counting all pixel locations for which the difference exceeds 9 radiance units. The occupancy in each bin has been expressed in percent of the total area of a subregion, thus providing an immediate appreciation of the fractional area matched to a given tolerance.

For example, the threshold images of Figure 5-2 show the spatial distribution of pixel locations included in bins $B_0$ and $B_1$ (difference $\leq 1$ radiance unit). These examples of nearest neighbor resampling resulted in fractional area occupancy of 86, 80, and 77 percent for Subscenes 4, 5, and 6, respectively. Occupancies for exact match are 53, 40, and 35 percent, respectively. Typical complete occupancy distributions for Scene C are shown in TABLE 5-8.

The occupancies obtained by the four resampling techniques have been averaged over the six subregions analyzed in Scene B (TABLE 5-5). This table summarizes occupancy corresponding to match ($B_0$), differences to 1 radiance unit ($B_1$), and all differences of 1 unit or less ($B_0$ + $B_1$). Additionally,

TABLE 5-5. COMPARISON OF RADIANCE VALUES IN RAW COLLATERAL AND WARPED COLLATERAL IMAGES, SCENE B

• TRAK REGISTRATION WITH FIXED PARAMETERS

| COMPARISON OF WARPED COLLATERAL RADIANCE WITH CONJUGATE VALUE ON RAW COLLATERAL | OCCUPANCY, PERCENT (1) | | | |
|---|---|---|---|---|
| | NEAREST NEIGHBOR | 4 POINT | SINX/X $-2\pi$ TO $+2\pi$ | SINX/X $-3\pi$ TO $+3\pi$ |
| MATCH | 37.2 | 34.6 | 31.6 | 28.7 |
| GREATER THAN | 24.7 | 17.3 | 18.2 | 19.5 |
| LESS THAN | 38.1 | 48.2 | 50.3 | 51.8 |
| DIFFER BY 1 LEVEL (2) | 38.7 | 43.2 | 44.7 | 43.8 |
| MATCH +1 LEVEL | 75.9 | 77.8 | 76.3 | 72.5 |

(1) OCCUPANCY IS GIVEN IN PERCENT OF TOTAL IMAGE AREA INCLUDED IN ANALYSIS

(2) TOTAL RANGE IS 64 RADIANCE VALUES

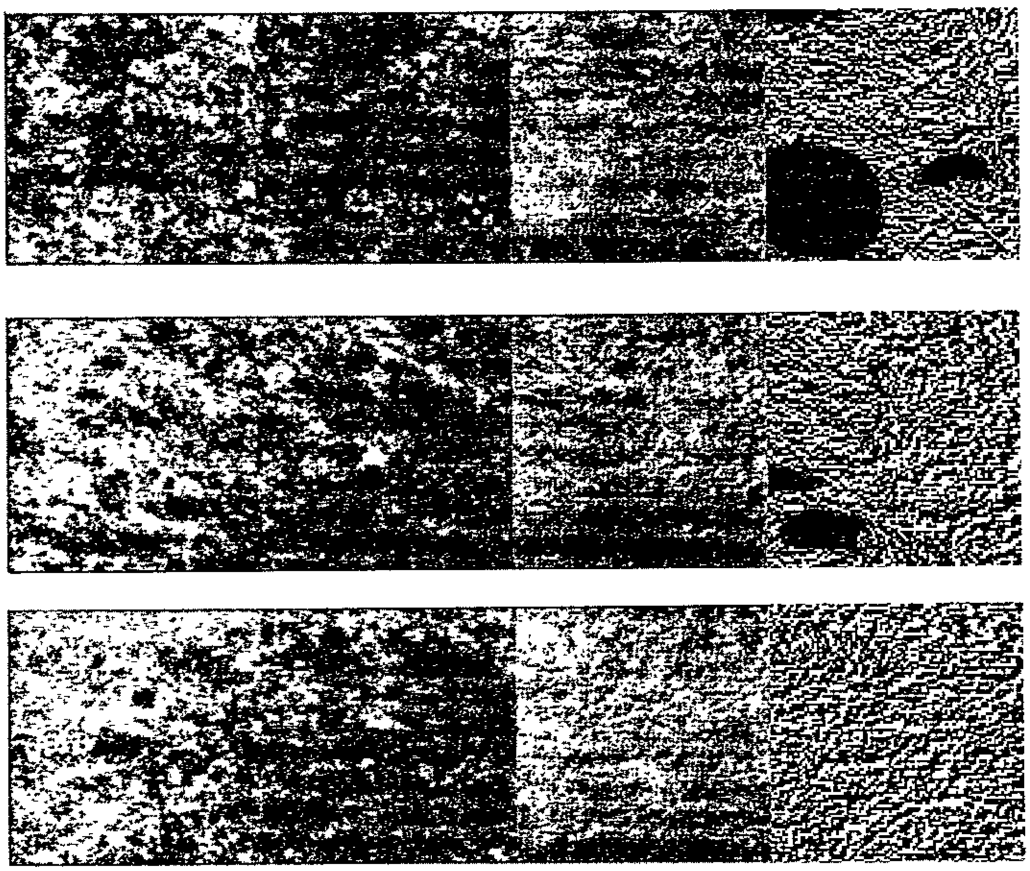

SUB-SCENE 4

SUB-SCENE 5

SUB-SCENE 6

WARPED COLLATERAL | RAW COLLATERAL | TONAL DIFFERENCE | THRESHOLD DIFFERENCE (T = $\pm 1$)

N

Figure 5-2. Analysis of Radiometric Degradation, Scene B
Nearest Neighbor Resampling

the occupancy for nonmatching areas is divided to show:

- Occupancy of radiance values in the warped collateral image which are greater than the conjugate values in the raw collateral image
- Occupancy of radiance values in the warped collateral image which are less than the conjugate values in the raw collateral image.

In these examples nearest neighbor resampling provides the greatest coverage of exact match, and 4-point bilinear resampling is marginally superior for a tolerance of $\pm 1$ radiance unit. This analysis demonstrates, too, the observation made previously that sin X/X and 4-point bilinear resampling depress the radiance values of the collateral image more than nearest neighbor. Even though correlations for Scene B are mediocre a significant fraction of the area ($>$ 72%) is matched to a tolerance of $\pm 1$ radiance unit.

5.3 Scene C

The investigation of radiometric degradation discussed in this section is based upon analyses of warped collateral data from Autoband processing of Scene C data (Section 4.3.1). The data is further identified in TABLE 3-1. The following discussion is limited to results obtained with nearest neighbor resampling.

Radiometric statistics are compiled over six subscenes, each 100 pixels square (TABLE 5-6). Comparisons of raw collateral and warped collateral data were obtained over these subscenes with Program DEGRAD (TABLE 5-7). Mean radial displacement error and cross correlation of the reference and warped collateral data were derived from WECK analysis over approximately the same subscenes.

Again, as would be expected, cross correlation of raw collateral and warped collateral data is substantially greater than that of reference and

TABLE 5-6. COORDINATES OF SUBSCENES USED IN TONAL DEGRADATION ANALYSIS, SCENE C

| SUB-SCENE NUMBER | CENTER COORDINATES | | | |
|---|---|---|---|---|
| | RAW COLLATERAL | | WARPED COLLATERAL | |
| | LINE | PIXEL | LINE | PIXEL |
| 1 | 793 | 59 | 1000 | 100 |
| 2 | 793 | 158 | 1000 | 200 |
| 3 | 793 | 258 | 1000 | 300 |
| 4 | 793 | 356 | 1000 | 400 |
| 5 | 793 | 455 | 1000 | 500 |
| 6 | 793 | 555 | 1000 | 600 |

warped collateral data. Mean radial displacement error between the reference and warped collateral images, averaging 0.13 pixel over the six subscenes, is somewhat better than the 0.18 pixel reported in Section 4.3.1 (TABLE 4-13).

Raw collateral and warped collateral data are very similar on the basis of all comparative statistics. The equation for the regression line interchanges position of the raw and warped collateral data relative to the equation used for Scenes A and B. Therefore, the equation for Scene C is as follows:

$$G_W = m\,G_0 + G_{W1}$$

where

$G_0$ = radiance of raw collateral image

$G_W$ = radiance of warped collateral image

$G_{W1}$ = intercept on warped collateral radiance axis

m = slope of regression line

# TABLE 5-7. ANALYSIS OF RADIANCE DEGRADATION, SCENE C

• TRAK REGISTRATION WITH AUTODAMP, AUTOVLIM, AND RESTART

| RESAMPLING | SUB-SCENE | MEAN RADIAL DISPLACEMENT PIXELS | AVERAGE RADIANCE | | | STANDARD DEVIATION OF RADIANCE | | | CORRELATION COEFFICIENT | | JOINT DISTRIBUTION REGRESSION LINE | | |
|---|---|---|---|---|---|---|---|---|---|---|---|---|---|
| | | | RAW COLLATERAL | WARPED COLLATERAL | DIFFERENCE | RAW COLLATERAL | WARPED COLLATERAL | DIFFERENCE | REFERENCE VS WARPED COLLATERAL | RAW COLLATERAL VS WARPED COLLATERAL | SLOPE | INTERCEPT | STANDARD DEVIATION PERPENDICULAR* |
| NEAREST NEIGHBOR | 1 | .13 | 33.55 | 33.65 | 30.84 | 7.93 | 7.99 | 1.71 | .791 | .910 | 1.008 | -.16 | 2.41 |
| | 2 | .17 | 28.28 | 28.27 | 30.84 | 7.73 | 7.73 | 1.46 | .617 | .930 | .999 | .01 | 2.04 |
| | 3 | .07 | 28.05 | 28.06 | 30.77 | 5.74 | 5.73 | 1.85 | .687 | .795 | .999 | .03 | 2.59 |
| | 4 | .09 | 24.89 | 24.91 | 30.94 | 4.68 | 4.74 | .85 | .512 | .938 | 1.013 | -.31 | 1.19 |
| | 5 | .12 | 27.74 | 27.80 | 30.91 | 6.53 | 6.55 | 1.21 | .675 | .933 | 1.003 | -.02 | 1.69 |
| | 6 | .19 | 25.49 | 25.45 | 30.75 | 5.40 | 5.41 | 1.83 | .546 | .777 | 1.002 | -.08 | 2.56 |
| | | .13 | 28.00 | 28.02 | 30.84 | 6.34 | 6.36 | 1.49 | .638 | .881 | 1.004 | -.09 | 2.08 |

*PERPENDICULAR TO JOINT DISTRIBUTION REGRESSION LINE

TABLE 5-8. COMPARISON OF RADIANCE VALUES IN RAW COLLATERAL AND WARPED COLLATERAL IMAGES, SCENE C

- TRAK REGISTRATION WITH AUTODAMP, AUTOVLIM, AND RESTART
- NEAREST NEIGHBOR RESAMPLING

| COMPARISON OF WARPED COLLATERAL RADIANCE WITH CONJUGATE VALUE ON RAW COLLATERAL | OCCUPANCY, PERCENT (1) | | | | | | |
|---|---|---|---|---|---|---|---|
| | SUBSCENE 1 | SUBSCENE 2 | SUBSCENE 3 | SUBSCENE 4 | SUBSCENE 5 | SUBSCENE 6 | SUBSCENE AVERAGE |
| MATCH | 45.9 | 55.2 | 30.5 | 81.1 | 65.8 | 33.1 | 51.9 |
| GREATER THAN | 22.0 | 17.9 | 28.6 | 7.5 | 14.1 | 26.2 | 19.4 |
| LESS THAN | 32.1 | 26.9 | 40.9 | 11.4 | 20.1 | 40.7 | 28.7 |
| DISTRIBUTION OF CHANGES: | | | | | | | |
| BIN CATEGORIES ARE DIFFERENCES IN RADIANCE VALUES (2) | | | | | | | |
| 1 | 33.4 | 26.2 | 36.8 | 11.4 | 19.8 | 37.2 | 27.5 |
| 2 | 10.8 | 10.2 | 18.1 | 4.7 | 8.2 | 15.2 | 11.2 |
| 3 | 4.3 | 4.3 | 7.9 | 1.9 | 3.4 | 7.6 | 4.9 |
| 4 | 2.2 | 2.1 | 3.5 | .6 | 1.6 | 3.6 | 2.3 |
| 5 | 1.3 | 1.0 | 1.8 | .2 | .7 | 1.8 | 1.1 |
| 6 | .8 | .5 | .8 | .1 | .3 | .7 | .5 |
| 7 | .5 | .3 | .4 | .05 | .1 | .4 | .3 |
| 8 | .4 | .2 | .2 | .03 | .03 | .1 | .2 |
| 9 | .3 | .1 | .07 | .01 | .01 | .09 | .1 |
| 10 or more | .08 | .02 | .04 | .02 | .01 | .09 | .04 |

(1) OCCUPANCY IS GIVEN IN PERCENT OF TOTAL IMAGE AREA
(2) TOTAL RANGE IS 64 RADIANCE VALUES

The slope and intercept are very near the perfect match for all six subregions. However, the standard deviation perpendicular to the regression line indicates typical scattering of data.

Goodness of match is analyzed further on the basis of the distribution of radiance values (TABLE 5-8 and Figure 5-3). On a pixel-by-pixel basis Subscenes 2, 4, and 5 match over more than one-half of their areas. It can be seen from the images of Figure 5-3b that Subscenes 4 and 5 contain extensive areas wherein radiometric values are precisely matched. The six subscenes can be viewed in context of the total warped collateral image for

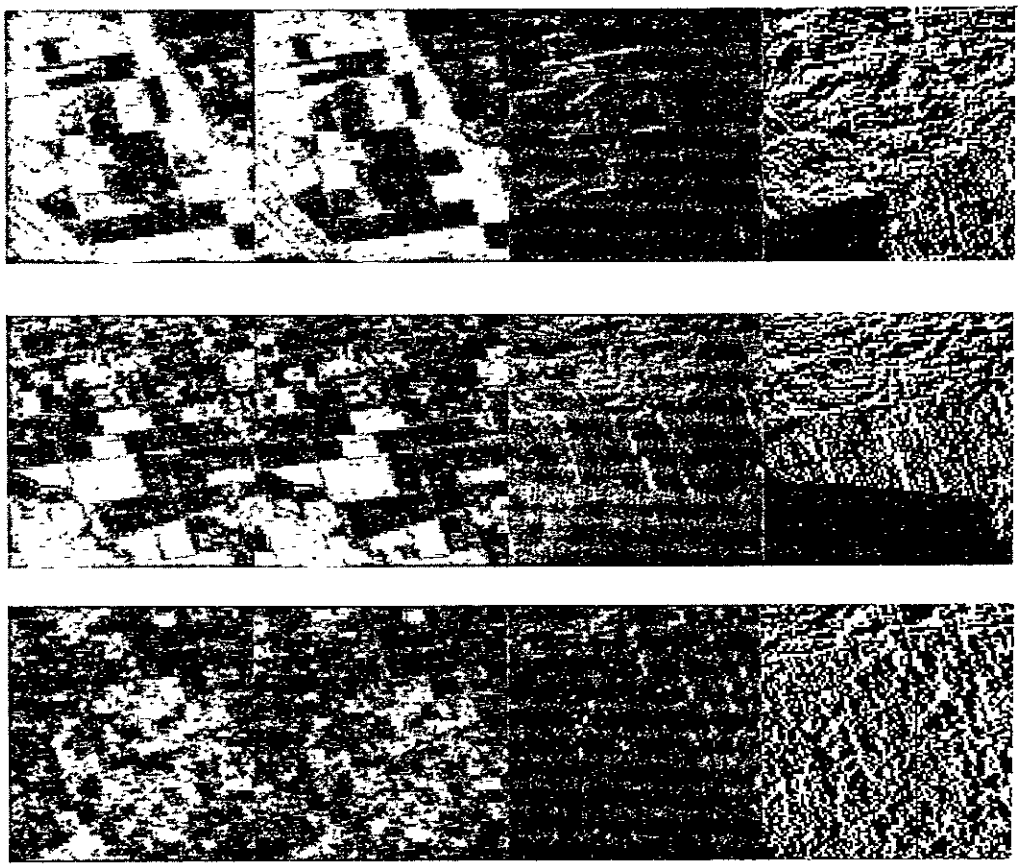


Figure 5-3a. Analysis of Radiometric Degradation, Scene C
Nearest Neighbor Resampling

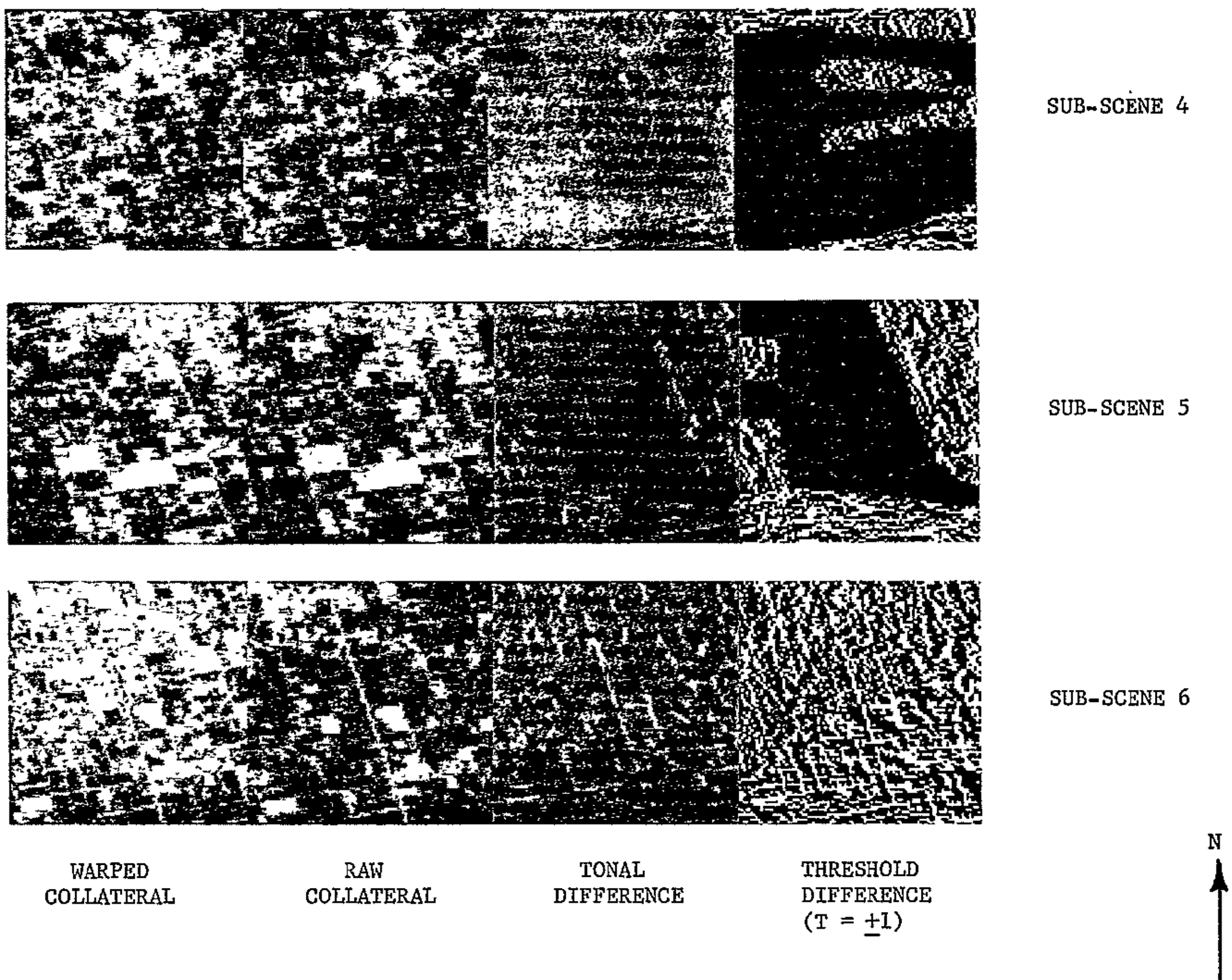


Figure 5-3b. Analysis of Radiometric Degradation, Scene C
Nearest Neighbor Resampling

Scene C by referring to Figure 4-8. The subscenes are about 20 millimeters square and extend from left to right just above the center of Scene C.

Subscene 4 matches over 81% of its area, and the average for all six subscenes is 52%. Complete distributions of differences for all six subscenes are presented in TABLE 5-8, and the descriptors are described in Section 5.2. On the average, the areas investigated match to a tolerance of $\pm 1$ radiance unit on a scale of 64 over 77% of the area. This is obtained from the sum of occupancies for bins 0 (match) and 1.

It is believed that subscenes 1, 3 and 6 should be comparable to the other scenes in this analysis. The relatively poor matches obtained for these areas is probably due to incorrect assignment of coordinates to the raw and warped collateral data. Some mismatch can be observed by close analysis of Figure 5-3 (for example, Subscenes 1 and 2).

## 5.4 Scene D

Scene D provides an opportunity to evaluate radiometric degradation resulting from automatic registration of data representing mountainous terrain. Data for the analysis was obtained from Autoband processing described in Section 4.4. Results for two resampling techniques are discussed: nearest neighbor and two dimensional sin X/X with 3 points weighted from $-\pi$ to $+\pi$ in both coordinate directions. The warped collateral data used for this analysis is further identified in TABLE 3-1.

Radiometric statistics are computed over six subscenes, each 100 pixels square (TABLE 5-9). These subscenes are outlined on the warped (collateral image which is shown in Figure 4-15. The subscenes are numbered 1 to 6 starting at the left and provide an interesting progression of image characteristics from cultural development to rugged mountains. Scene D consists of 700 lines of 810 pixels each. Line 1000 corresponds to the north edge, and pixel 0 to the west edge.

TABLE 5-9. COORDINATES OF SUBSCENES USED IN TONAL DEGRADATION ANALYSIS, SCENE D

| SCENE NUMBER | CENTER COORDINATES | | | |
|---|---|---|---|---|
| | RAW COLLATERAL | | WARPED COLLATERAL | |
| | LINE | PIXEL | LINE | PIXEL |
| 1 | 1098 | 51 | 1300 | 104 |
| 2 | 1098 | 150 | 1300 | 204 |
| 3 | 1098 | 249 | 1300 | 304 |
| 4 | 1098 | 348 | 1300 | 404 |
| 5 | 1098 | 448 | 1300 | 504 |
| 6 | 1098 | 547 | 1300 | 604 |

Radiance values of raw and warped collateral data are statistically compared in each of these subscenes with Program DEGRAD (TABLE 5-10). Mean radial displacement error and cross correlation of the reference and warped collateral data were derived from WECK analysis over approximately the same subscenes. The reference data is that of Scene D described in TABLE 3-1 and is precisely the data used in the process runs discussed in Section 4.4.

With two exceptions, cross correlation of warped collateral data and raw collateral data exceeds the correlation between warped collateral and reference data. The correlation of warped collateral and raw collateral data is very high (0.955) in the culturally developed area of Subscene 1, and decreases progressively through the foothills to the rugged mountains in Subscenes 5 and 6. A trend of decreasing mean radial displacement error with increasing correlation coefficient between the reference and warped collateral data is also suggested. The approximate trend line for these examples is

$$r = -0.54\,\rho + 0.62, \quad 0.5 < \rho < 1$$

where r = mean radial displacement error in pixels

ρ = correlation coefficient between reference and warped collateral data.

# TABLE 5-10. ANALYSIS OF RADIANCE DEGRADATION, SCENE D

• TRAK REGISTRATION WITH AUTODAMP, AUTOVLIM, AND RESTART

| RESAMPLING | SUB-SCENE | MEAN RADIAL DISPLACE-MENT PIXELS | AVERAGE RADIANCE | | | STANDARD DEVIATION OF RADIANCE | | | CORRELATION COEFFICIENT | | JOINT DISTRIBUTION REGRESSION LINE | | |
|---|---|---|---|---|---|---|---|---|---|---|---|---|---|
| | | | RAW COLLATERAL | WARPED COLLATERAL | DIFFERENCE | RAW COLLATERAL | WARPED COLLATERAL | DIFFERENCE | REFERENCE VS WARPED COLLATERAL | RAW COLLATERAL VS WARPED COLLATERAL | SLOPE | INTERCEPT | STANDARD DEVIATION PERPENDICULAR* |
| NEAREST NEIGHBOR | 1 | .12 | 33.81 | 33.71 | 30.78 | 8.81 | 8.80 | 1.34 | .903 | .955 | .999 | -.08 | 1.86 |
| | 2 | .57 | 40.31 | 40.30 | 30.81 | 3.13 | 3.13 | .92 | .642 | .842 | .999 | .02 | 1.24 |
| | 3 | .25 | 37.52 | 37.62 | 30.82 | 3.75 | 3.69 | 1.32 | .698 | .755 | .976 | .98 | 1.80 |
| | 4 | .14 | 31.01 | 31.12 | 30.82 | 4.85 | 4.88 | 1.56 | .819 | .798 | 1.009 | -.16 | 2.21 |
| | 5 | .23 | 24.74 | 24.84 | 30.81 | 4.04 | 3.97 | 1.71 | .694 | .642 | .974 | .73 | 2.33 |
| | 6 | .18 | 23.09 | 23.17 | 30.80 | 6.00 | 5.92 | 2.12 | .523 | .749 | .981 | .53 | 2.93 |
| | AVERAGE | .25 | 31.75 | 31.79 | 30.81 | 5.10 | 5.07 | 1.50 | .713 | .790 | .990 | .34 | 2.06 |
| SIN X/X 3 POINTS -π TO +π | 1 | .14 | 33.81 | 33.25 | 30.47 | 8.81 | 8.83 | 1.27 | .909 | .960 | 1.003 | -.66 | 1.77 |
| | 2 | .49 | 40.31 | 39.82 | 30.51 | 3.13 | 3.12 | .89 | .659 | .857 | .996 | -.31 | 1.18 |
| | 3 | .26 | 37.52 | 37.11 | 30.54 | 3.75 | 3.68 | 1.24 | .725 | .787 | .975 | .53 | 1.67 |
| | 4 | .21 | 31.01 | 30.61 | 30.55 | 4.85 | 4.89 | 1.46 | .835 | .826 | 1.010 | -.71 | 2.05 |
| | 5 | .26 | 24.74 | 24.33 | 30.55 | 4.04 | 3.98 | 1.68 | .712 | .658 | .979 | .12 | 2.29 |
| | 6 | .20 | 23.09 | 22.65 | 30.53 | 6.00 | 5.93 | 2.11 | .544 | .754 | .984 | -.06 | 2.91 |
| | AVERAGE | .26 | 31.75 | 31.30 | 30.53 | 5.10 | 5.07 | 1.44 | .731 | .807 | .991 | -.18 | 1.98 |

*PERPENDICULAR TO JOINT DISTRIBUTION REGRESSION LINE

It should be noted that Subscene 2 is substantially above this trend and Subscene 6 is substantially below. The latter may be explained by wispy clouds over Subscene 6 which would reduce the correlation there (Figure 4-17).

Somewhat higher correlations were obtained with two dimensional sin X/X resampling than with nearest neighbor, but mean radial displacement was essentially equivalent for both, ranging from 0.12 to 0.57 pixel. The average mean radial error of 0.25 pixel over the six subscenes is to be compared with 0.20 pixel reported in Section 4.4 for the entire scene (TABLE 4-22).

Raw collateral and warped collateral data are statistically very similar. However, the correlation coefficient and regression line fit are slightly inferior to results for Scene C. Definition of the regression line is the same as for Scene C and is defined in Section 5.3. Resampling techniques are ranked as follows on the basis of radiance parameters presented in TABLE 5-10:

| RESAMPLING TECHNIQUE | RANK VALUE |
|---|---|
| Two Dimensional sin X/X with 3 Points weighted over $-\pi$ to $+\pi$ | 2.8 |
| Nearest neighbor | 2.2 |

These weighted rank values were obtained using the procedure described in Section 5.1 and assigning rank values of 3 and 2 in the calculation. The order obtained for Scene D agrees with the results for Scenes A and B.

The extent of exact match of radiance values in the raw collateral and warped collateral subscenes decreases drastically in moving from culturally developed areas to rugged mountain terrain (TABLE 5-11). Nearest neighbor resampling produces 59 percent occupancy for the culturally developed terrain of Subscene 1. Occupancy steadily declines as the terrain shifts to foothills and finally to rugged mountains where occupancy reaches a low of 26 percent.

TABLE 5-11. COMPARISON OF RADIANCE VALUES IN RAW COLLATERAL AND WARPED COLLATERAL IMAGES, SCENE D

- TRAK REGISTRATION WITH AUTODAMP, AUTOVLIM, AND RESTART

| COMPARISON OF WARPED COLLATERAL RADIANCE WITH CONJUGATE VALUE ON RAW COLLATERAL | | OCCUPANCY, PERCENT[1] | | | | | | |
|---|---|---|---|---|---|---|---|---|
| | | SUBSCENE 1 | SUBSCENE 2 | SUBSCENE 3 | SUBSCENE 4 | SUBSCENE 5 | SUBSCENE 6 | SUBSCENE AVERAGE |
| NEAREST NEIGHBOR | MATCH | 59.3 | 55.3 | 37.4 | 30.6 | 27.9 | 25.9 | 39.4 |
| | GREATER THAN | 14.0 | 15.2 | 25.4 | 30.0 | 30.5 | 32.3 | 24.6 |
| | LESS THAN | 26.7 | 29.5 | 37.2 | 39.4 | 41.6 | 41.8 | 36.0 |
| | DIFFER BY 1 LEVEL[2] | 27.5 | 35.5 | 41.0 | 39.8 | 39.1 | 35.2 | 36.4 |
| | MATCH + 1 LEVEL | 86.8 | 90.8 | 78.4 | 70.4 | 67.0 | 61.1 | 75.8 |
| SINX/X | MATCH | 38.0 | 41.3 | 33.5 | 28.6 | 26.2 | 24.2 | 32.0 |
| | GREATER THAN | 11.8 | 9.2 | 17.6 | 22.7 | 25.2 | 27.2 | 19.0 |
| | LESS THAN | 50.2 | 49.5 | 48.9 | 48.7 | 48.6 | 48.6 | 49.1 |
| | DIFFER BY 1 LEVEL [2] | 46.3 | 48.5 | 44.9 | 42.3 | 39.4 | 35.6 | 42.8 |
| | MATCH + 1 LEVEL | 84.3 | 89.8 | 78.4 | 70.9 | 65.6 | 59.8 | 74.8 |

(1) OCCUPANCY IS GIVEN IN PERCENT OF TOTAL IMAGE AREA

(2) TOTAL RANGE IS 64 RADIANCE VALUES

The tonal difference image (Figure 4-17) displays ghosting in Subscenes 4, 5, and 6, thus indicating misregistration. It also appears that there are some wispy clouds over Subscenes 5 and 6. This together with the clouds north of this area may contribute to less precise registration of the reference and warped collateral data. Since that warp data is used to define the subscene coordinates in the raw and warped collateral data, any inaccuracy would be reflected in the match occupancies.

Reliability of the occupancy calculation would be improved by computing the center coordinates for each subscene on the basis of cross correlation of raw and collateral data. Yet, to a degree, this would defeat the intent of testing the results of the original TRAK registration.

Two dimensional sin X/X resampling as applied to Scene D produces significantly lower match occupancies. As in the previous examples sin X/X resampling decreases the average radiance values of warped data relative to raw data.

In conclusion, then, nearest neighbor resampling is superior to the particular sin X/X resampling used over Scene D on the basis of occupancies in the radiance difference distribution. Also, correlation and registration with TRAK processing as implemented here are better over culturally developed areas than over mountainous terrain.

## 5.5 Summary

TRAK registration has been shown to register a wide variety of image terrain examples very effectively under conditions of temporal change and different sensor spectral bands. The four scenes which are analyzed in this report represent terrain of the following types: cultural development, foothills, rugged mountains, and amorphous desert-like terrain. All were registered to a mean radial error of less than 0.25 pixel by TRAK automatic processing. In worst cases radiance values in the raw and warped data were within a tolerance of $\pm 1$ radiance unit (on a scale of 64) over at least 70 percent of the registered area. In some cases this tolerance was met in excess of 90% of the area.

Some general conclusions from the preceding analyses of radiometric degradation resulting from TRAK registration can be made:

- Correlation of raw and warped data is greater for cultural development than for natural terrain and is perhaps lowest in rugged mountainous and desert terrains.
- Mean radial displacement error decreases with increasing correlation.
- Two dimensional sin X/X and 4-point bilinear resampling (as implemented in this work) decrease the average radiance in the warped data by about 0.5 radiance unit (on a scale of 64).
- 4-point bilinear resampling blurs the image.

- Nearest neighbor resampling causes local fluctuations corresponding to pixel displacements as great as 0.5 pixel and decreases average gray level at feature edges.
- Sin X/X maintains high radiometric spatial fidelity without blurring.

It is difficult to conclude from this investigation which resampling technique gives superior overall performance with regard to radiometric qualities. It is anticipated that sin X/X with appropriate improvements would allow TRAK registration to reach its maximum performance as theoretical considerations suggest.

Reviewing the summary conclusions stated above the following order of decreasing performance is suggested for the three resampling techniques: (1) sin X/X, (2) nearest neighbor, and (3) 4-point bilinear. This is precisely the order obtained for all four scenes when the techniques were ranked on the basis of statistical radiometric parameters. Yet, an important and very sensitive measure involving matching on a pixel-by-pixel basis in the tonal difference image revealed best performance with nearest neighbor interpolation.

1. Lillestrand, R. L., "Remote Sensing of Earth Resources", Thirteenth Meeting of Panel on Science and Technology, Proceedings Before the Committee on Science and Astronautics, House of Representatives, Second Session of Ninety-Second Congress, No. 13, pps 290-374, January 25, 26, and 27, 1972.

2. Rosenfeld, A., "Automatic Detection of Changes in Reconnaissance Data", Proc. 5th Conv. Mil. Electron., pp 492-499, 1961.

3. Lillestrand, R. L., "Techniques for Change Detection", IEEE Transactions on Computers, Vol. C-21, Number 7, pp 654-659, July, 1972.

4. Ulstad, M. L., "An Algorithm for Estimating Small Scale Differences Between Two Digital Images", PATTERN RECOGNITION, Pergamon Press, Vol. 5, pp 323-333.

5. Bonrud, L. O. and P. J. Henrikson, "Correlation and Registration of ERTS Multispectral Imagery," Final Report, Contract NAS9-13114, April 1974.

6. Bonrud, L. O. and P. J. Henrikson, "Digital Registration of ERTS-1 Imagery", 13th Symposium on Adaptive Processes, 1974 IEEE Conference on Decision and Control, November, 1974.

7. Thomas, Valerie L., "Generation and Physical Characteristics of the ERTS MSS System Corrected Computer Compatible Tapes", Goddard Space Flight Center, July 1973.

8. Klass, P. J., "Analyzer Pinpoints Radar Changes", Aviation Week and Space Technology, May 26, 1975.

9. Lillestrand, R. L, and R. R. Hoyt, "The Design of Advanced Digital Image Processing Systems", Photogrammetric Engineering, Vol. XL, No. 10, October, 1974.